Model Development Report: Salmon Creek Watershed

SUBMITTED TO:

State Water Resources Control Board
1001 I Street, 14th Floor
Sacramento, CA 95814

PREPARED BY:

Paradigm Environmental
9320 Chesapeake Drive, Suite 100
San Diego, CA 92123

AUGUST 26, 2025

THIS PAGE INTENTIONALLY LEFT BLANK

Contents

Figures

Tables

1 INTRODUCTION

This report provides a detailed discussion of the development and configuration of a hydrology model which was developed for the Salmon Creek watershed to support decision making by the California State Water Resources Control Board (Water Board) regarding water supply, demand, and use. In April 2021, Governor Gavin Newsom issued a state of emergency proclamation for specific watersheds across California in response to exceptionally dry conditions throughout the state. The April 2021 proclamation, as well as subsequent proclamations, directed the Board to address these emergency conditions to ensure adequate, minimal water supplies for critical purposes. To support Water Board actions to address emergency conditions, hydrologic modeling and analysis tools are being developed to contribute to a comprehensive decision support system that assesses water supply and demand, and the flow needs for watersheds throughout California.

This model development report builds on the Salmon Creek watershed modeling work plan (SWRCB 2024), which has additional information on the model background and over-arching model approach; the Loading Simulation Program in C++ (LSPC) was used to simulate hydrology within the watershed. The model provides an evaluation platform for (1) simulating existing instream flows that integrate current water management activities and consumptive uses, (2) evaluating the range of impacts of alternative management scenarios. Key components for model development are detailed in this report. Model development refers to the basic building blocks for defining the surface water model domain. It includes catchment delineation, reach segments (cross-sections, hydraulic characteristics, and routing network), and Hydrologic Response Units (HRUs). Model development also includes creating and assigning representative climate-forcing inputs. The final sections of this report provide details on the model calibration approach and present calibration and validation results.

- Section 2.1 describes the Catchment Delineation. Catchments are the highest-resolution spatial boundaries in the model. Delineated catchments were compiled from best-available topographic layers and refined as needed to align outlets with monitoring flow stations.
- Section 2.2 describes the Hydraulic Network. Hydraulic routing features include reaches, lakes/reservoirs, and other network routing elements that convey flow and pollutants from one catchment to another.
- Section 3 describes the Hydrologic Response Units. HRUs are the smallest spatial unit within the model, representing unique combinations of spatial data layers including land use/land cover/cropland, hydrologic soil group, and slope.
- Section 4 describes the climate-forcing inputs. Forcing inputs include precipitation and potential evapotranspiration that drive the model's rainfall-runoff response.
- Section 5 describes the representation of surface water withdrawals and irrigation in the model.
- Section 6 describes the model calibration approach and results.
- Section 7 presents the model validation results.
- Section 8 presents a summary of the report.

2 CATCHMENT NETWORK

2.1 Catchment Delineation

The United States Geological Survey (USGS) delineates watersheds nationwide based on surface hydrological features and organizes the drainage units into a nested hierarchy using hydrologic unit codes (HUC). These HUCs have a varying number of digits to denote scale ranging from 2-digit HUCs (largest) at the regional scale to 12-digit HUCs (smallest) at the subwatershed scale. The Salmon Creek watershed is defined as a single HUC-12 subwatershed.

For units smaller than the HUC-12 subwatershed, the National Hydrography Dataset Plus v2 (NHDPlus) has further discretized the subwatershed into catchments ranging in size between 0.01 square miles to approximately 7.6 square miles. Figure 2-1 is a map of the NHDPlus catchments within the Salmon Creek watershed (HUC-12 subwatershed). Table 2-1. presents summary statistics of NHDPlus catchment sizes by HUC-12 subwatershed. Where necessary, catchments were either merged to eliminate braiding in the stream network or sub-delineated using the hydrologically conditioned 30-meter resolution digital elevation model (DEM), flow direction, and flow accumulation rasters available with the NHDPlus dataset to better represent points of interest. No catchments were merged in the Salmon Creek watershed. Sub-delineation was necessary in one case in the Salmon Creek watershed, where a catchment was split based on the USGS stream flow station location. Figure 2-2 shows the final delineated catchments for the LSPC model.

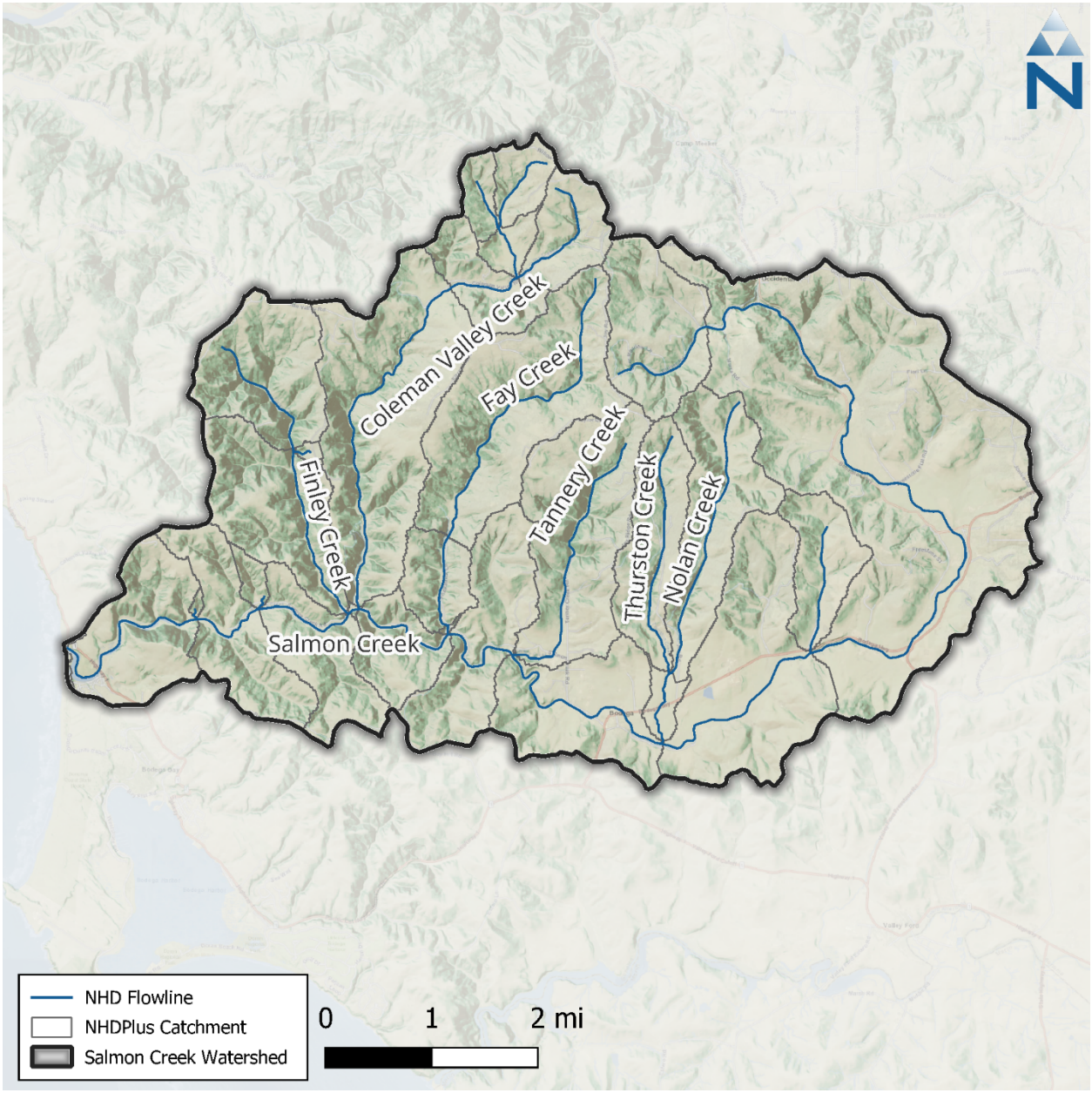

Figure 2-1. Initial NHDPlus catchment segmentation for the Salmon Creek watershed.

Table 2-1. Summary of finalized NHDPlus catchments within the Salmon Creek watershed (HUC-12 subwatershed)

HUC-12	HUC-12 Name	Catchment Count	Catchment Area (acre)			
			Minimum	Average	Maximum	Total
18010109020	Salmon Creek	30	6.9	746.9	4,856.4	22,395.7

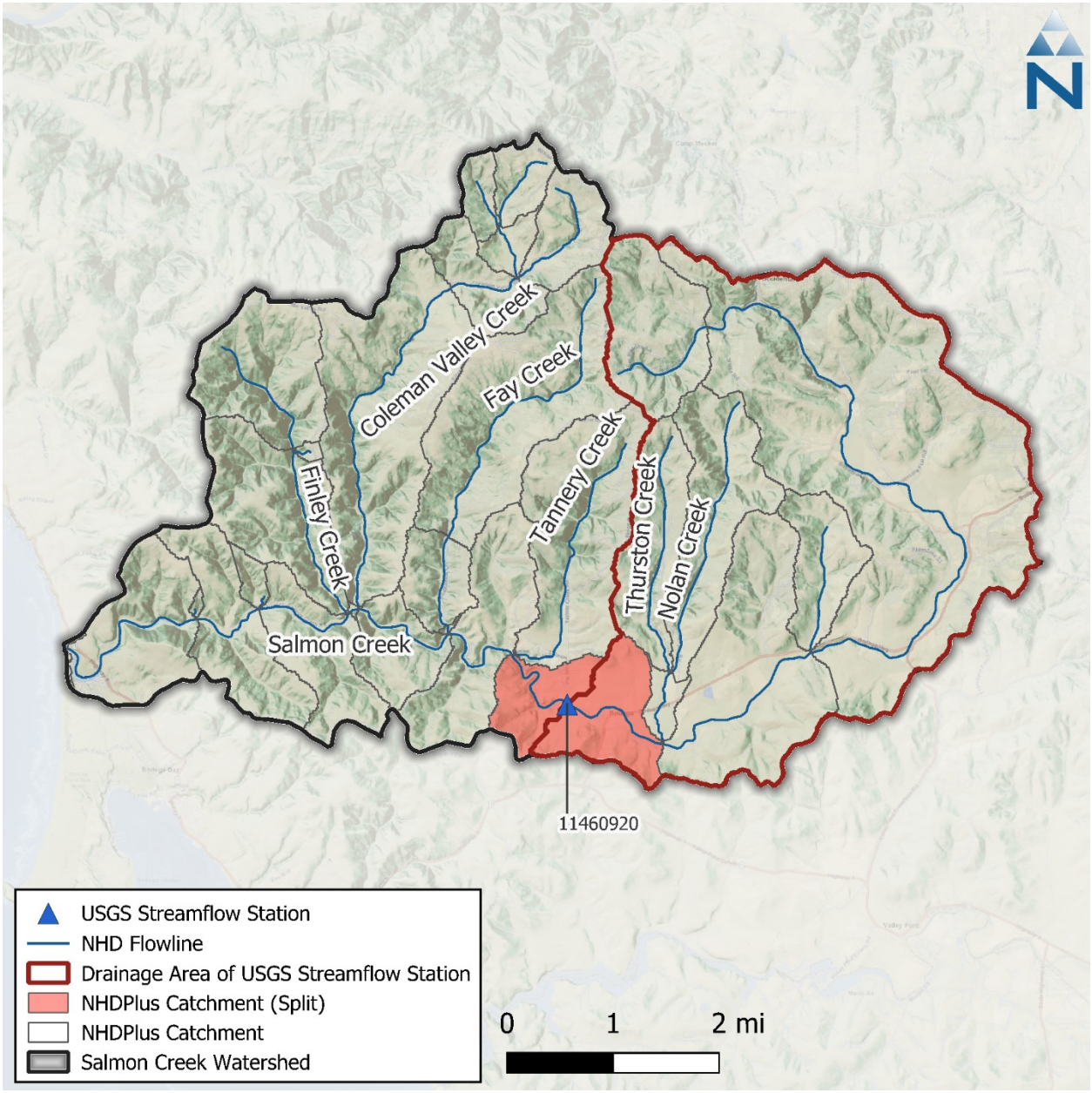

Figure 2-2. Final NHDPlus catchment segmentation for the Salmon Creek watershed.

2.2 Routing & Connectivity

Once catchments have been delineated, the connectivity of flow within and between each catchment needs to be specified so that water can be routed from upstream to downstream areas. Within the Salmon Creek watershed model, surface flow is conveyed through a reach network with no more than one representative reach segment for each catchment. Within a catchment, water from all other upstream physical conveyances is routed directly to the top of and through the representative stream segment.

The reach network for the Salmon Creek watershed is based on the NHD flowlines available with the NHDPlus dataset. These flowlines were edited as described in Section 2.1 to eliminate braiding and are shown in Figure 2-2. Within the NHDPlus schema, catchments can be related to flowlines through

the catchment *FEATUREID* and flowline *COMID*. The flowline *COMID* was joined to the PlusFlowlineVAA (value-added attributes) table available with the NHDPlus dataset to determine flow routing.

2.3 Stream Characteristics

The discharge for each stream segment is calculated in LSPC using Manning's equation, presented below as Equation 1:

$$Q = VA = (1.49/n)\, AR^{2/3}\sqrt{S}]$$

where (A) is the cross-sectional area in square feet, (R) is the hydraulic radius in feet, (V) is the velocity in feet per second, (S) is the longitudinal slope, and (n) is the channel roughness coefficient.

Length and slope are derived from the PlusFlowlineVAA table, which includes precalculated reach characteristics based on local conditions. For reaches that were merged, split, or edited, the slope was recalculated as the length-weighted average slope (derived from the DEM described in Section 3.4) based on the new reach length. The default cross-section representation in LSPC is a symmetrical trapezoidal channel defined using the terms shown in Figure 2-3. Stream segments are represented in the model as having the same cross-section for the entire reach length. Numerous studies have developed empirical relationships between stream channel geometry and upstream contributing area (Bent and Waite, 2013; McCandless, 2003a, 2003b; McCandless and Everett, 2002); these were used to derive channel geometry for each stream segment in LSPC. An initial estimate of n = 0.04 representing natural streams with vegetation was used for all reach segments and may be updated as needed during model calibration (Arcement and Schneider, 1989).

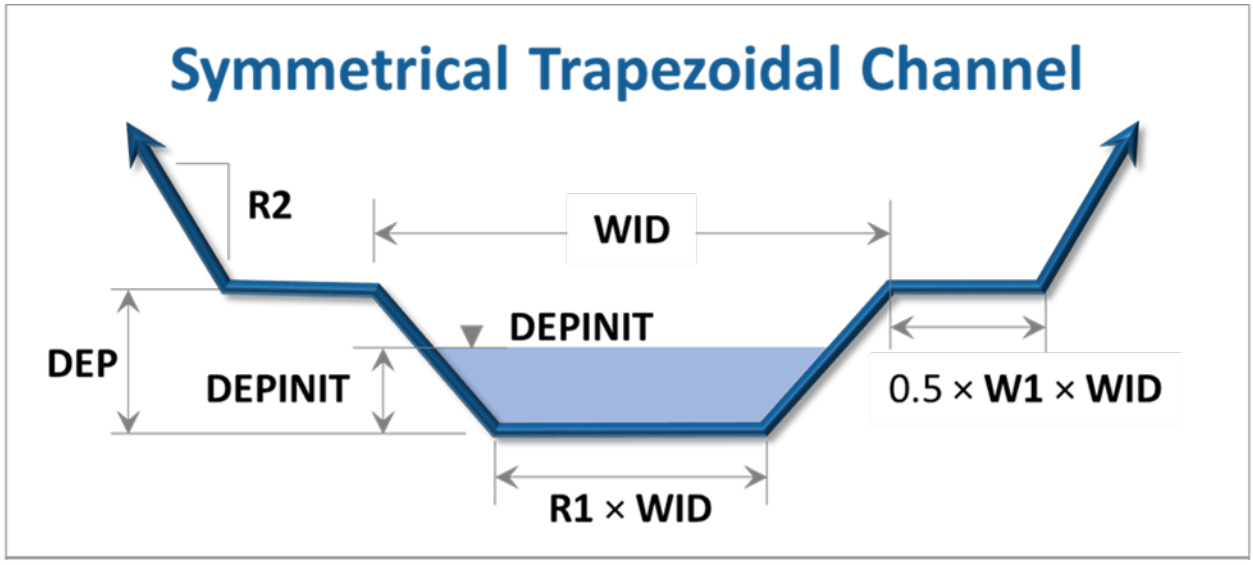

WID	Estimated Bankfull-Width	**R1**	Ratio of channel bottom width to **WID**
DEP	Estimated Bankfull-Depth	**R2**	Side slope for floodplain
DEPINIT	Initial water depth	**W1**	Floodplain width parameter

Figure 2-3. Example cross-section representations in LSPC.

3 HYDROLOGIC RESPONSE UNITS

Within LSPC, the land is categorized into HRUs, which are the core hydrologic modeling land units in the watershed model. Each HRU represents areas of similar physical characteristics attributable to certain processes. The HRU development process uses data types that are typically closely associated with hydrology (and water quality, when applicable) in the watershed. For the Salmon Creek watershed, this includes data such as land cover, cropland, soil type, and slope. The HRUs are developed by overlaying these datasets in raster format and identifying the unique combinations over catchments. Ultimately, some consolidation of HRUs was implemented to balance the model computational efficiency and optimal spatial resolution, resulting in a set of meaningful HRUs for model configuration. Percent tree canopy was also summarized as a secondary attribute by HRU and used to estimate initial values for the interception storage and lower-zone evapotranspiration rate for model configuration.

Table 3-1 lists the spatial data used in the HRU analysis along with the corresponding data sources. The following subsections summarize the data that were used to develop each of these spatial layers and the processes for consolidating them as HRUs.

Table 3-1. Summary of input datasets detailing data source and type

GIS Layer	Data Source	Site	Description	Date Downloaded
Digital Elevation Model	USGS 3D Elevation Program (3DEP)	Science Base	2024 – 27.66m resolution grid	August 1, 2024
Land Cover	MRLC (NLCD)	MRLC	2021 – 30m resolution grid	June 30, 2023
Cropland	USDA (CDL)	USDA	2022 – 30m resolution grid	January 2, 2023
Percent Imperviousness	MRLC (NLCD)	MRLC	2021 – 30m resolution grid	June 30, 2023
Percent Tree Canopy	MRLC	MRLC	2021 – 30m resolution grid	October 5, 2023
Soil Survey Geographic Database (SSURGO)	USDA (NRCS)	USDA	2022 – polygon layer	October 5, 2023
U. S. General Soil Map (STATSGO2)	USDA (NRCS)	USDA	2016 – polygon layer	December 29, 2022

3.1 Land Cover

The land cover data were obtained from the 2021 National Land Cover Database (NLCD) maintained by the Multi-Resolution Land Consortium (MRLC), a joint effort between multiple federal agencies. The primary objective of the MRLC NLCD is to provide a current data product in the public domain with a consistent characterization of land cover across the United States. The 2021 NLCD provides a 16-class scheme at a 30-meter grid resolution.

Table 3-2 summarizes the NLCD 2021 land cover distribution for the Salmon Creek watershed; Figure 3-1 shows the land cover for the Salmon Creek watershed. Evergreen forest is the dominant land cover classification, covering approximately 41% of the watershed area. When combined, the undeveloped categories of evergreen forest, deciduous forest, mixed forest, shrub/scrub, and grassland/herbaceous account for close to 93% of the total watershed area. Developed land cover, which is concentrated in small portions of the watershed, makes up less than 6% of the total watershed area and is classified mostly as "Developed, Open Space." None of the watershed areas are categorized as cultivated cropland. For HRU development, similar NLCD classes (i.e., forest and grassland) were grouped.

Table 3-2. Distribution of 2021 NLCD land cover classes within the Salmon Creek watershed

NLCD Class	Description	Model Group[1]	Area	
			Acres	%
22	Developed, Low Intensity	Developed_Low_Intensity	127.2	0.57%
23	Developed, Medium Intensity	Developed_Medium_Intensity	36.0	0.16%
24	Developed, High Intensity	Developed_High_Intensity	4.0	0.02%
21	Developed, Open Space	Developed_Open_Space	1,050.8	4.69%
31	Barren Land (Rock/Sand/Clay)	Barren	0.9	0.00%
41	Deciduous Forest	Forest	92.5	0.41%
42	Evergreen Forest	Forest	9,086.6	40.57%
43	Mixed Forest	Forest	1,352.8	6.04%
52	Shrub/Scrub	Scrub	6,081.8	27.16%
71	Grassland/Herbaceous	Grassland	4,097.6	18.30%
81	Pasture/Hay	Pasture	23.1	0.10%
82	Cultivated Crops	Agriculture	0.0	0.00%
90	Woody Wetlands	Forest	164.1	0.73%
95	Emergent Herbaceous Wetlands	Grassland	254.0	1.13%
11	Open Water	Water	24.2	0.11%
		Total	**22,396**	**100%**

1: Developed land cover was refined and redistributed into effective Developed_Impervious and Developed_Pervious areas as described in Section 3.6. All other model groups categories are mapped for consolidation as shown.

Color Gradient: Lowest | Low | Med | High | Highest

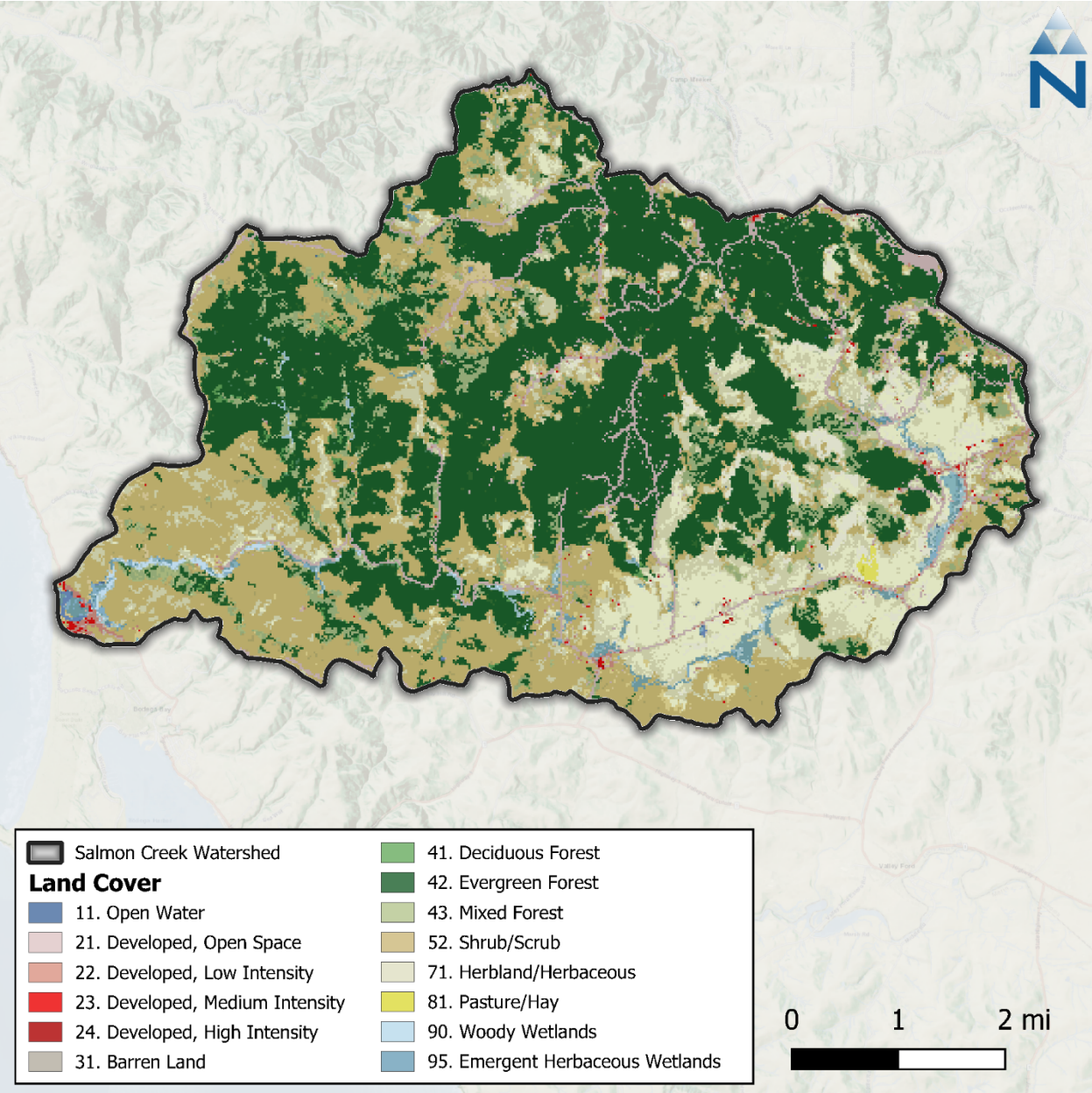

Figure 3-1. NLCD 2021 land cover within the Salmon Creek watershed.

3.2 Agriculture and Crops

Land cover data for the Salmon Creek watershed (see Section 3.1) was analyzed to identify predominant cropland vegetation classes. This analysis revealed that only 0.1% of the watershed area was classified as Pasture/Hay (class 81), 27% was classified as Shrub/Scrub (class 52), and 18% was classified as Grassland/Herbaceous (class 71); of these areas, a portion may include areas of cultivated crops that were not automatically recognized through processing of the remote sensing data or include cultivated crops on a rotating schedule. To reflect these situations, supplemental information published by the United States Department of Agriculture (USDA) was used.

The USDA Cropland Data Layer (CDL) is an annually updated raster dataset that geo-references crop-specific land use (USDA 2024). The dataset comes as a 30-meter resolution raster with a linked

lookup table of 85 standard crop types that can be used to classify agricultural land. Figure 3-2 shows the spatial distribution of these classes through the study area, and Table 3-3 summarizes their areal coverage. The CDL Land use layer was intersected with the NLCD Land Cover layer, and CDL Agriculture and Pasture land use classifications overwrote the original NLCD classifications—all other HRUs retained their or original NLCD classifications. The combined Land Use/Land Cover (LULC) increased "Cropland" to 617 acres (2.8%), which was classified as "Agriculture" in the final HRU layer— "Pasture" area was also updated to match CDL land use. The LULC intersection redistributes HRU area between originally classified Grassland, Pasture, and Agriculture categories from NLCD.

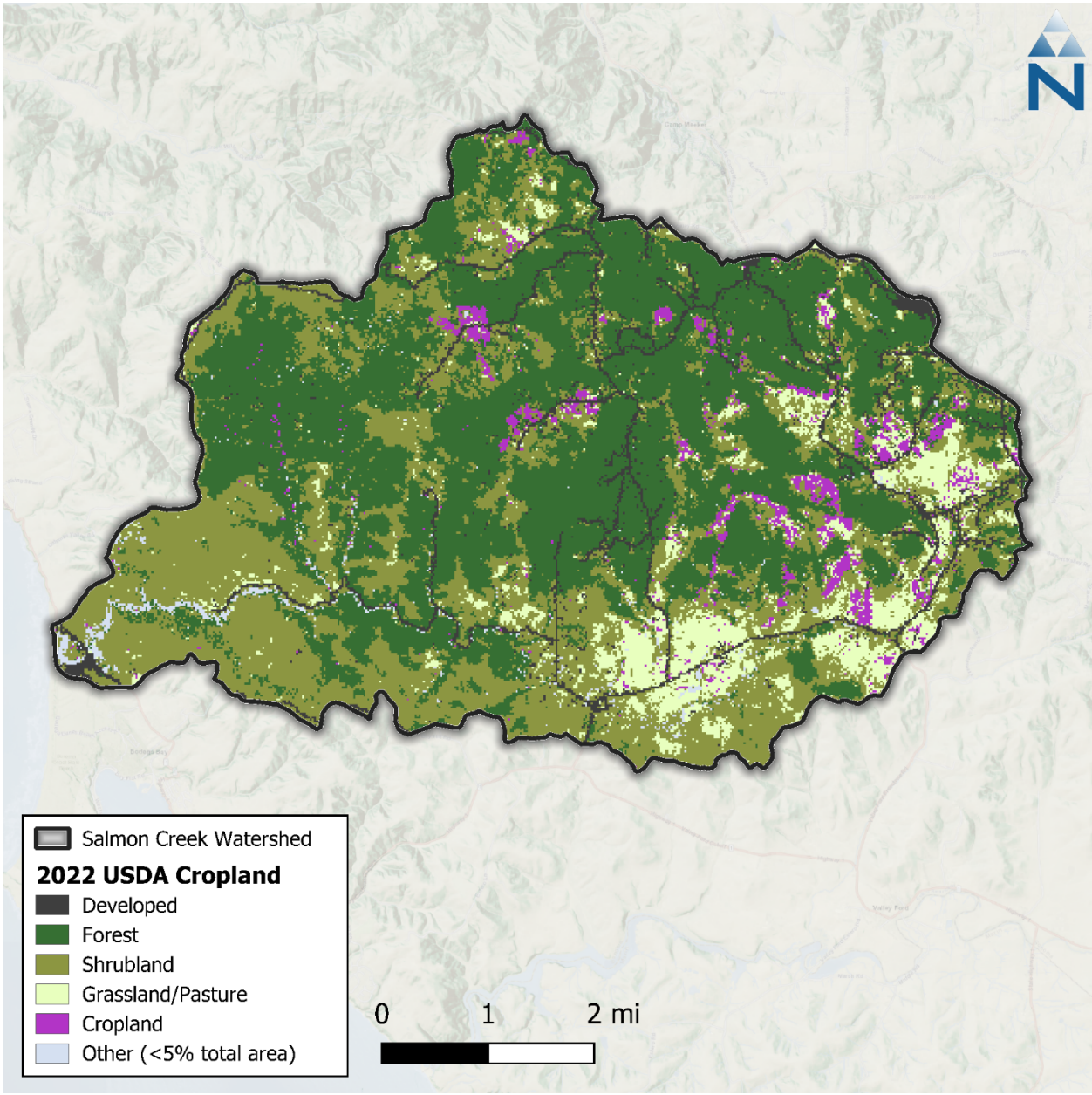

Figure 3-2 USDA 2022 Cropland Data within Salmon Creek watershed.

Table 3-3 USDA 2022 Cropland Data Summary within the Salmon Creek watershed

Crop Type	Area (acre)	Area (%)
Forest	10,352.2	46.2%
Shrubland	8,090.7	36.1%
Grassland/Pasture	1,868.6	8.3%
Cropland	617.1	2.8%
Other (<5% Total Area)	1,467.1	6.6%
Total	**22,396**	**100%**

Color Gradient: Lowest | Low | Medium | High | Highest

Table 3-4 shows the impact that intersecting NLCD with CDL has on mapped cropland and pasture areas. It also shows which NLCD categories were reclassified into Cropland and Pasture, and which were unchanged.

Table 3-4 Intersection of NLCD and USDA 2022 Cropland Data Layer for the Salmon Creek watershed

NLCD Class	Description	NLCD (acres)		Crop Data Layer Intersect (acres)		
		Original	Changed[1]	No Change	Cropland	Pasture
22	Developed, Low Intensity	127.2	0.0%	127.2	0.0	0.0
23	Developed, Medium Intensity	36.0	0.0%	36.0	0.0	0.0
24	Developed, High Intensity	4.0	0.0%	4.0	0.0	0.0
21	Developed, Open Space	1,050.8	0.0%	1,048.8	2.0	0.0
31	Barren Land (Rock/Sand/Clay)	0.9	0.0%	0.7	0.0	0.2
41	Deciduous Forest	92.5	0.0%	91.4	0.4	0.7
42	Evergreen Forest	9,086.6	0.2%	9,045.7	21.6	19.3
43	Mixed Forest	1,352.8	0.1%	1,336.1	12.2	4.4
52	Shrub/Scrub	6,081.8	1.5%	5,753.3	171.2	157.2
71	Grassland/Herbaceous	4,097.6	9.1%	2,068.3	377.8	1,651.5
81	Pasture/Hay	23.1	0.1%	2.0	20.7	0.4
82	Cultivated Crops	0.0	--	--	--	--
90	Woody Wetlands	164.1	0.0%	161.2	0.9	2.0
95	Emergent Herbaceous Wetlands	254.0	0.2%	211.1	10.2	32.7
11	Open Water	24.2	0.0%	24.2	0.0	0.0
Total:		**22,396**	**11%**	**19,910.0**	**617.1**	**1,868.6**

1: Expressed as a percentage of the entire Salmon Creek Watershed

3.3 Soils

Soil data for the Salmon Creek watershed were obtained from the Soil Survey Geographic Database (SSURGO) published by the Natural Resource Conservation Service (NRCS). Four primary hydrologic soil groups (HSG) are used to characterize soil runoff potential. Group A generally has the lowest runoff potential, whereas Group D has the highest runoff potential. The SSURGO soils database is composed of a GIS polygon layer of map units and a linked tabular database with multiple layers of soil properties.

Table 3-5 and Figure 3-3 present summaries of the SSURGO hydrologic soil groups for the Salmon Creek watershed. The dominant soil group in the watershed is Group C (66%), containing sandy clay loam. Group B (26%) is the next most common soil group in the watershed, containing silt and silty loam. Group D, with the lowest infiltration rates, makes up approximately 7% of the watershed. Less than 1% of the watershed has mixed soil. For modeling purposes, mixed soils were grouped with the nearest primary group as follows: A/D → B, B/D → C, and C/D → D About 0.6% of the watershed HSG area is classified as unknown in the SSURGO database and reside primarily near the watershed outlet. For these areas, the corresponding HSG from the STATSGO dataset was used to supplement the data gaps; this reduced the unknown soil areas to about 0.01%. Since most of the soil in the watershed is Group C, the unknown soil areas are also considered to be Group C in this analysis.

Table 3-5. NRCS Hydrologic soil groups in the Salmon Creek watershed

Soil Group	Model Group	Area (acre)	Area (%)
A	A	217.5	1.0%
B	B	5,848.1	26.1%
C	C	14,771.9	66.0%
C/D	D	12.7	0.1%
D	D	1,543.9	6.9%
Unclassified	C	1.8	0.0%
	Total	**22,396**	**100%**

Color Gradient: Lowest | Low | Medium | High | Highest

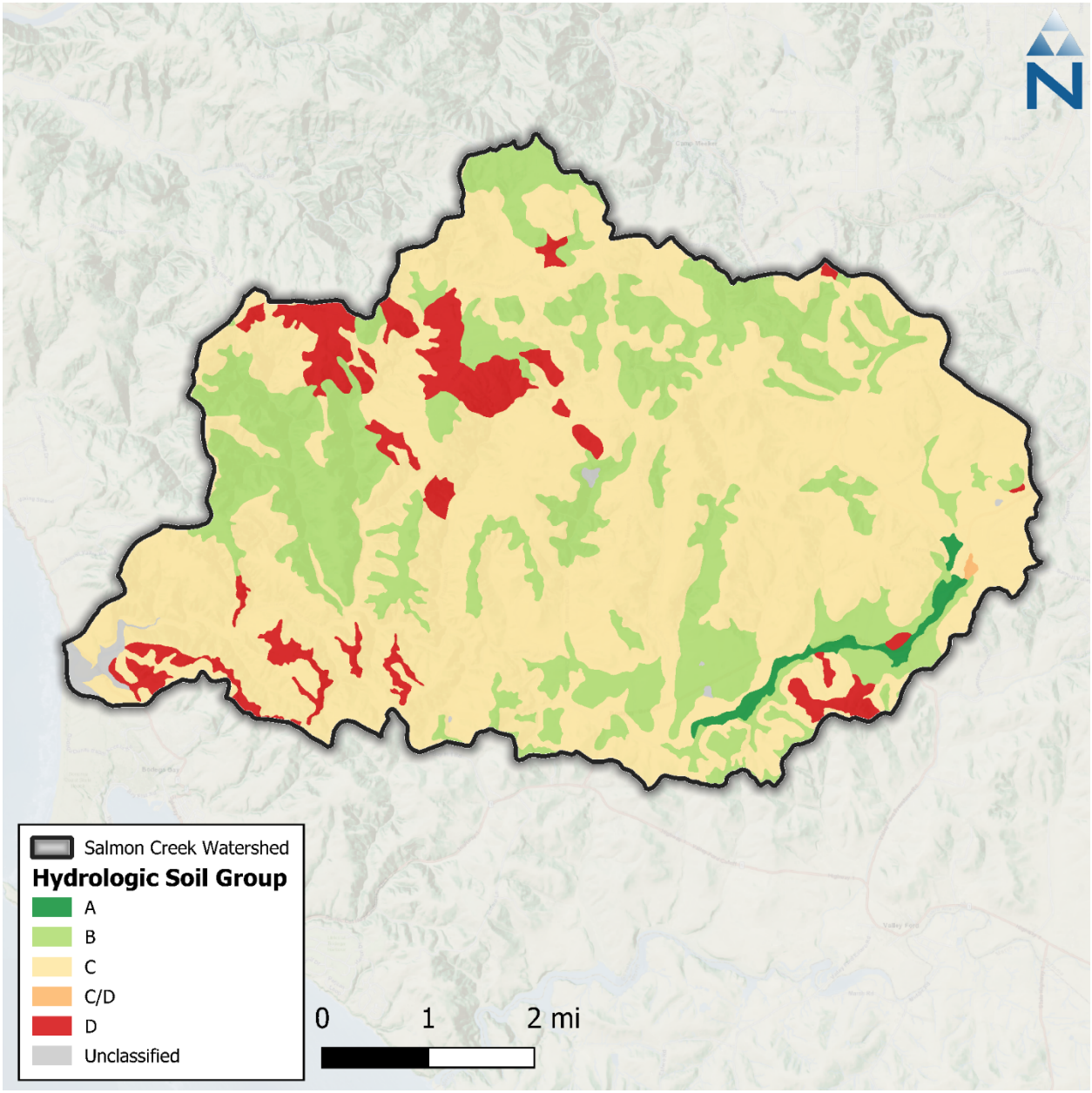

Figure 3-3. SSURGO hydrologic soil groups within the Salmon Creek watershed.

3.4 Elevation and Slope

The United States Geological Survey (USGS) 3D Elevation Program (3DEP) publishes DEMs expressing landscape elevation through a raster grid data product with a 1 arc-second (approximately 30-meter) horizontal resolution. The 1 arc-second data covering the Salmon watershed had a resolution of 27.66-meters and thus was resampled to 30-meters for consistency with the rest of the datasets for the HRU analysis. The Salmon Creek watershed ranges in elevation from near sea level at the mouth of the watershed in the west to over 402 meters in the northern portion of the watershed.

The 30-meter DEM was used to generate a slope (percent rise) raster for the watershed. Figure 3-4 illustrates the cumulative distribution function (CDF) of the slope raster values across the model

domain as a percentage of the total watershed land area (i.e., excluding major water bodies). The CDF was used to identify appropriate bins for HRU slope categories during the HRU definition process. Slopes were categorized as low (< 5%), medium (5 to 15%), and high (>15%) according to their distribution and overlap with the land cover layer. Table 3-6 and Figure 3-5 present the distribution of slope categories within the watershed.

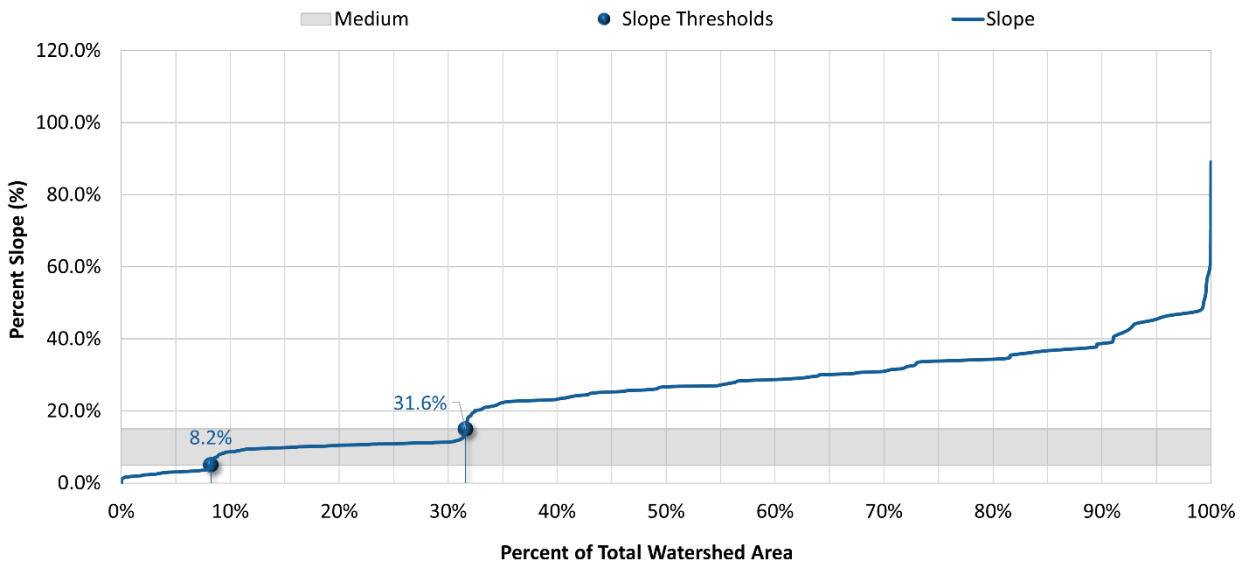

Figure 3-4. Cumulative distribution of slope categories within the Salmon Creek watershed.

Table 3-6. Distribution of slope categories within the Salmon Creek watershed

Slope (%)	Slope Category	HRU Group	Area (ac)	Area (%)
0-5	Low	Low	1,842.1	8.2%
5-15	Medium	Med	5,232.9	23.4%
>15	High	High	15,320.7	68.4%
		Total	**22,396**	**100%**

Color Gradient: Lowest | Low | Medium | High | Highest

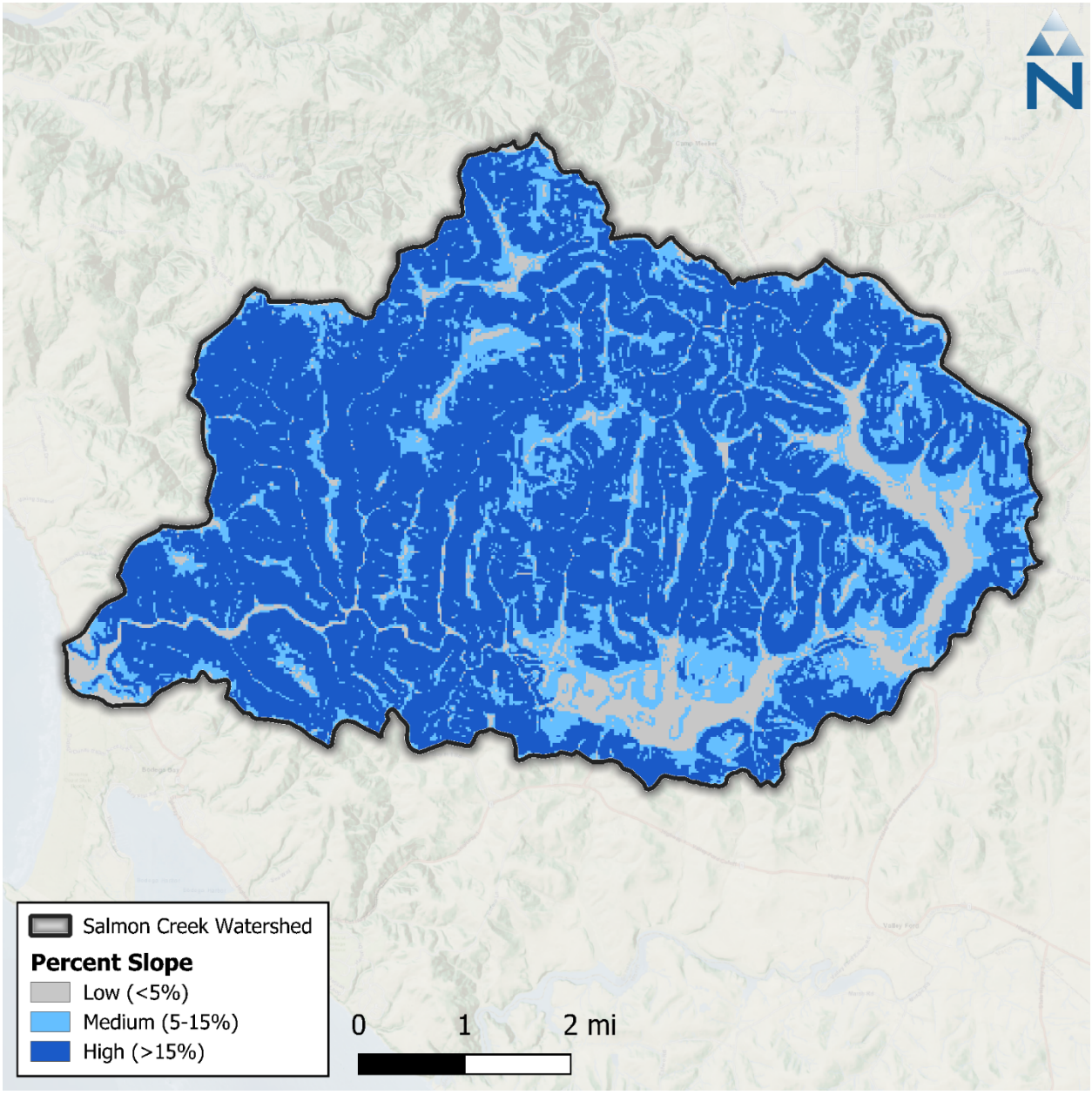

Figure 3-5. Percent Slope derived from the DEM within the Salmon Creek watershed.

3.4.1 Length and Slope of Overland Flow

Overland flow lengths on high slopes are generally shorter and more direct and have faster travel times on high slopes, but generally longer and less direct with slower travel times on lower slopes. It was found during previous modeling efforts that using an empirical relationship shown in Figure 3-6, derived by inversely scaling length of overland flow (LSUR) with slope of overland flow (SLSUR), improved model prediction of peak flow timing. Figure 3-7 is the resulting cumulative distribution of LSUR and SLSUR in the Salmon Creek watershed. Longer flow lengths on shallow sloped areas increase the opportunity for attenuation, surface storage, and infiltration. On the other hand, shorter flow lengths on steeper slopes retain the flashiness where applicable. Similar modeling efforts have historically used discrete/fixed values and ranges for SLSUR and LSUR to better manage the degrees

of freedom among model variables. However, because SLSUR can be measured by HRU from remotely-sensed data, applying a relationship to also estimate LSUR as a function of SLSUR preserves some natural variability throughout the watershed that (1) can provide some improvement relative to initial hydrology prediction using constant values and (2) helps to reduce the chance of adjusting other parameters during calibration that are better explained by the influence of LSUR and SLSUR.

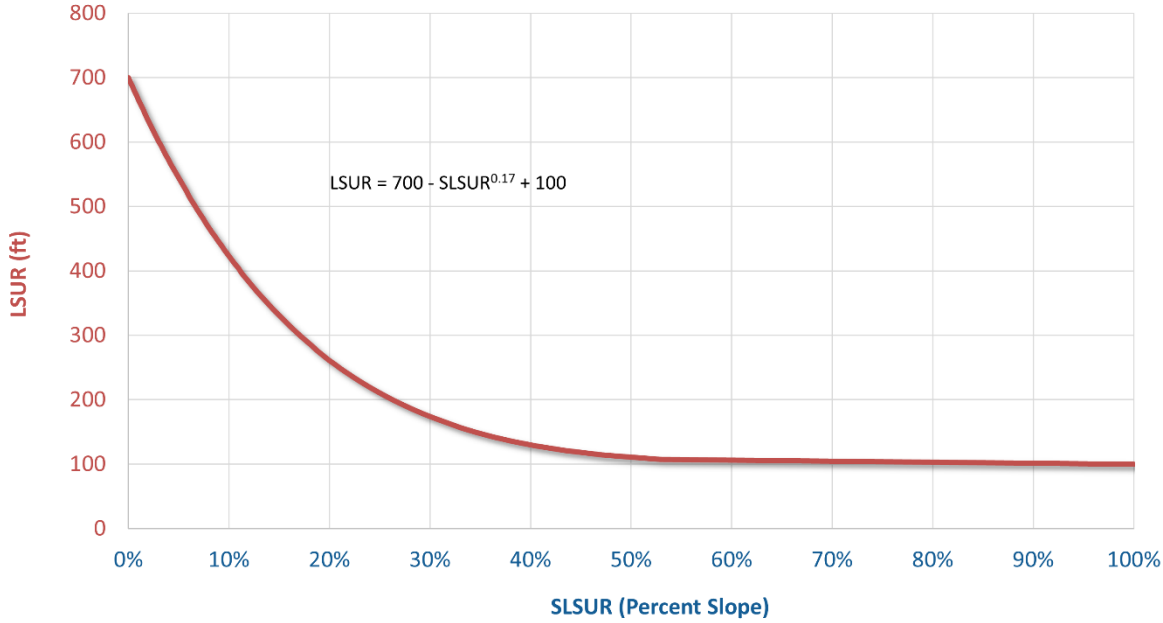

Figure 3-6. Empirical relationship of LSUR vs. SLSUR.

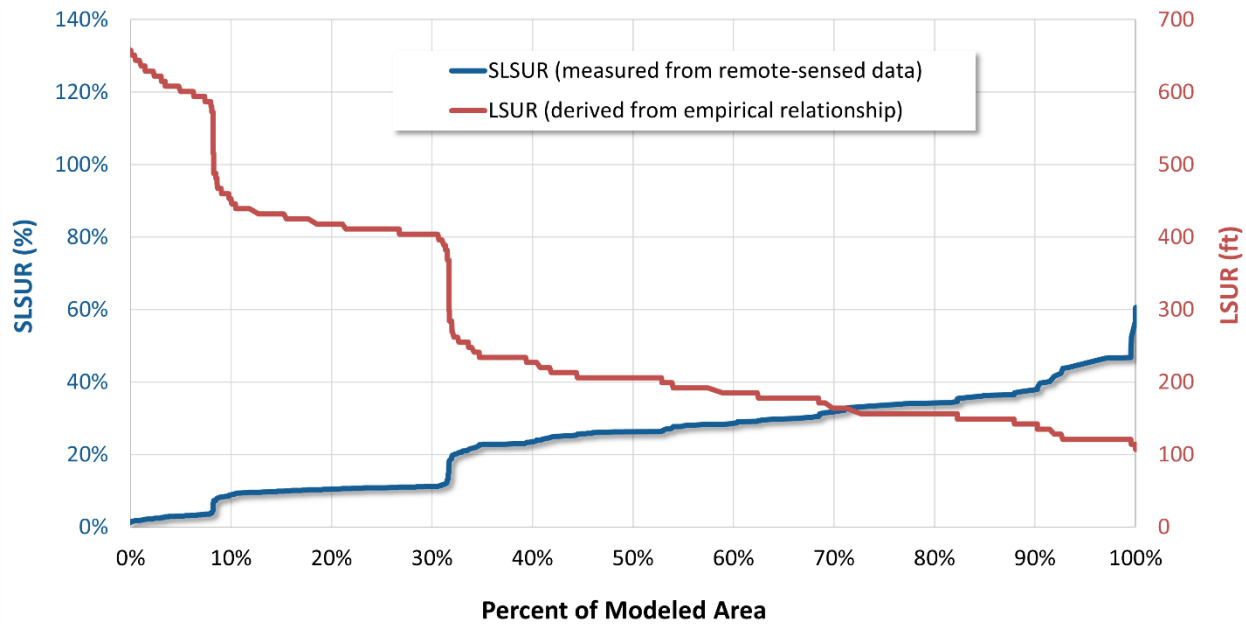

Figure 3-7. Cumulative distribution of LSUR and SLSUR in the Salmon Creek watershed derived from the generalized empirical relationship.

3.5 Secondary Attributes

Secondary attributes can be included in the HRU development process to provide additional information not directly mapped in the HRU categories. Secondary attributes used for the Salmon Creek watershed include impervious and tree canopy cover percentages. The impervious cover percentage is used for the translation of mapped impervious cover to effective impervious cover, while percent canopy estimates can inform certain hydrologic parameters but will not be represented in the HRUs as a category.

3.5.1 Impervious Cover

MRLC publishes a developed impervious cover dataset as a companion to the NLCD land cover. This dataset is also provided as a raster with a 30-meter grid resolution. Impervious cover is expressed in each raster pixel as a percentage of the total area ranging from 0 to 100 percent. Figure 3-8 shows the NLCD impervious 2021 cover dataset for the Salmon Creek watershed. Because this data set provides impervious cover estimates for areas classified as developed, non-zero values closely align with developed areas (NLCD classification codes 21 through 24). The percentage impervious cover was used in HRU development to further group developed land cover classes into pervious or impervious and to distinguish between mapped impervious area (MIA) and effective impervious area (EIA), as discussed in Section 3.6.1.

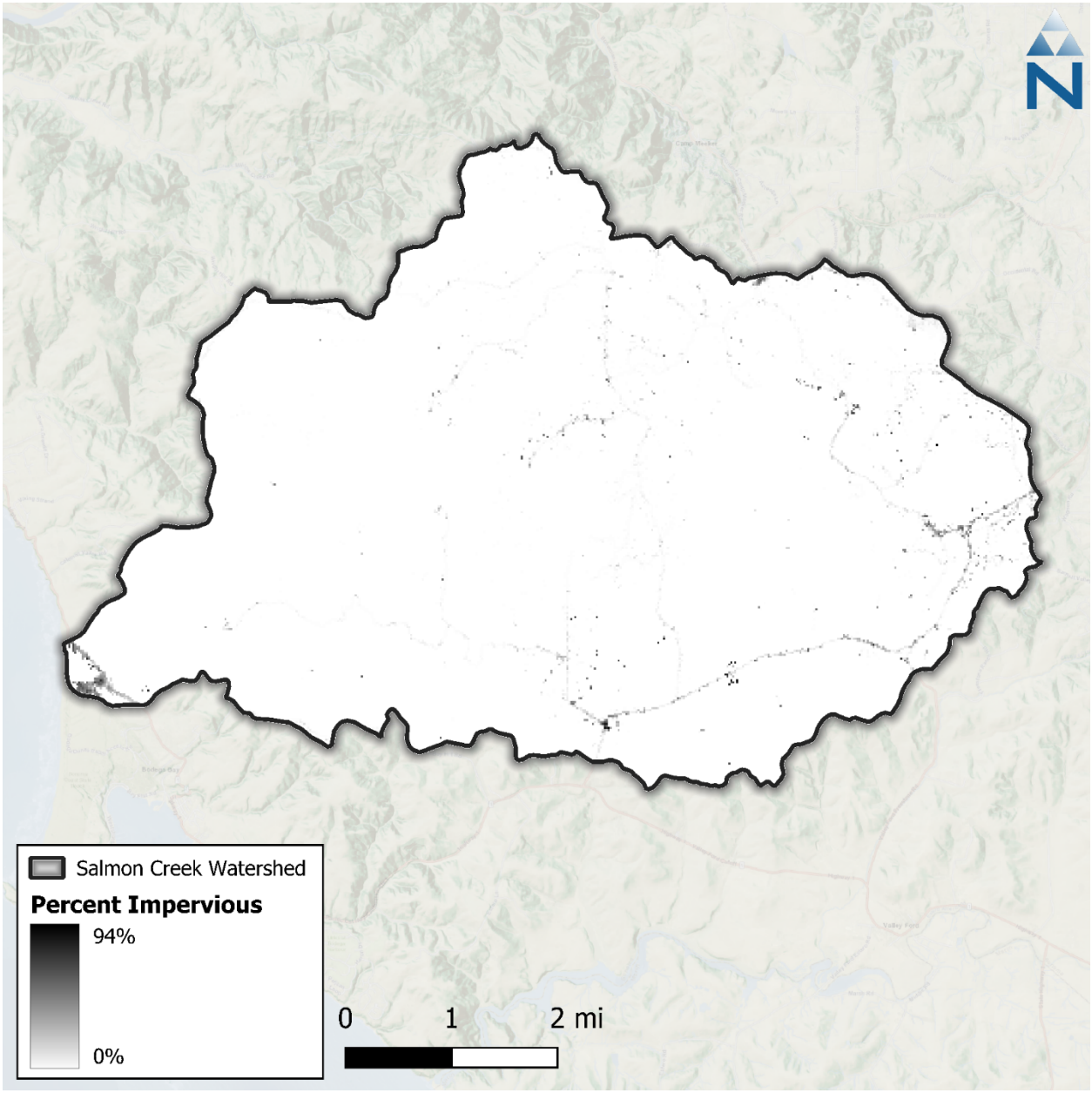

Figure 3-8. NLCD 2021 percent impervious cover in the Salmon Creek watershed.

3.5.2 Tree Canopy

MRLC publishes a tree canopy dataset as a companion to the NLCD land cover dataset that estimates the percentage of tree canopy cover spatially. The United States Forest Service (USFS) developed the underlying data model, which is available through its partnership with the MRLC. This dataset is also provided as a raster with a 30-meter grid resolution. Similar to the impervious cover dataset, each raster grid cell expresses the percentage of grid cell area covered by tree canopy with values ranging from 0 to 100 percent. The Salmon watershed has the highest canopy coverage (up to 90%) from the center of the watershed toward the northern boundary (Figure 3-9). Tree canopy cover data was used to estimate model parameters such as interception storage and lower-zone evapotranspiration rates.

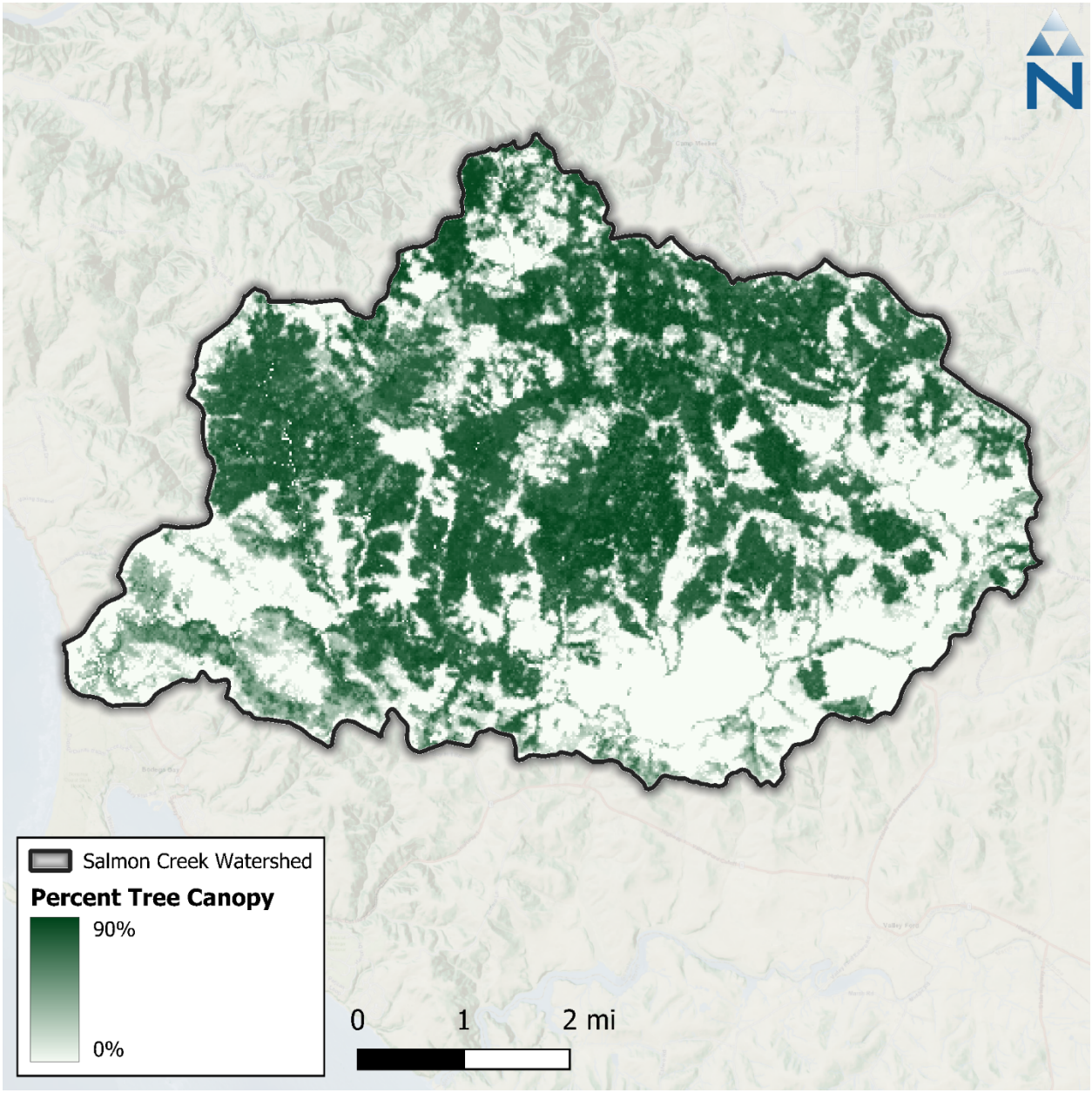

Figure 3-9. NLCD 2021 percent tree canopy cover in the Salmon Creek Watershed.

3.6 HRU Consolidation

The five spatial datasets described above (land cover, cropland, impervious cover, soils, and slope) were spatially overlayed in GIS to derive a composite raster where each grid cell shows the combination of the values from the overlayed datasets. A zonal statistics operation was then performed in GIS to generate a summary table identifying unique grid cell values (i.e., HRUs) from the composite raster and corresponding areas across catchments. The combination of these datasets resulted in 132 potential HRUs. To balance model computational efficiency, the impervious HRUs were consolidated for soil and slope combinations to reduce the overall number of unique HRUs. This step was necessary to develop a model with a reasonable run time while maintaining the optimal model resolution to characterize hydrologic conditions adequately. The HRU refinement process involves analyzing the

percentage of the model area attributed to each unique HRU combination as shown in Table 3-7. The spatial distribution of mapped HRUs across the watershed is shown in Figure 3-10. Additionally, the impervious percentage is used to adjust and group developed land cover classes (Section 3.6.1) and agriculture areas located in the catchments of point diversions were assigned as irrigation HRUs (Section 5.1.2). The final 98 modeled HRU categories are described in Section 3.6.2.

Table 3-7. Percent land cover distribution by mapped HRU category for the Salmon Creek watershed

LULC	Total Area (%)	Soil Group (% LULC Area)				Slope (% LULC Area)		
		A	B	C	D	0-5	5-15	>15
Developed_Low_Intensity	0.6%	4.4%	19.8%	65.2%	10.7%	29.5%	47.2%	23.3%
Developed_Medium_Intensity	0.2%	3.1%	14.2%	58.0%	24.7%	33.3%	53.1%	13.6%
Developed_High_Intensity	0.0%	0.0%	38.9%	61.1%	0.0%	27.8%	55.6%	16.7%
Developed_Open_Space	4.7%	1.5%	23.9%	70.5%	4.1%	15.6%	44.4%	39.9%
Barren	0.0%	0.0%	0.0%	0.0%	100.0%	33.3%	33.3%	33.3%
Forest	47.5%	0.3%	31.4%	64.9%	3.4%	2.4%	12.8%	84.9%
Scrub	25.7%	0.4%	16.9%	68.3%	14.4%	5.8%	26.7%	67.5%
Grassland	10.2%	3.5%	18.9%	69.0%	8.6%	21.7%	29.7%	48.6%
Pasture	8.4%	2.5%	36.3%	57.7%	3.5%	22.8%	43.7%	33.5%
Agriculture	2.8%	1.3%	22.7%	71.7%	4.3%	17.3%	46.5%	36.3%
Water	0.1%	1.8%	15.6%	17.4%	65.1%	74.3%	22.0%	3.7%
Total	**100.0%**	**1.0%**	**26.1%**	**66.0%**	**7.0%**	**8.2%**	**23.4%**	**68.4%**

Color gradients indicate more Watershed Area and an increasing percentage of Soil and Slope, respectively.

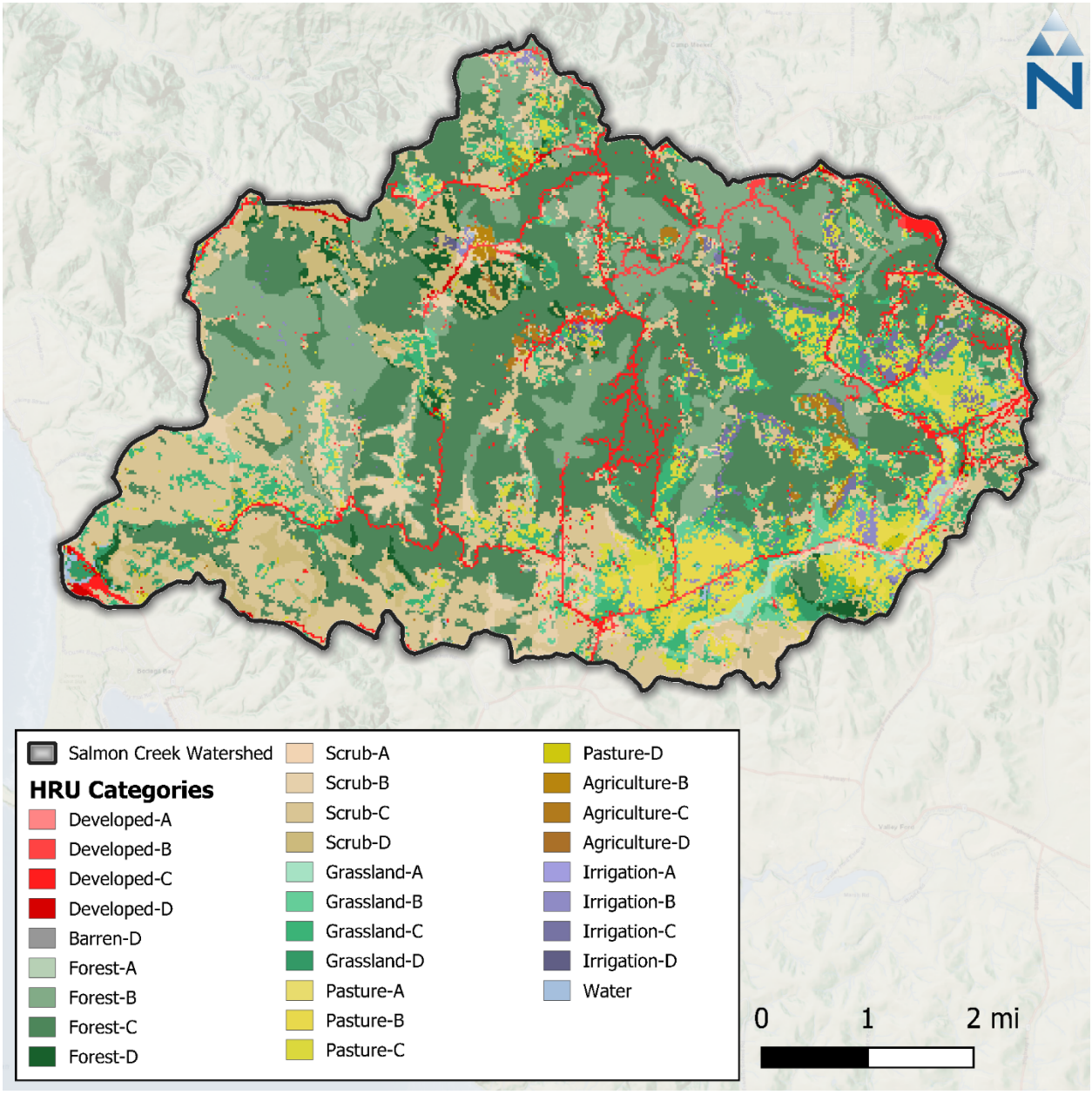

Figure 3-10. Mapped HRU categories within the Salmon Creek watershed. Note that slope categories are grouped for visual clarity.

3.6.1 Directly Connected Impervious Area

The HRU approach not only highlights the predominant composition of an area within the catchment but also provides additional texture and physical basis for parameterizing and representing natural processes. Within a given modeled catchment, HRU segments are modeled as being parallel to one another. Each HRU segment flows directly to the routing stream segment without any interaction with neighboring HRU segments. However, in the physical environment, the lines between impervious and pervious land are not as clearly distinguished—impervious land may flow downhill over pervious land on route to a storm drain or watercourse.

For modeling purposes, Effective Impervious Area (EIA) represents the portion of the total, or Mapped Impervious Area (MIA), that routes directly to the stream segments. It is derived as a function of the percent Directly Connected Impervious Area (DCIA), with other adjustments as needed to account for other structural and non-structural management practices in the flow network. Figure 3-11 illustrates the transitional sequence from MIA to DCIA. Impervious areas that are not connected to the drainage network can flow onto pervious surfaces, infiltrate, and become part of the pervious subsurface and overland flow. Because segments are modeled as being parallel to one another in LSPC, this process can be approximated using a conversion of a portion of impervious land to pervious land. On the open landscape, runoff from disconnected impervious surfaces can overwhelm the infiltration capacity of adjacent pervious surfaces during large rainfall/runoff events creating sheet flow over the landscape—therefore, the MIA→EIA translation is not actually a direct linear conversion. Finding the right balance between MIA and EIA can be an important part of the hydrology calibration effort.

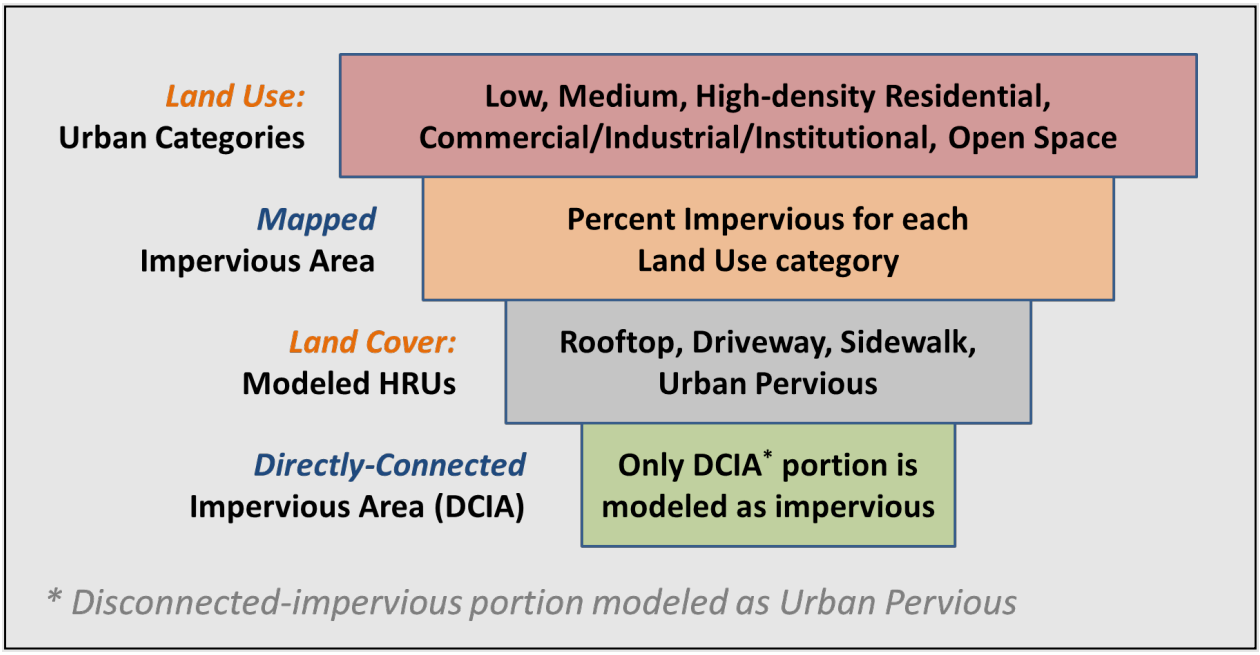

Figure 3-11. Generalized translation sequence from MIA to DCIA.

Empirical relationships like the Sutherland Equations (Sutherland, 2000) presented in Figure 3-12 show a strong correlation between the *density* of developed areas and DCIA. The curve for high-density developed land trends closer to the line of equal value than the curve for less developed areas. Similarly, as the density of the mapped impervious area approaches 100%, the translation to DCIA also approaches 100%. An initial estimate of EIA is equal to MIA × DCIA. This empirical approximation can be further refined during model calibration to account for other flow disconnections resulting from structural or non-structural Best Management Practices (BMPs) or other inline hydraulic routing features.

For the Salmon Creek watershed, each developed land cover category was assigned a DCIA curve as shown in Table 3-. The MIA, which is the impervious portion of each grid, was converted to EIA areas using these equations. Sutherland (2000) notes that areas with less than 1% MIA effectively behave like 100% pervious areas; therefore, EIA adjustments were only applicable to "Developed" areas. Table 3-9 is a summary of resampled MIA and calculated EIA by the land cover groups.

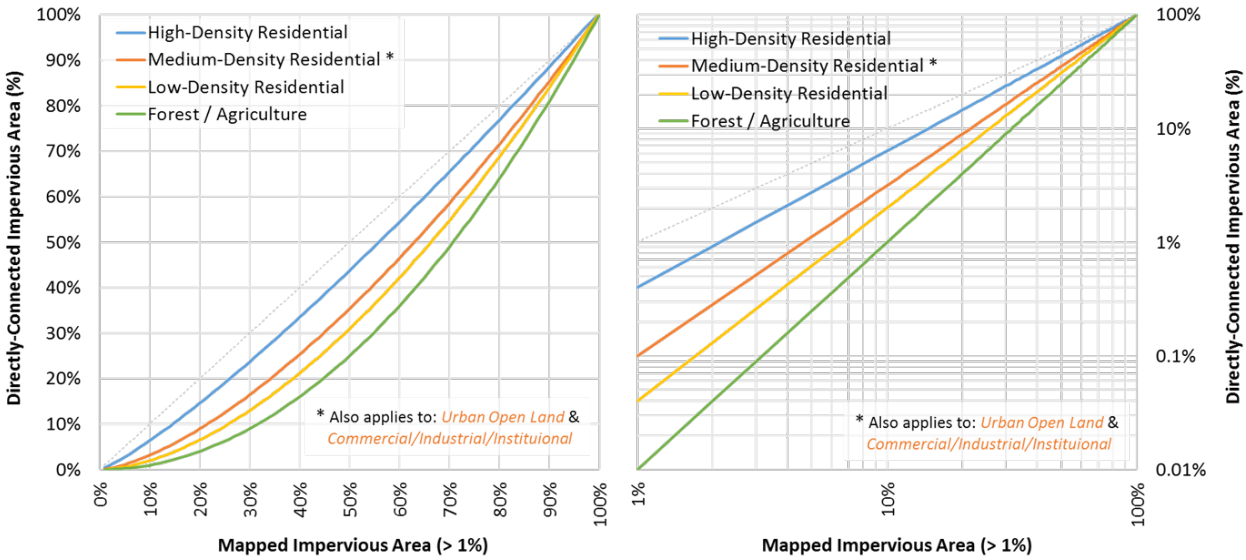

Figure 3-12. Mapped and directly connected impervious area relationships (Sutherland, 2000).

Table 3-8. Assignment of DCIA curves by land cover category

Land Cover	MIA	EIA	EIA:MIA	Equation
High Density Developed	86.78%	84.76%	98%	$DCIA=0.4(MIA)^{1.2}$
Medium Density Developed	60.23%	46.76%	78%	$DCIA=0.1(MIA)^{1.5}$
Low Density Developed	31.80%	14.37%	45%	$DCIA=0.04(MIA)^{1.7}$
Open Space	3.41%	0.13%	4%	$DCIA=0.01(MIA)^{2.0}$
Undeveloped*	0.00%	0.00%	0%	DCIA=0

* Assume no DCIA (100% disconnection, EIA = 0)

Color Gradient:	Lowest	Low	Medium	High	Highest

Table 3-9. Distribution of impervious area by grouped NLCD land cover class

Model Group	Total Area		Impervious (acre)		Impervious (%)	
	Acre	%	MIA	EIA	MIA	EIA
Developed_Low_Intensity	127.2	0.57%	40.45	18.28	31.8%	14.4%
Developed_Medium_Intensity	36.0	0.16%	21.70	16.84	60.2%	46.8%
Developed_High_Intensity	4.0	0.02%	3.47	3.39	86.8%	84.8%
Developed_Open_Space	1,048.8	4.68%	35.75	1.39	3.4%	0.1%
Barren	0.7	0.00%	0.00	0.00	0.0%	0.0%
Forest (Deciduous)	91.4	0.41%	0.00	0.00	0.0%	0.0%
Forest (Evergreen)	9,045.7	40.39%	0.00	0.00	0.0%	0.0%
Forest (Mixed)	1,336.1	5.97%	0.00	0.00	0.0%	0.0%
Scrub	5,753.3	25.69%	0.00	0.00	0.0%	0.0%
Grassland (Herbaceous)	2,068.3	9.24%	0.00	0.00	0.0%	0.0%
Pasture	1,870.6	8.35%	0.00	0.00	0.0%	0.0%
Agriculture	617.1	2.76%	0.05	0.00	0.0%	0.0%
Forest (Woody Wetlands)	161.2	0.72%	0.00	0.00	0.0%	0.0%
Grassland (Herbaceous Wetland)	211.1	0.94%	0.00	0.00	0.0%	0.0%
Water	24.2	0.11%	0.00	0.00	0.0%	0.0%
Total	**22,396**	**100%**	**101**	**40**	**--**	**--**

Color gradients indicate model groups with more Watershed Area and Imperviousness, respectively.

3.6.2 Modeled HRU Categories

The combinations of LULC, HSG, and slope represent the physical characteristics that influence hydrology. After accounting for DCIA, the four developed land cover classes were rolled up as either a single "Developed Impervious" category or "Developed Pervious," stratified by HSG and slope. Agriculture HRUs (i.e., 4 HSGs × 3 slopes = 12 combinations) were further divided into irrigated and non-irrigated counterparts for a total of 24 HRUs. Altogether, a total of 98 HRU categories comprised the basic building blocks used in LSPC to represent hydrologic responses in the watershed. The "Agriculture" HRU areas within catchments where streamflow was withdrawn for irrigation were re-assigned to their "Irrigation" HRU counterparts. Irrigation was simulated for those HRUs as described in Section 5.1. The final HRU distribution in the watershed is shown in Table 3-10.

Table 3-10. Modeled HRU distribution within the Salmon Creek watershed

HRU ID	Land Use - Land Cover	HSG	Slope	Area	
				Acre	%
1000	Developed_Impervious	All	All	39.908	0.2%
2110	Developed_Pervious	A	Low	7.376	0.0%
2120	Developed_Pervious	A	Med	11.513	0.1%
2130	Developed_Pervious	A	High	2.324	0.0%
2210	Developed_Pervious	B	Low	36.902	0.2%
2220	Developed_Pervious	B	Med	121.818	0.5%
2230	Developed_Pervious	B	High	116.210	0.5%

HRU ID	Land Use - Land Cover	HSG	Slope	Area	
				Acre	%
2310	Developed_Pervious	C	Low	143.637	0.6%
2320	Developed_Pervious	C	Med	364.667	1.6%
2330	Developed_Pervious	C	High	312.989	1.4%
2410	Developed_Pervious	D	Low	14.321	0.1%
2420	Developed_Pervious	D	Med	29.379	0.1%
2430	Developed_Pervious	D	High	15.007	0.1%
3110	Barren	A	Low	0.000	0.0%
3120	Barren	A	Med	0.000	0.0%
3130	Barren	A	High	0.000	0.0%
3210	Barren	B	Low	0.000	0.0%
3220	Barren	B	Med	0.000	0.0%
3230	Barren	B	High	0.000	0.0%
3310	Barren	C	Low	0.000	0.0%
3320	Barren	C	Med	0.000	0.0%
3330	Barren	C	High	0.000	0.0%
3410	Barren	D	Low	0.222	0.0%
3420	Barren	D	Med	0.222	0.0%
3430	Barren	D	High	0.222	0.0%
4110	Forest	A	Low	20.238	0.1%
4120	Forest	A	Med	9.118	0.0%
4130	Forest	A	High	6.449	0.0%
4210	Forest	B	Low	47.815	0.2%
4220	Forest	B	Med	323.361	1.4%
4230	Forest	B	High	2,968.514	13.3%
4310	Forest	C	Low	171.466	0.8%
4320	Forest	C	Med	994.768	4.4%
4330	Forest	C	High	5,732.204	25.6%
4410	Forest	D	Low	10.453	0.0%
4420	Forest	D	Med	33.581	0.1%
4430	Forest	D	High	316.467	1.4%
5110	Scrub	A	Low	7.561	0.0%
5120	Scrub	A	Med	9.341	0.0%
5130	Scrub	A	High	6.894	0.0%
5210	Scrub	B	Low	96.074	0.4%
5220	Scrub	B	Med	372.732	1.7%
5230	Scrub	B	High	504.612	2.3%
5310	Scrub	C	Low	210.607	0.9%
5320	Scrub	C	Med	953.625	4.3%
5330	Scrub	C	High	2,765.469	12.3%

HRU ID	Land Use - Land Cover	HSG	Slope	Area	
				Acre	%
5410	Scrub	D	Low	19.348	0.1%
5420	Scrub	D	Med	203.046	0.9%
5430	Scrub	D	High	604.022	2.7%
6110	Grassland	A	Low	68.053	0.3%
6120	Grassland	A	Med	9.785	0.0%
6130	Grassland	A	High	2.002	0.0%
6210	Grassland	B	Low	89.625	0.4%
6220	Grassland	B	Med	181.918	0.8%
6230	Grassland	B	High	158.122	0.7%
6310	Grassland	C	Low	306.014	1.4%
6320	Grassland	C	Med	457.909	2.0%
6330	Grassland	C	High	809.292	3.6%
6410	Grassland	D	Low	30.913	0.1%
6420	Grassland	D	Med	27.799	0.1%
6430	Grassland	D	High	137.884	0.6%
7110	Pasture	A	Low	36.028	0.2%
7120	Pasture	A	Med	10.008	0.0%
7130	Pasture	A	High	1.334	0.0%
7210	Pasture	B	Low	145.890	0.7%
7220	Pasture	B	Med	425.884	1.9%
7230	Pasture	B	High	107.194	0.5%
7310	Pasture	C	Low	241.520	1.1%
7320	Pasture	C	Med	349.159	1.6%
7330	Pasture	C	High	488.600	2.2%
7410	Pasture	D	Low	3.114	0.0%
7420	Pasture	D	Med	32.025	0.1%
7430	Pasture	D	High	29.801	0.1%
8110	Agriculture	A	Low	5.860	0.0%
8120	Agriculture	A	Med	0.756	0.0%
8130	Agriculture	A	High	0.000	0.0%
8210	Agriculture	B	Low	33.871	0.2%
8220	Agriculture	B	Med	64.105	0.3%
8230	Agriculture	B	High	27.121	0.1%
8310	Agriculture	C	Low	54.442	0.2%
8320	Agriculture	C	Med	188.090	0.8%
8330	Agriculture	C	High	157.088	0.7%
8410	Agriculture	D	Low	1.112	0.0%
8420	Agriculture	D	Med	4.492	0.0%
8430	Agriculture	D	High	18.859	0.1%

HRU ID	Land Use - Land Cover	HSG	Slope	Area	
				Acre	%
9000	Water	All	All	24.241	0.1%
10110	Irrigation	A	Low	1.034	0.0%
10120	Irrigation	A	Med	0.133	0.0%
10130	Irrigation	A	High	0.000	0.0%
10210	Irrigation	B	Low	4.604	0.0%
10220	Irrigation	B	Med	7.506	0.0%
10230	Irrigation	B	High	2.902	0.0%
10310	Irrigation	C	Low	5.604	0.0%
10320	Irrigation	C	Med	21.183	0.1%
10330	Irrigation	C	High	16.379	0.1%
10410	Irrigation	D	Low	0.000	0.0%
10420	Irrigation	D	Med	0.400	0.0%
10430	Irrigation	D	High	1.601	0.0%
			Total	**22,396**	**100%**

Color Gradient: Lowest | Low | Med | High | Highest

4 CLIMATE FORCING INPUTS

The only USGS flow station 11460920 within the Salmon Watershed has flow data available from August 1, 1962, to October 1, 1975. Additionally, the only precipitation station (see, Table 4-1) located within the watershed has historical data dating back to the 1960s, with a complete dataset available from January 1, 1960, to December 31, 1969, compared to the observed flow data. As a result, the climate data inputs for this watershed were developed for two periods: the historical period from 1960 to 1969 and the more recent period from the water years 2004 to 2023.

The Salmon Creek watershed LSPC model uses hourly climate data forcing inputs to drive the hydrology module. In general, hydrologic models are highly dependent on the quantity and quality of meteorological input data (Quirmbach and Schultz, 2002). Conventionally, meteorological boundary conditions for stormwater modeling rely on ground-based stations across an area; however, challenges arise when trying to associate point-sampled weather station data over complex and/or large terrain (Henn et al., 2018). Model representation of precipitation in regions with low station density is susceptible to distortion when using linearized downscaling methods (e.g., Thiessen polygons).

The hybrid approach supplements spatial and temporal gaps in observed meteorological data with gridded meteorological products from the Parameter-elevation Regressions on Independent Slopes Model (PRISM) and North American Land Data Assimilation System-2 (NLDAS). NLDAS and PRISM are Land Surface Model (LSM) datasets with 1/8th degree and 4-km spatial resolution, respectively, which are ideal for supplementing spatial gaps in the observed station network as well as patching missing or erroneous temporal gaps in the observed time series data. The use of a hybrid approach that blends ground-based stations with remotely sensed precipitation products, i.e., increasing the rainfall gauge density over the watershed, has been shown to improve the representation of rainfall and increase forecast accuracy more than using ground-based stations alone (Kim et al., 2018; Looper and Vieux, 2012; Xia et al., 2012a, 2012b). This approach has been applied for large watershed-scale modeling applications in Los Angeles County (LACFCD, 2020).

Potential evapotranspiration (PEVT) is another critical forcing input for hydrology simulation. Section 4.2 describes how PEVT was derived for this modeling effort.

4.1 Precipitation

Figure 4-1 presents a summary of the hybrid approach to blend observed precipitation with gridded meteorological products. Observed data and gridded products were processed in parallel (1) to identify the highest quality gauge data and (2) to merge gridded products to produce continuous hourly time series. Gridded products were used to fill spatial and temporal gaps in the observed precipitation coverage. The final coverage shown in Figure 4-2 comprises the highest quality observed time series, supplemented by gridded products only where spatial and temporal gaps occurred in the observed coverage. The parallel processing of observed and gridded precipitation is presented in Section 4.1.1. Section 4.1.2 describes how those outputs were synthesized into the model's final set of precipitation time series.

f

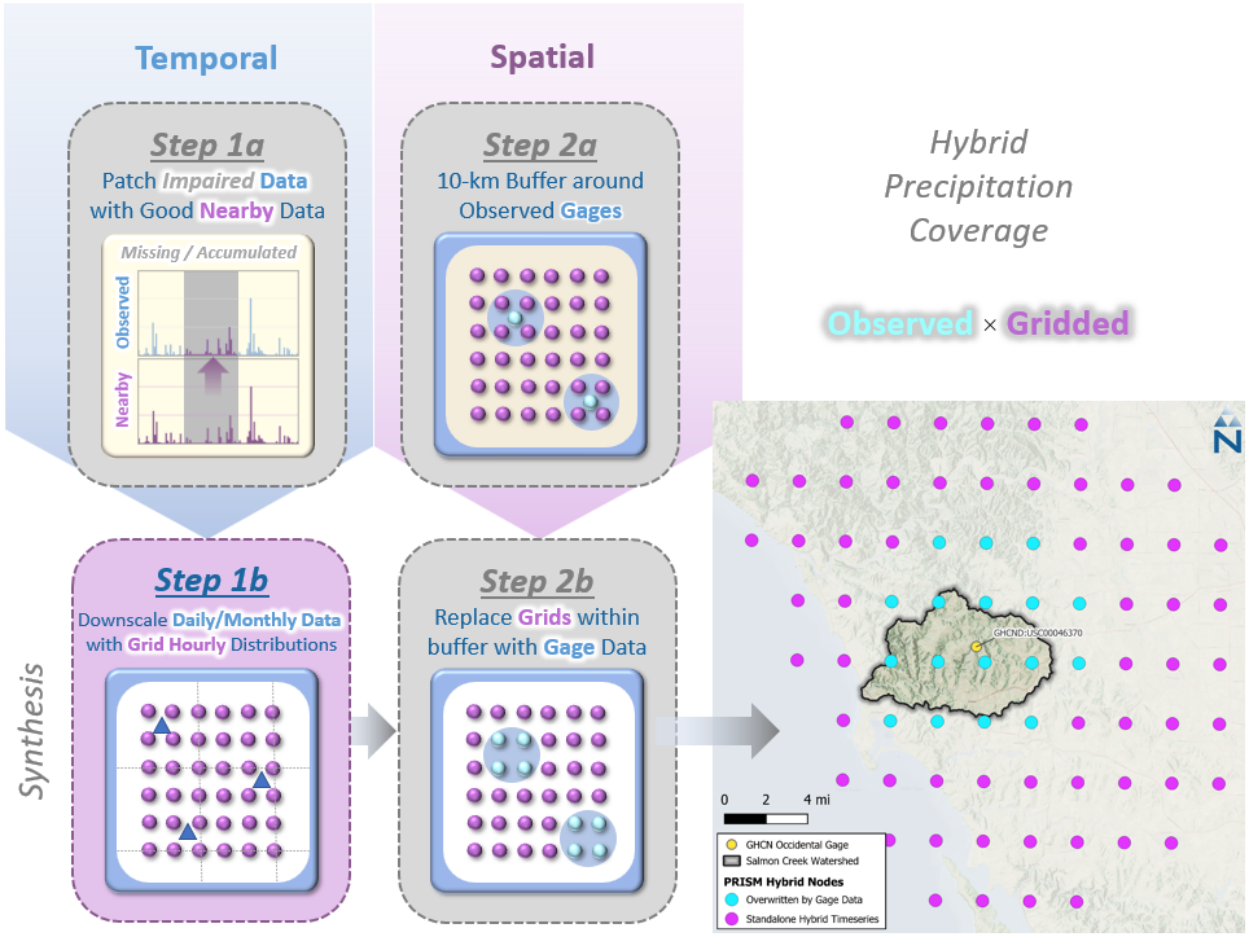

Figure 4-1. Hybrid approach to blend observed precipitation with gridded meteorological products.

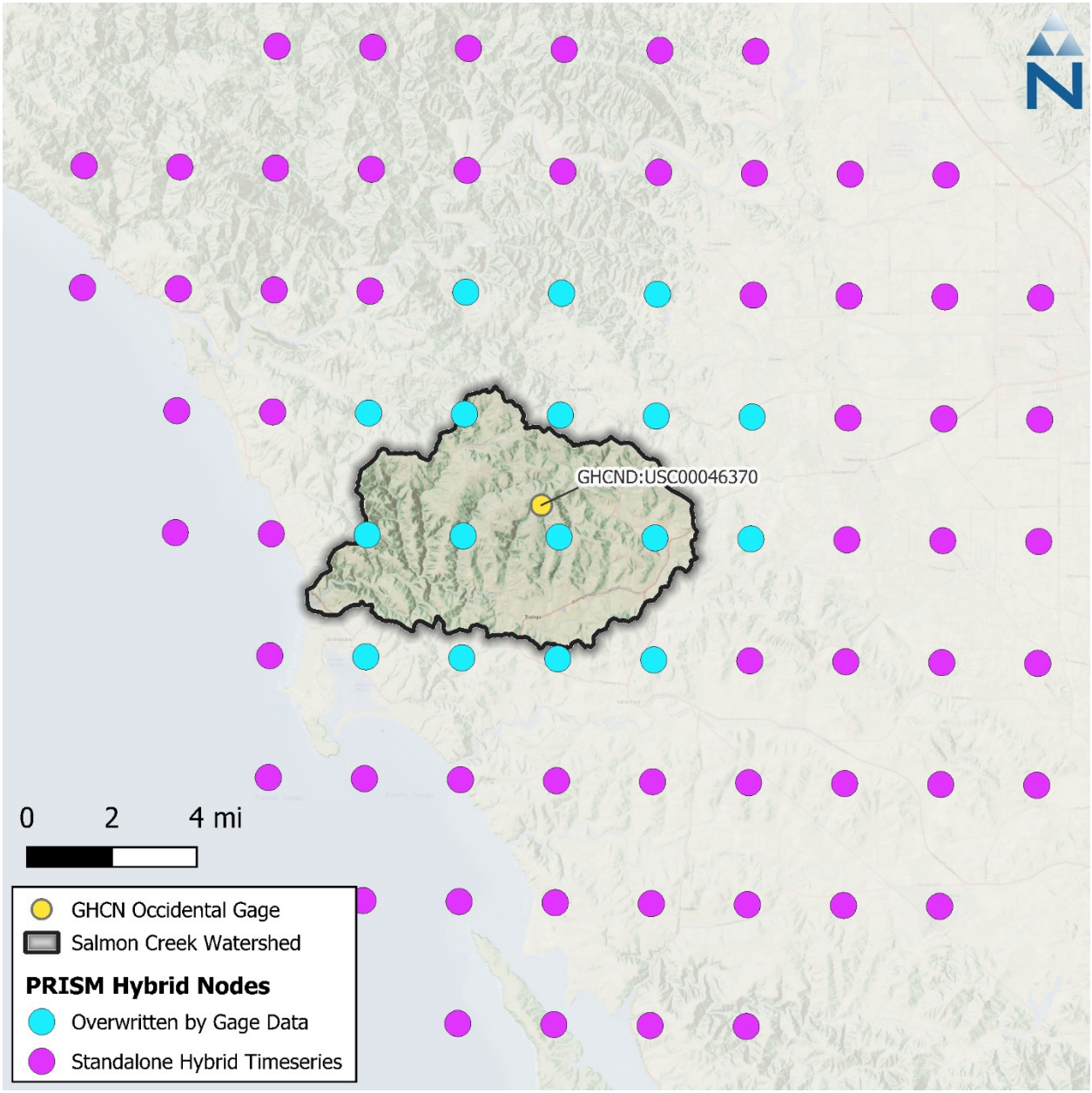

Figure 4-2. Spatial coverage of PRISM nodes by hybrid data source.

4.1.1 Parallel Processing of Observed Data and Gridded Products

Observations from one precipitation gauge, summarized in Table 4-1, were processed for use in the hybrid precipitation time series. This station reports daily precipitation totals, which were disaggregated to hourly based on the distribution of the nearest NLDAS grid cell, while maintaining observed daily totals. The station is from the Global Historical Climatology Network Daily (GHCND) database which is operated by The National Ocean and Atmospheric Association (NOAA). The relationship between the annual average total precipitation and elevation for this station is shown in Figure 4-3. The Salmon Creek work plan had additional precipitation gauges listed, however those stations were dropped from further use as either duplicates or were outside of the 10km buffer used to create hybrid time series.

Table 4-1. Precipitation station used to develop hybrid precipitation time series

Agency	Station ID[1]	Name	Start Date	End Date	Lat.	Long.	Elevation (meters)	Data Coverage (%)[2]
NOAA-GHCN	GHCND:USC00046370	OCCIDENTAL, CA US	4/30/1943	4/5/2021	38.3858	-122.9661	263.7	92%

[1] Stations presented have at least 90% data coverage.

[2] NOAA data coverage as reported.

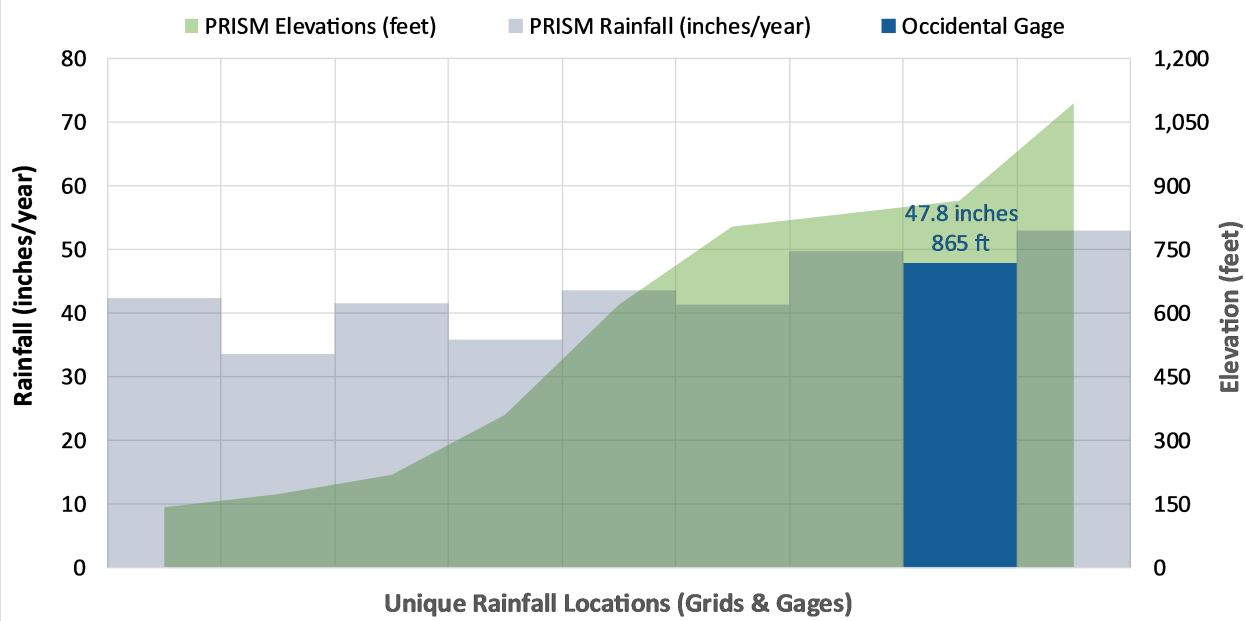

Figure 4-3. Annual average precipitation totals and elevation of selected precipitation stations.

The gridded meteorological products were processed in parallel with the observed data and used to patch spatial and temporal gaps in the observed data record. PRISM monthly precipitation time series data are available at a 4-km spatial resolution across the conterminous United States (Daly et al., 1997, 1994; Gibson et al., 2002). PRISM combines point data and spatial datasets (primarily DEMs) via statistical methods to generate estimates of annual, monthly, and event-based precipitation in a gridded format from as early as 1961 (Daly et al., 2000). PRISM has undergone several iterations of refinement, extensive peer review, and performance validation through case study applications.

NLDAS is a quality-controlled meteorological dataset designed specifically to support continuous simulation modeling activities (Cosgrove et al., 2003; Mitchell et al., 2004). NLDAS provides hourly predictions of meteorological data at a 1/8th degree spatial resolution for North America (approximately 8.6-mile intervals), with retrospective simulations beginning in January 1979. For this model, hourly NLDAS precipitation distributions were mapped to the nearest PRISM grid cell and used to disaggregate the monthly PRISM totals to hourly—the resulting set of gridded precipitation time series reflects monthly PRISM totals that have hourly distributions from the nearest NLDAS grid. Using monthly PRISM totals with hourly NLDAS, as opposed to daily PRISM totals, eliminates the need to estimate distributions for occasional but rare instances where an hourly distribution does not coincide with a daily total.

Since NLDAS hourly data were unavailable before January 1979, hourly observed precipitation data from another station from 1960 to 1969 were used to disaggregate the observed daily precipitation data patched with PRISM monthly precipitation for those periods. The hourly precipitation data were obtained from the San Francisco International Airport NOAA station (WBAN:23234), which is the closest station with hourly precipitation records dating back to the 1960s.

4.1.2 Synthesis of Observed Data and Gridded Products

Where available, observed precipitation data were preferentially selected over gridded data where data quantity and quality were adequate. Impaired intervals are gaps in the observed record flagged as missing, deleted, or accumulated rainfall. Gridded time series are used to patch impaired intervals as follows. First, a 10-km buffer was created around the Occidental GHCND station—had there been

more gauges, this would have been done for each of the observed gauges that were prescreened for quality. Next, the 10-km gauge buffer was intersected with the PRISM grid layer. The time series at any grid falling within the buffer is overridden by the associated observed gauge time series, except for impaired intervals, where the gridded data are retained to patch those temporal impairments. Consequently, most of the observed data at a PRISM grid location was identical to a neighboring grid within a 10-km buffer of the gauge but will have slightly different PRISM time series for impaired intervals. The available daily observed precipitation data from the Occidental GHCND station ended on 4/5/2021. Therefore, the period from 4/6/2021 to 12/31/2023 was considered an impaired interval and was patched using a gridded time series following the steps outlined above.

After the creation of the hybrid precipitation time series, each catchment is assigned a time series based on the Thiessen polygon its centroid falls within. Figure 4-4 illustrates the final assignment of gauge-based or LSM-based hybrid time series by catchment. Figure 4-5 and Figure 4-6 show the distribution of monthly total precipitation across all hybrid time series within the watershed. The graphs suggest that the distribution of monthly rainfall totals has become more extreme between 2004-2024 compared to 1960-1969, with lower lows and higher highs. Figure 4-7 illustrates the spatial distribution of annual average precipitation from the hybrid time series by catchment. The color gradient suggests a more dramatic variation; however, it should be noted that annual average rainfall varies between 45 and 50 inches per year. There is a slight increase in annual rainfall volume between the southern and northern portions of the watershed.

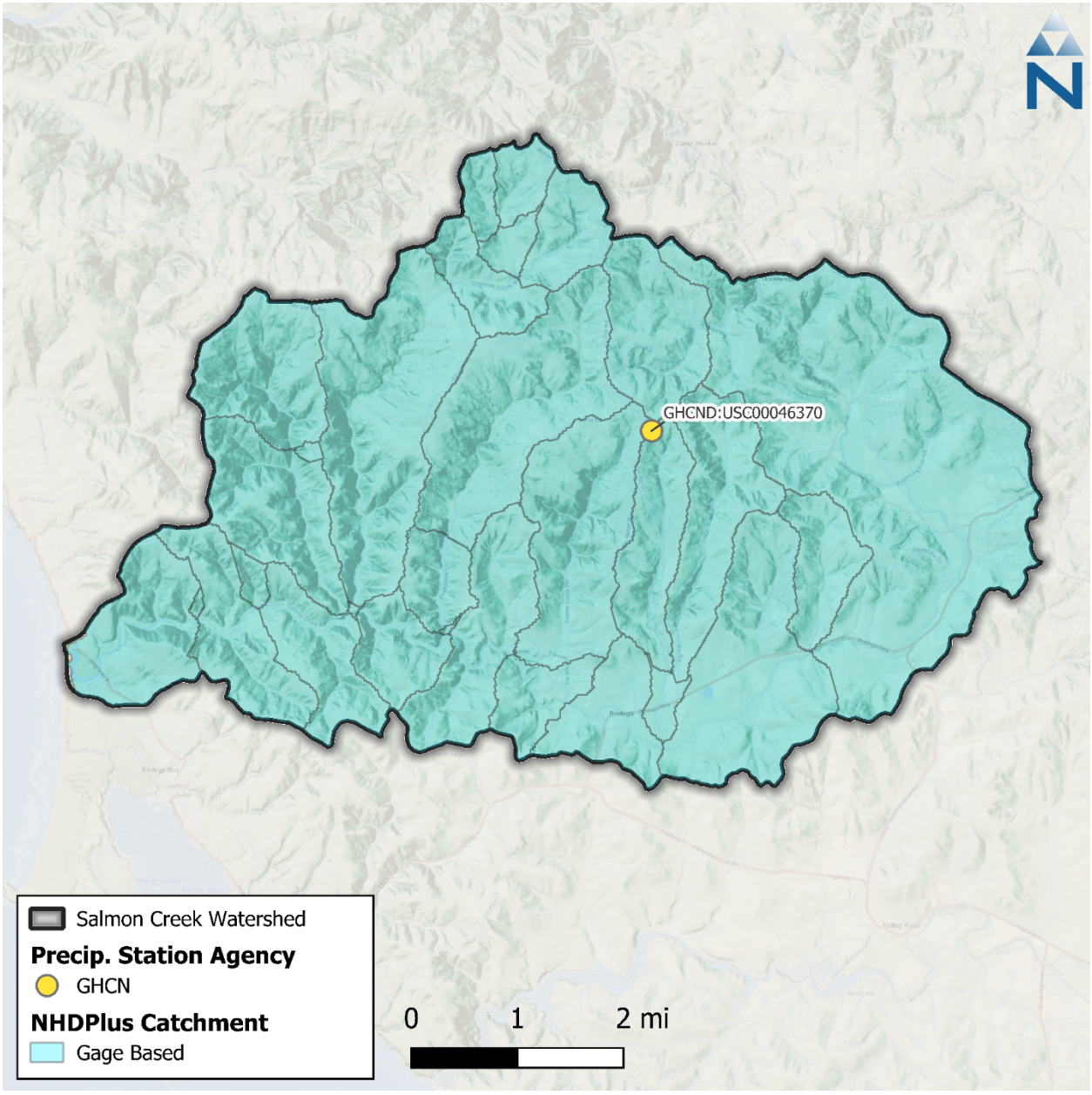

Figure 4-4. Final spatial coverage of precipitation time series by catchment.

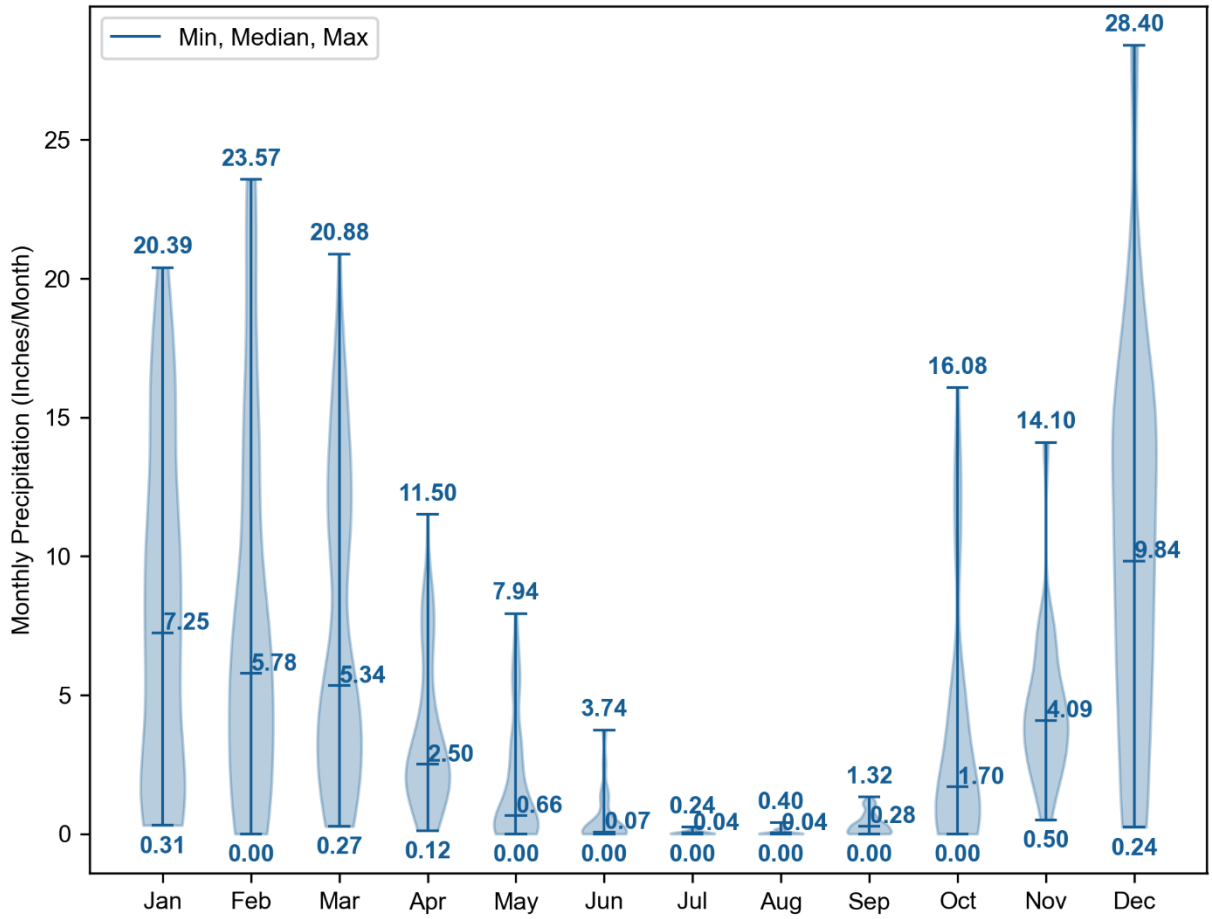

Figure 4-5. Distribution of monthly total precipitation across all hybrid time series within the Salmon Creek watershed for Water Years 2004-2023.

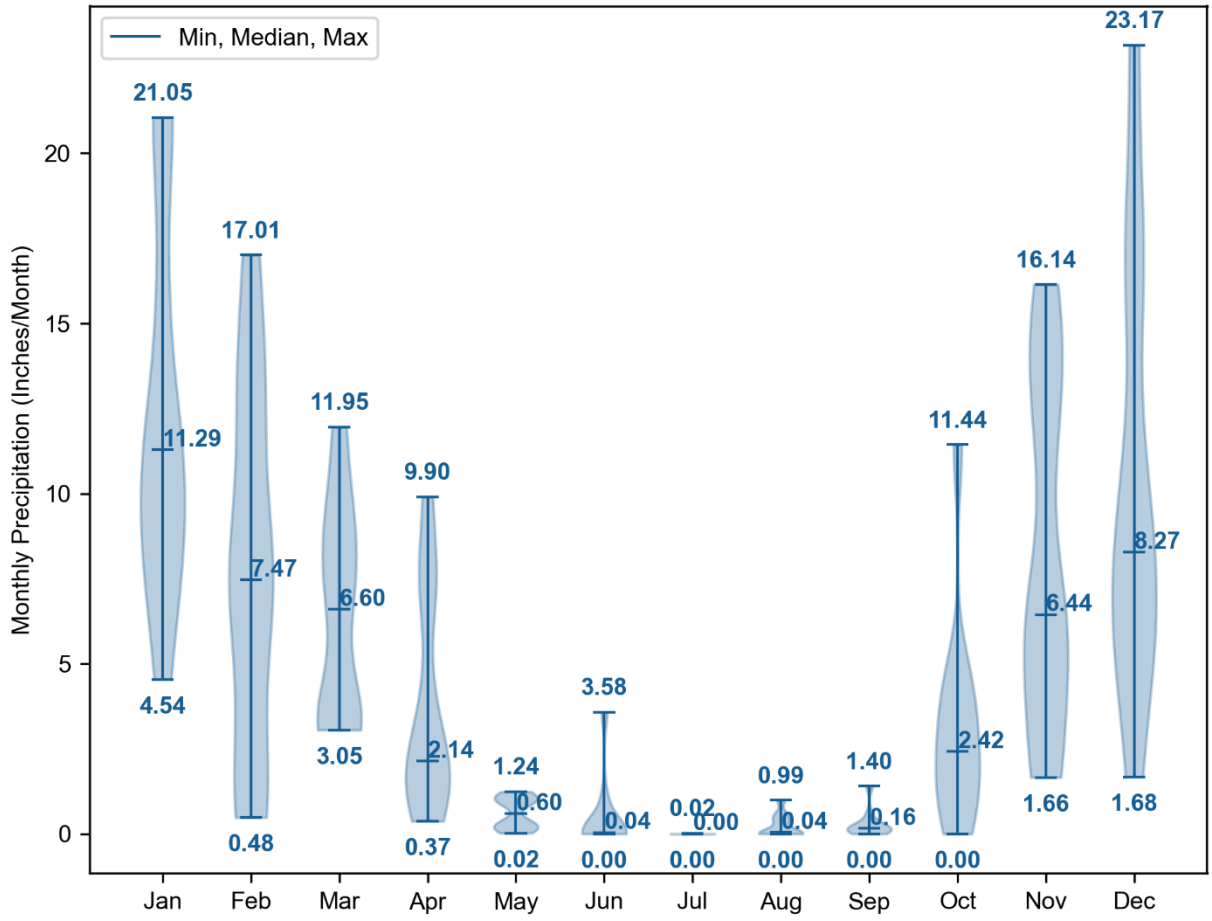

Figure 4-6. Distribution of monthly total precipitation across all hybrid time series within the Salmon Creek watershed for Years 1960-1969.

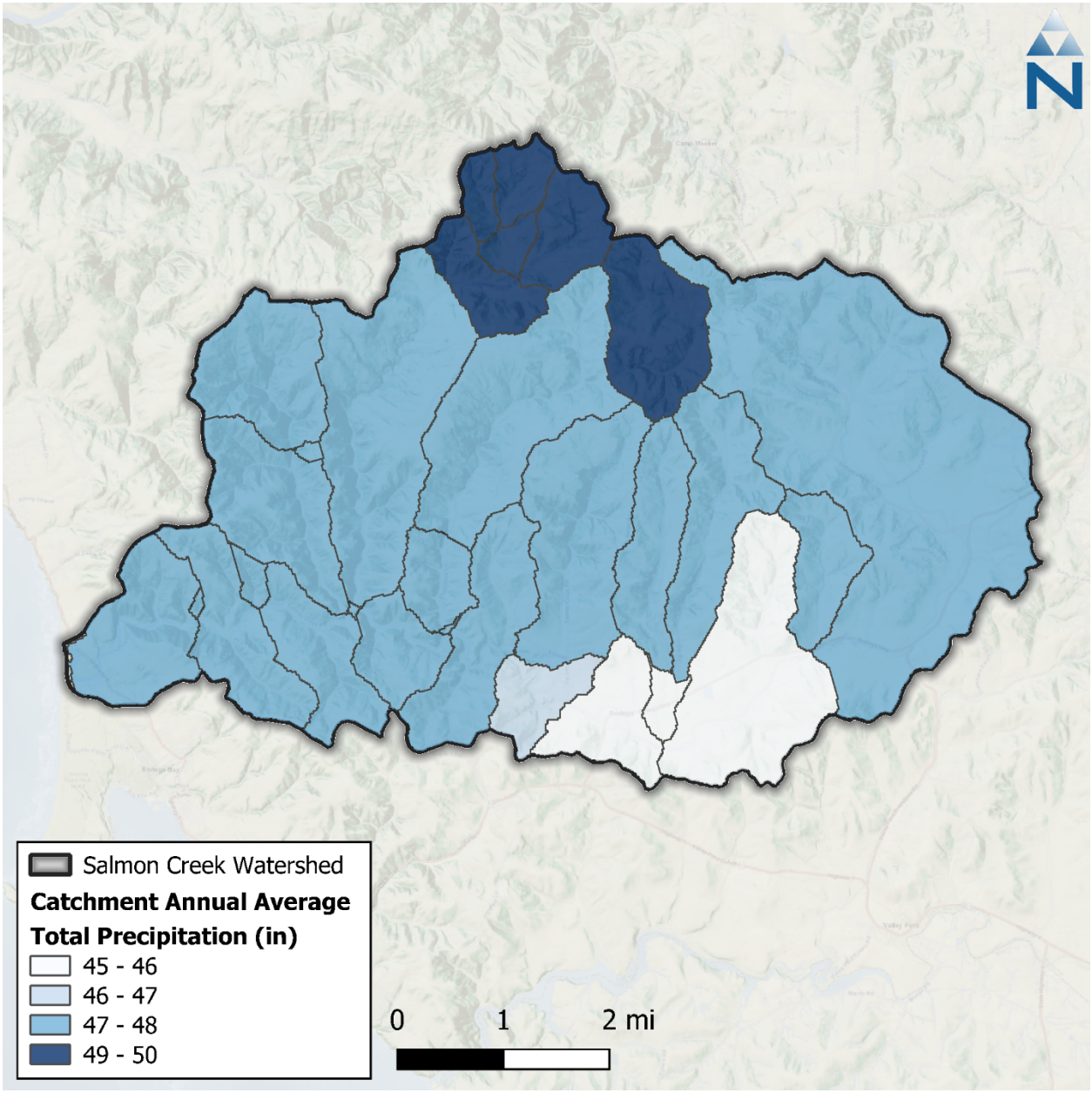

Figure 4-7. Annual average hybrid precipitation totals by catchment from 2000-2023.

4.2 Potential Evapotranspiration

In addition to precipitation, potential evapotranspiration forcing input time series were created and assigned to each catchment. Daily total reference evapotranspiration (ET_o) from the California Irrigation Management Information System (CIMIS) Spatial dataset was downscaled to hourly using the NLDAS hourly solar radiation. CIMIS Spatial expresses daily ET_o estimates calculated at a statewide 2-km spatial resolution using the American Society of Civil Engineers version of the Penman-Monteith equation (ASCE-PM). This product provides a consistent spatial estimate of ET_o that is California-specific, implicitly captures macro-scale spatial variability and orographic influences, is available from 2004 through the Present, and is routinely updated. Within each catchment, actual ET is calculated for each Hydrologic Response Unit (HRU) during the model simulation as a function

of parameters representing differences in vegetation (type, height, and density) and soil conditions. Figure 4-8 and Figure 4-9 show the distribution of monthly total ET_o across all grid points within the watershed. Figure 4-10 shows the spatial distribution of CIMIS annual average total ET_o across the watershed. The color gradient suggests a more dramatic variation; however, it should be noted that annual average potential evaporation rainfall varies between 38 and 41 inches per year. There is a slight increase in annual potential evapotranspiration traveling from west to east in the watershed.

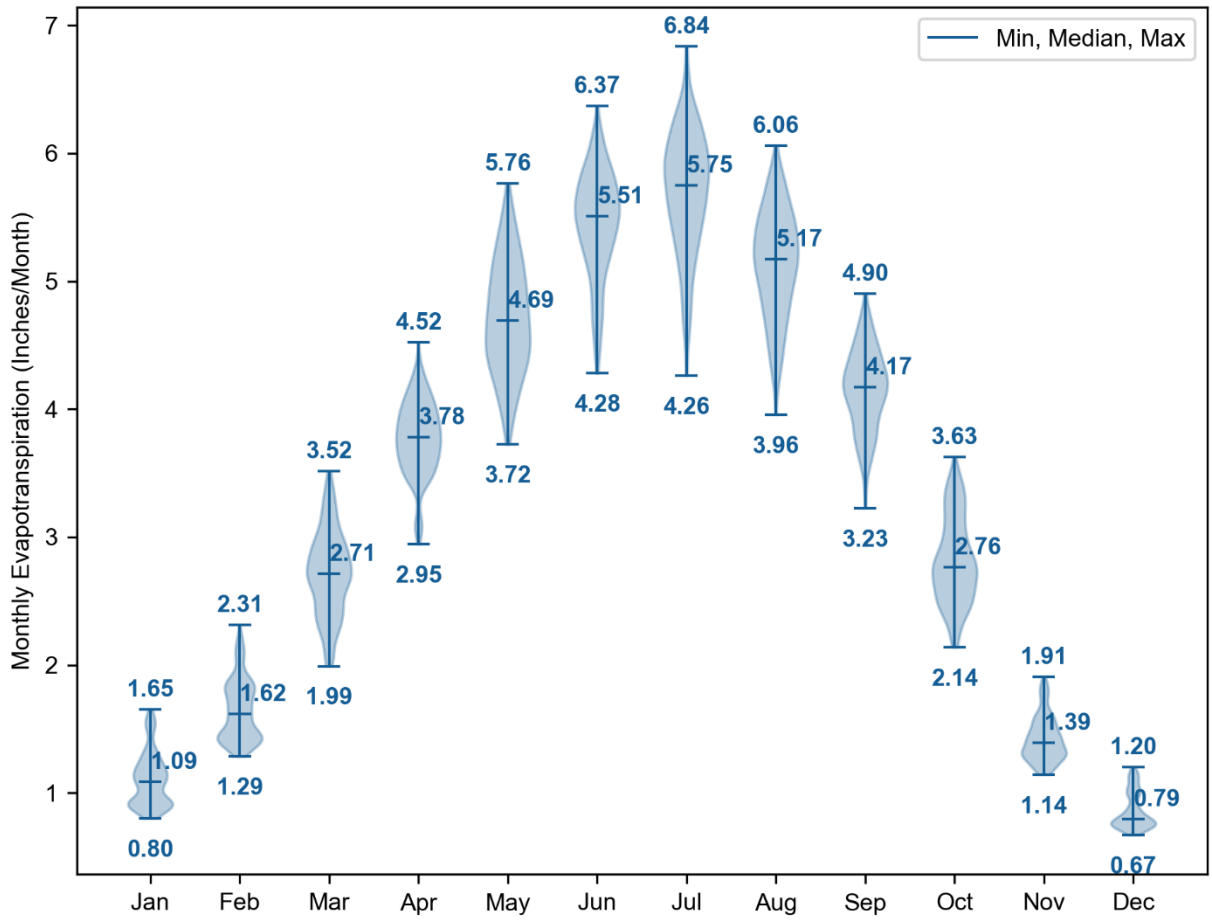

Figure 4-8. Distribution of monthly total ET_o across all CIMIS spatial grid points within the Salmon Creek watershed for Water Years 2004 to 2023.

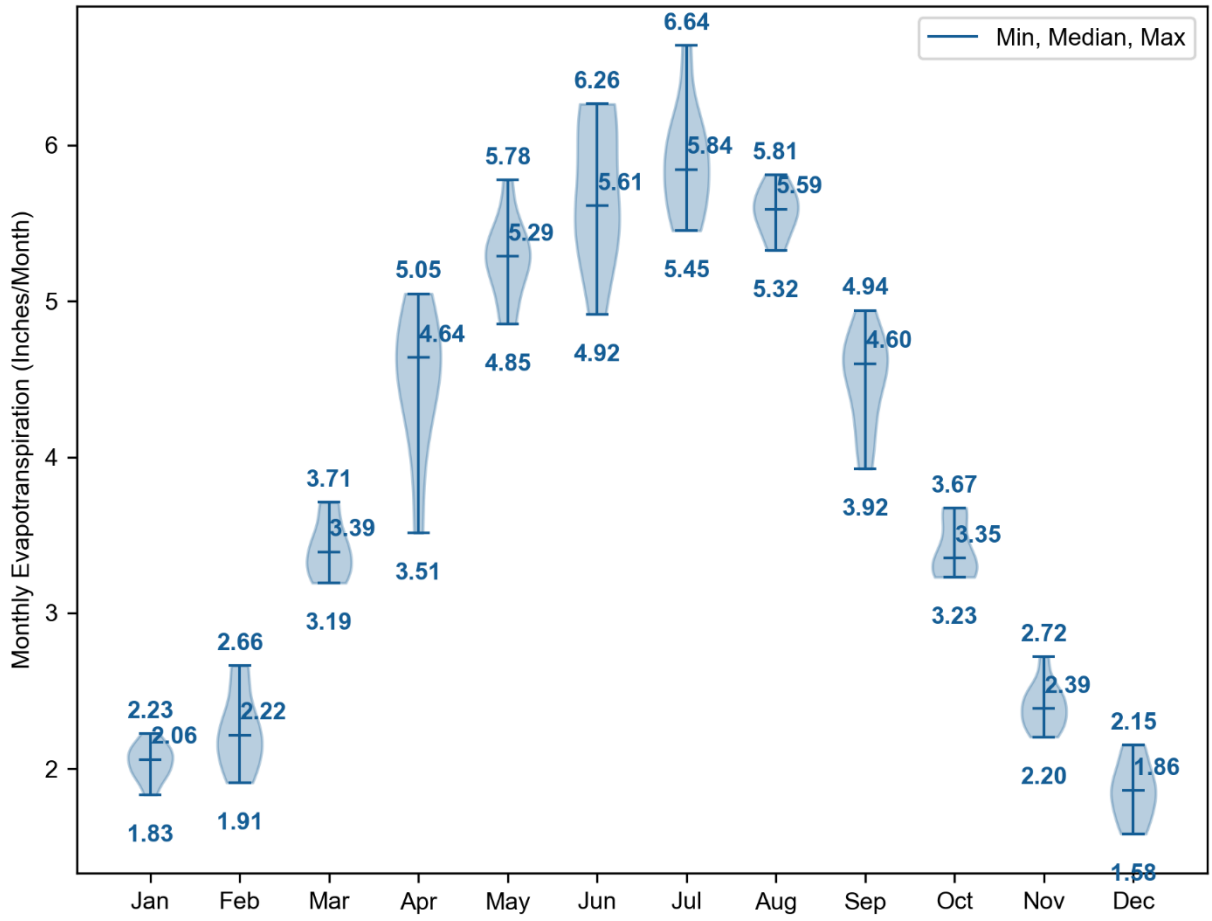

Figure 4-9. Distribution of monthly total ET_o across all CIMIS spatial grid points within the Salmon Creek watershed for Years 1960 to 1969

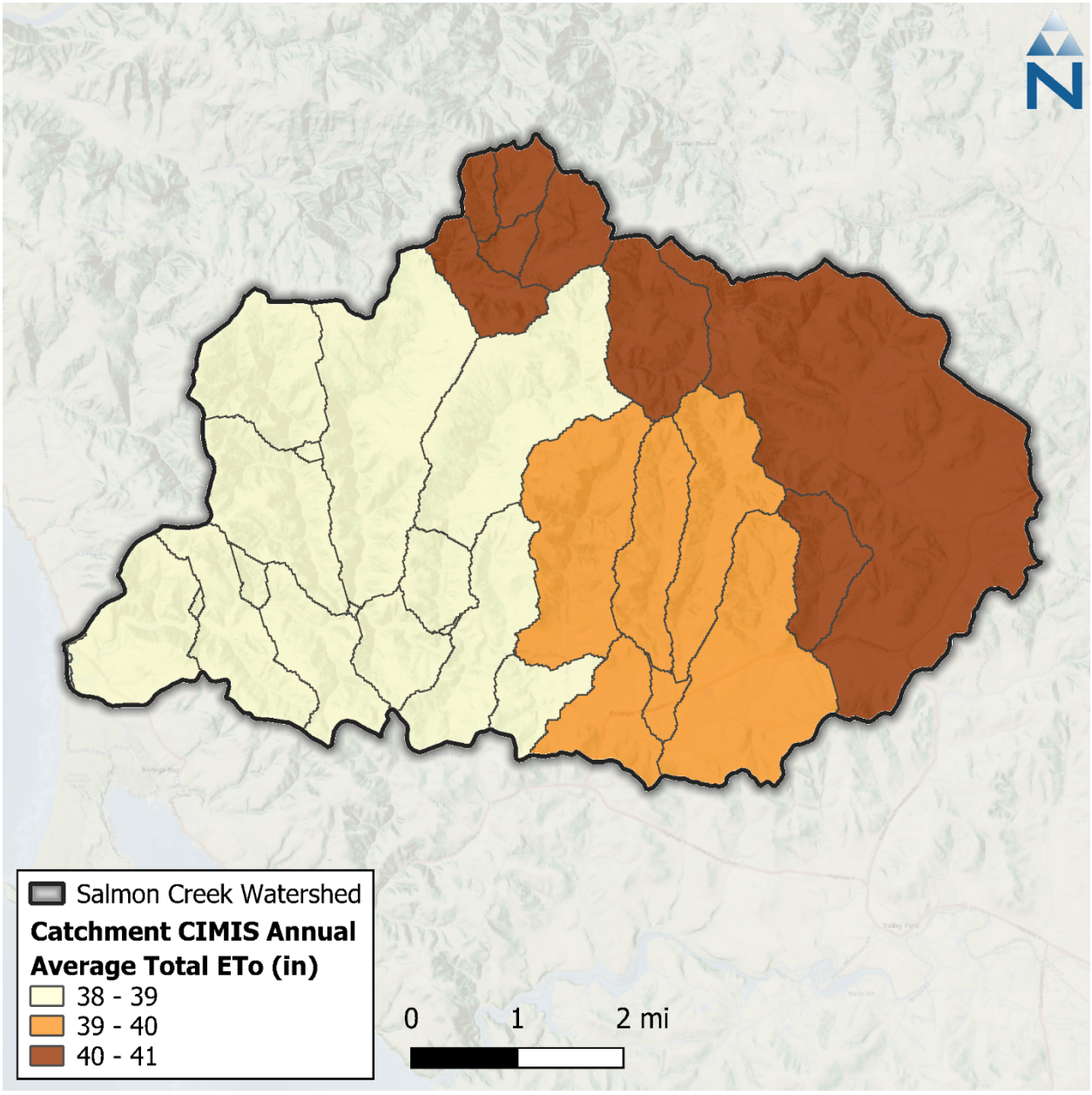

Figure 4-10. CIMIS annual average total ET_o by catchment within the Salmon Creek watershed

Due to the unavailability of NLDAS hourly data prior to January 1979, potential evapotranspiration for the years 1960 to 1969 was calculated using ground-measured daily temperatures and the Hamon formula. First, daily maximum and minimum temperatures were obtained from the GHCND station, USC00043578 Graton. For missing values, measurements from a nearby GHCND station, USC00047965 Santa Rosa, were used, adjusting those values based on the monthly average ratio between Graton and Santa Rosa. Next, daily potential evapotranspiration was determined using the Hamon method, which requires daily average temperature and daylight length (see Equations 2, 3, and 4).

$$PEVT = 0.165 \times 216.7 \times \frac{N}{12} \times \left(\frac{e_s}{T + 273.3}\right) \quad \text{Equation 2}$$

$$e_s = 6.108e^{\left(\frac{17.27T}{T+237.3}\right)} \quad \text{Equation 3}$$

$$PT = \frac{T_{max} + T_{min}}{2} \quad \text{Equation 4}$$

Where PEVT is the potential evapotranspiration (mm/day), N is the daytime length (hrs), e_s is the saturation vapor pressure (mb), T is the average daily temperature (°C), T_{max} is the daily maximum temperature (°C), and T_{min} is the daily minimum temperature (°C). Daylight hours were estimated following the approach outlined in the Qual2K model (Chapra et al., 2008). Finally, the hourly PEVT was adjusted to ensure that the monthly averages aligned with CIMIS Zone 4 reference ET_o values.

5 SURFACE WATER WITHDRAWS

Datasets related to water rights, points of diversion (PODs), and irrigation use were identified through the Water Board's eWRIMS database and a University of California Cooperative Extension (UCCE) study assessing agricultural water needs in the nearby the Navarro River and Russian River watersheds (McGourty et al. 2020). These data were used to represent diversions and withdraws in the watershed model. Monthly data from forty-nine active water rights within the Salmon Creek watershed from 2017 to 2023 were received from the Board's Supply and Demand Unit staff. Of these, forty-six had reported withdrawals; surface water withdrawals from these active water rights occur from the PODs as illustrated in Figure 5-1. By count, water usage is predominately Irrigation (52%) and Domestic (30%) (Figure 5-2). Here, the 'Other' category only includes the stock-watering primary use. By volume, the Irrigation category accounts for more than half of the usage (58%).

For the non-irrigated water demand, the received monthly data in acre-feet are converted to a flow rate for withdrawal from the appropriate catchment's modeled reach segment. Irrigation demand is similarly converted from monthly volume into a withdrawal rate by application number. These water demand data are added to the LSPC model as surface water withdrawals from the appropriate reach segments based on the following considerations.

- Diversions were classified based on primary usage (irrigation, municipal, industrial, recreational, and others) as well as by allocation type (direct and storage).
- During simulations, diverted streamflow was routed out of the system to represent the different uses (e.g., irrigation).
- For instances where PODs in different catchments share the same application/permit number, water demand was proportionally distributed based on the magnitude of the upstream drainage area.

As described in Section 4, the full model simulation period spans from the calendar years 1960 to 1969 and includes water years from 2004 to 2023. Estimations of historical withdrawal values were necessary for periods without observed POD data. To carry out these estimations, the monthly average withdrawals for each permit were calculated based on available data from 2017 to 2023. These monthly averages were then uniformly applied to the corresponding months in earlier periods from 2003 to 2016 and no withdrawals were applied during the period from 1960 to 1969. This approach assumes that monthly withdrawal patterns remain constant, suggesting that estimated withdrawal volumes for any given month would be the same for the same month in a different year throughout the extrapolated time frames.

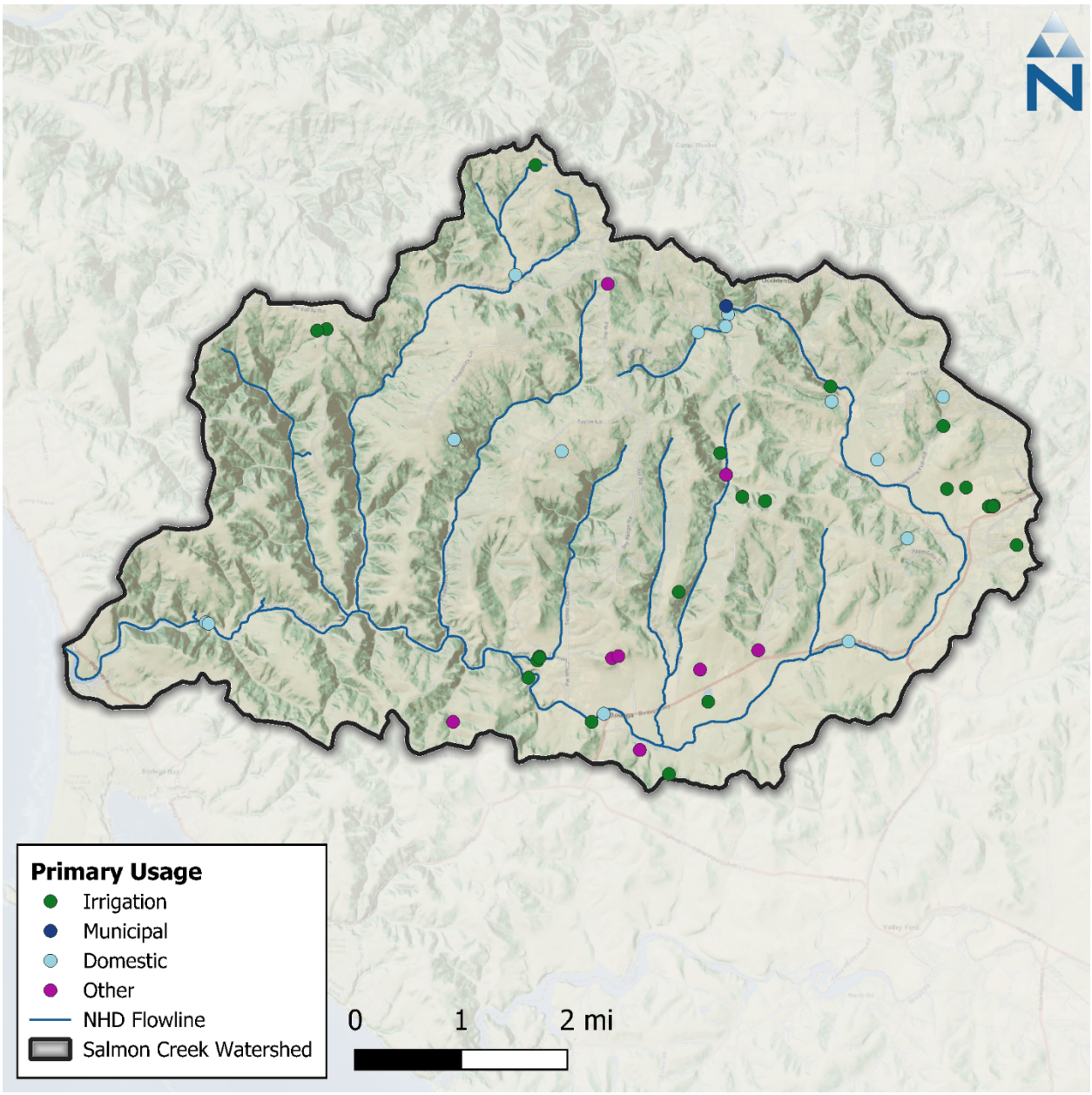

Figure 5-1. Points of diversion within the Salmon Creek watershed.

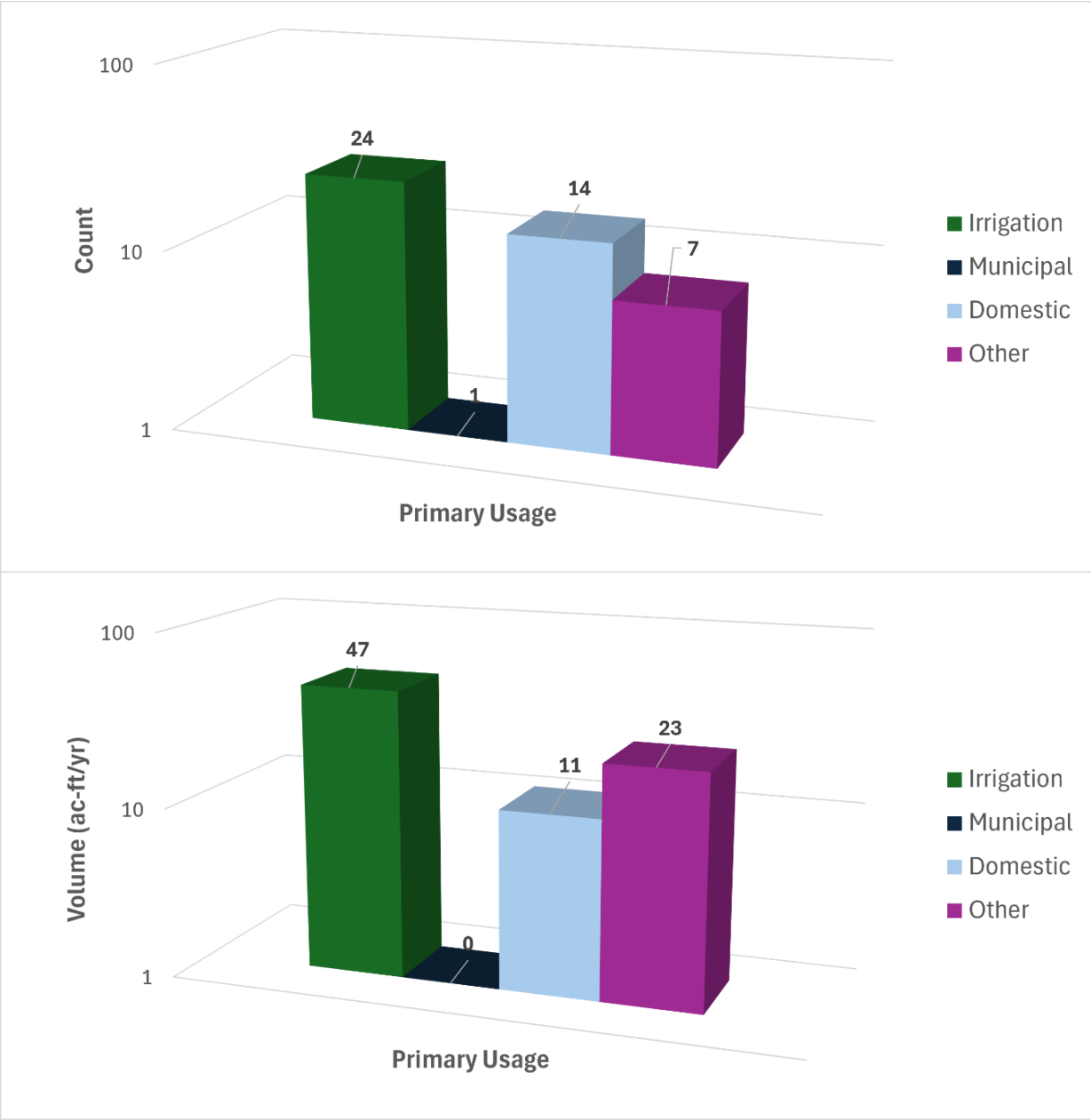

Figure 5-2. Primary water usage for points of diversion within the Salmon Creek watershed. Note that the count and volume are presented on a log scale.

5.1 Irrigation

The LSPC irrigation module is designed to streamline the spatial and temporal representation of water demand, irrigation application, and associated return flows. In practice, irrigation demand is estimated as the deficit of precipitation from the product of a crop-specific evaporative coefficient (ET_c) and reference evapotranspiration (PEVT). This LSPC configuration uses a similar approach but instead works backwards to estimate the monthly crop coefficients for agricultural HRUs by using observed irrigation demand and climate data. Those crop coefficients are then used with observed climate data to calculate irrigation application rates during LSPC simulations. The equation used to calculate monthly evaporative crop coefficients for agricultural HRUs is shown as Equation 5:

$$V_{irr} = (PEVT \times ET_c - PREC) \times A_{irr}$$

where (V_{irr}) is the volume of irrigation demand in acre-feet, (A_{irr}) is the cropland being irrigated in acres, (PEVT) is the reference evapotranspiration depth in feet, ET_c is the crop-specific evaporative coefficient, and (PREC) is the observed precipitation depth in feet. As mentioned above, irrigation demand was inferred from stream diversion records for each catchment. Because the exact location of irrigated vs. non-irrigated parcels was unknown, it was assumed that agricultural land located in catchments immediately draining to reach segments with irrigation PODs were irrigated.

The process for representing irrigation in the Salmon Creek watershed is summarized by the following steps:

1. Estimate irrigation demand.
2. Define irrigated hydrologic response units.
3. Calculate crop evaporative coefficients.

5.1.1 Estimation of Irrigation Demand

Irrigation demand was inferred from eWRIMS stream diversion data for records between 2017 and 2023. For each LSPC catchment, the total monthly irrigation demand was estimated as the sum of all irrigation-associated stream diversions. As mentioned above, stream diversions were either directly used for the application or routed to a storage facility for later use. Due to data limitations, it was unknown exactly when and how stored streamflow was used for irrigation; because evaporative demand is higher during the warmer and drier growing season, it was assumed that irrigation of directly diverted and stored water would follow a similar pattern that scales in proportion to evaporative demand. Figure 5-3 shows average monthly diversion volumes vs. potential evapotranspiration.

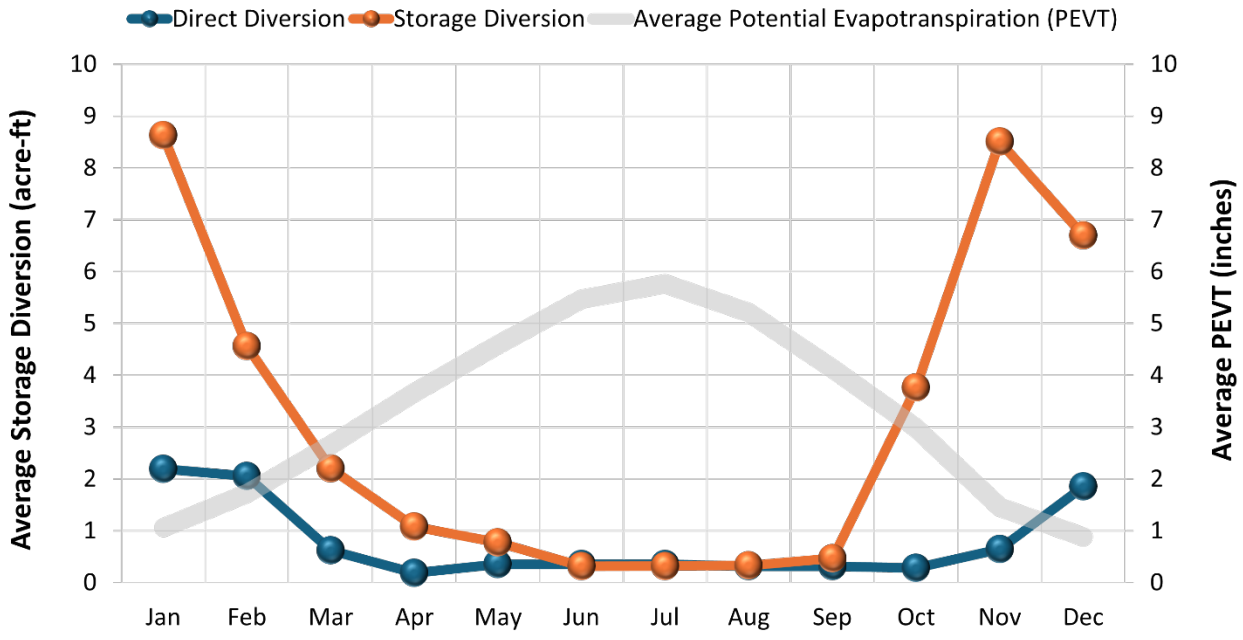

Figure 5-3. Total reported direct and storage diversions vs. average potential evapotranspiration.

5.1.2 Defining Irrigated Hydrologic Response Units

The LSPC model simulates irrigation on a unit-area basis. Agricultural HRUs were partitioned into irrigated and non-irrigated HRU counterparts, as previously described in Section 3.6.2. Because the exact location of irrigated vs. non-irrigated parcels was unknown, it was assumed that 15% of agricultural land located in catchments immediately draining to reach segments with irrigation PODs were irrigated; there were nine out of the 30 catchments that were irrigated. Only 15% of agricultural footprints, identified through the NLCD and CDL datasets within those catchments, were irrigated, totaling 61 acres, which is 0.5% of the total area of the nine irrigated catchments.

As shown in Figure 5-4, the irrigated footprint area is a small portion of the Salmon Creek model domain. The sum of all cropland, pasture, and grassland areas represents 21.3% of the watershed. Of that area, about 72% is within the nine catchments with irrigation. The "Irrigated" area, where the modeled unit-area response is applied, is 61 acres—about 0.3% of the Salmon Creek watershed, as shown in Figure 5-5. For the unit-area model representation, it was assumed that 50 percent of irrigation water was applied as sprinkler and 50 percent as flood irrigation. Sprinkler irrigation enters the model at the same layer as precipitation, making it subject to interception storage and associated evaporation. Flood irrigation enters the model below interception storage and is only subject to surface ponding and infiltration.

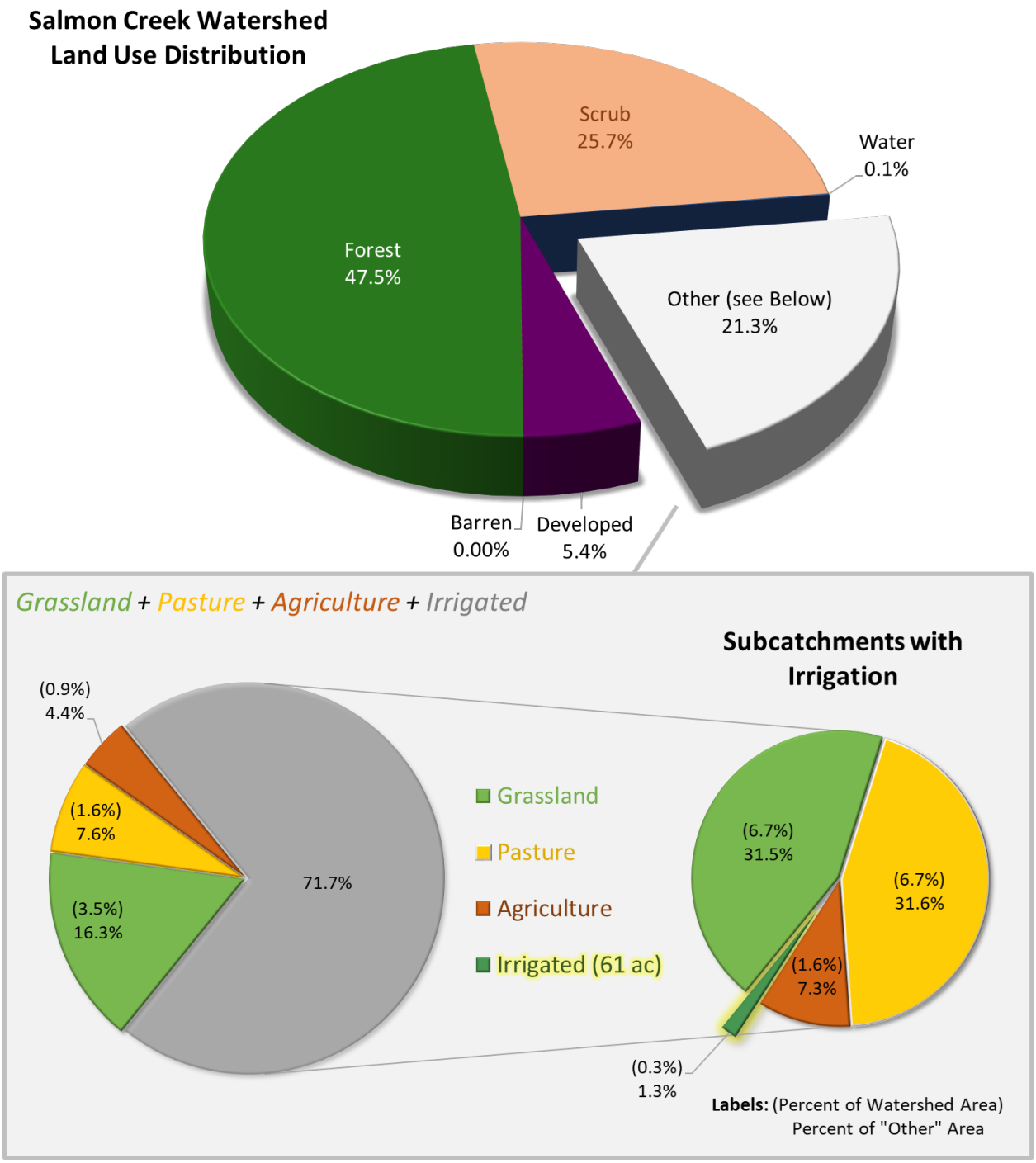

Figure 5-4. Irrigated area as a subset of the Salmon Creek watershed. Note that for each pie, values in parentheses represent the percentage of total watershed area.

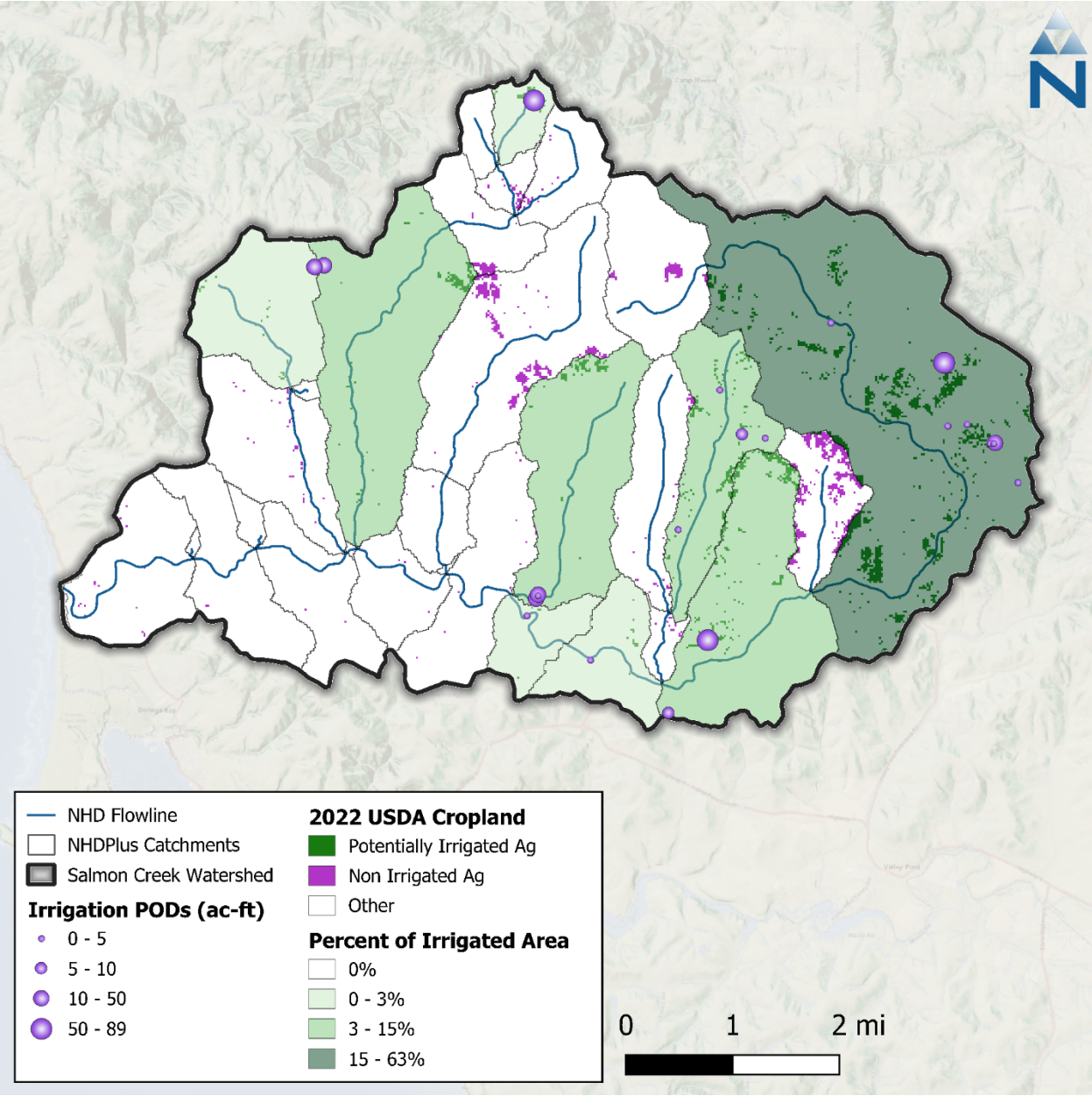

Figure 5-5 Irrigated and non-irrigated agriculture and pasture areas within the Salmon Creek watershed.

5.1.3 Calculation of Crop Evaporative Coefficients

Crop evaporative coefficients (ET_c) are used to adjust reference evapotranspiration rates to better represent an evaporative demand for a specific vegetation type. In the absence of high-resolution irrigation data, this crop-specific evaporative demand can be used with observed precipitation and PEVT data to predict irrigation demand. For this LSPC model instance, distinct crop types were not represented in hydrologic response units; therefore, one value of crop evaporative coefficient per calendar month was used to represent all irrigated areas.

The initial coefficients used in the model were derived by optimizing ET_c in Equation 5 using Microsoft Excel solver to match total irrigation demand volume (V_{irr}) with the total withdrawal volume for irrigation use. Storage diversion and management were not explicitly modeled. By using

these coefficients, it was assumed that the same total water diverted for irrigation (storage + direct diversion) was eventually irrigated in proportion to monthly potential evapotranspiration. However, these coefficients were adjusted during streamflow calibration to improve the water balance. Final estimates for these coefficients are provided in Table 5-1.

Table 5-1. Estimated crop evaporative coefficients (ET_c) by month

Jan	Feb	Mar	Apr	May	Jun	Jul	Aug	Sep	Oct	Nov	Dec
0.678	0.160	0.126	0.170	0.323	0.448	0.524	0.535	0.508	0.522	0.416	0.556

6 MODEL CALIBRATION

The goal of the hydrology model calibration is to adjust model parameters to improve predictive performance based on comparisons to observed data. The desired outcome of the calibration process is a set of modeling parameters that characterize existing conditions for all processes in LSPC that vary by HRU (as described in Section 3) and process-based parameters group. The model development approach prioritizes model configuration over calibration by investigating and expressing known physical characteristics of the watershed wherever possible and practical, and only leaving responses that cannot be explained by physical characteristics to calibration of model parameters. The resulting model is parameterized in such a way that variability trends in the observed data are replicated relative to hydrological conditions (e.g. wet and dry streamflow conditions and rainfall magnitude). The resulting calibrated parameters are consistent by HRU with responses varying as a function of HRU distribution and weather variability minimizes spatial biases and reduces the possibility of over tuning during model calibration. A robustly calibrated model can then serve as the starting point for future watershed-specific applications and investigations and management scenarios.

Figure 6-1 shows how the model configuration and calibration components are layered in the model. LSPC makes clear distinctions between inputs that are physical characteristics and process parameters. The term "parameters" refers to the rates and constants used to represent physical processes in the model. All other model inputs previously described such as weather data, HRU distribution, and the length and slope of overland flow for individual HRUs are generally considered physical characteristics of the watershed because they can be directly measured, assigned, or reasonably estimated from available spatial and temporal data sources. Those components are generally set during model configuration and are not varied during model calibration unless new information is received that justifies a systemwide change to those components.

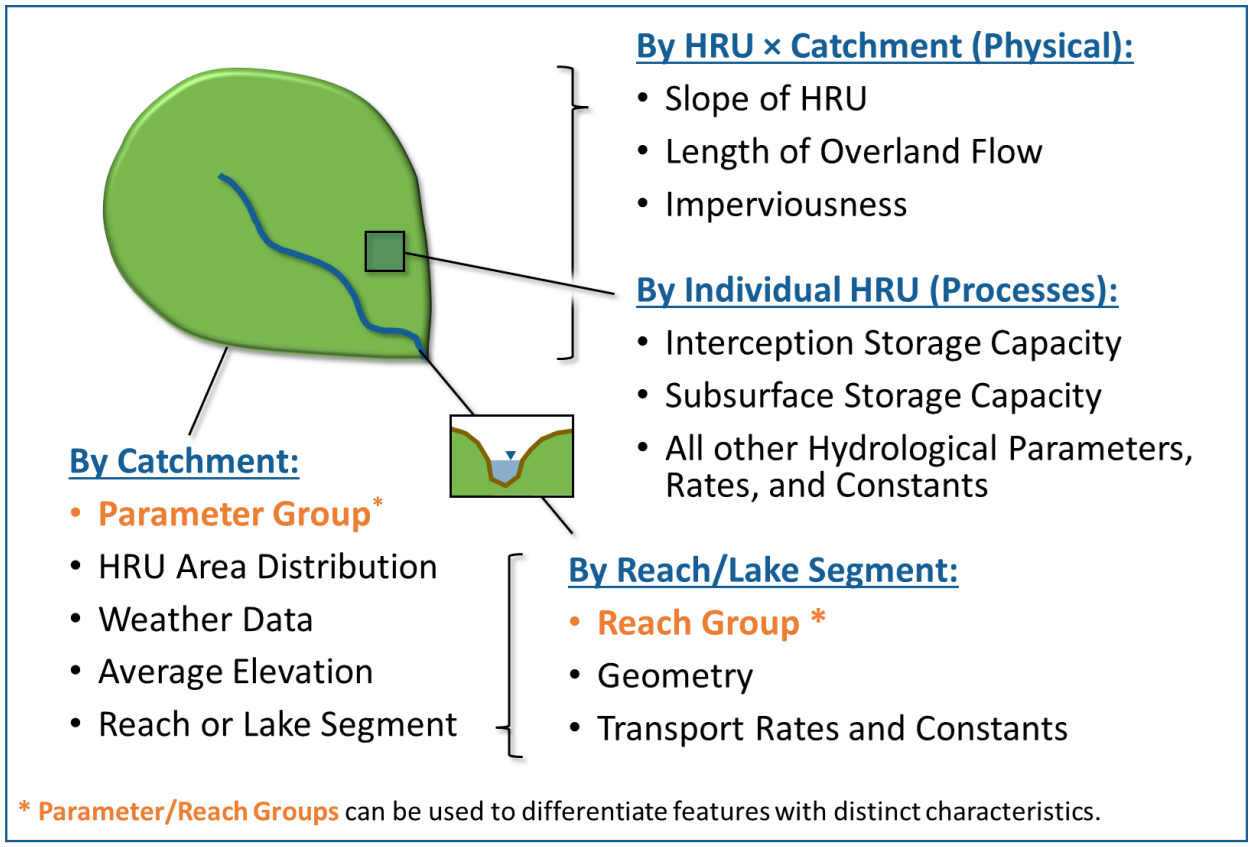

Figure 6-1. LSPC model configuration and calibration components.

Developing modeling parameters begins with specifying one set of parameters systemwide. The Salmon Creek model comprises 98 possible HRUs per catchment and 8 unique combinations of meteorological boundary conditions (i.e., unique combinations of precipitation time series and potential evapotranspiration time series). As described in Section 3.4.1, LSUR and SLSUR are uniquely computed by HRU and catchment; therefore, the initial degrees of freedom are already quite broad. Consequently, using one parameter group, the model represents 1,032 unique non-zero area HRU × meteorological responses over the model domain of 30 catchments. Wherever model responses diverge from observed data in ways that the modeling parameters cannot explain, further investigation may warrant introducing a new parameter group or reach group to add more degrees of freedom to the range of model parameters. This methodical calibration sequence can also help to identify areas where additional data collection may be warranted to characterize the physical system better.

Figure 6-2 shows the model calibration sequence, a top-down data approach that began with the extensive model configuration and quality control process previously described in Section 2 through Section 5. The sequence begins with climate-forcing data, followed by edge-of-stream land hydrology and water budget estimates and representation of the stream routing network. This sequencing minimizes the propagation of uncertainty and error by distinguishing physical characteristics of the watershed that can be measured and configured from process-based parameters, which are rates and constants that can be estimated within a reasonable range of variability by HRU.

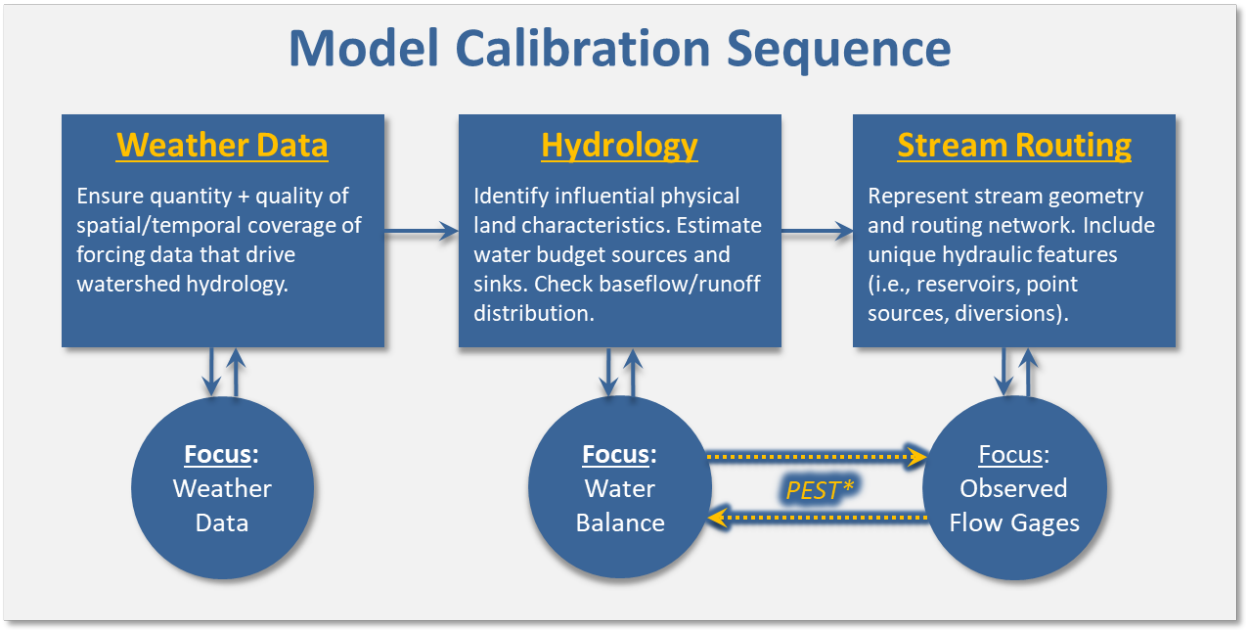

Figure 6-2. Top-down calibration sequence for hydrology model calibration.

Ten years of meteorological forcing data between January 1960 and December 1969 and twenty water years of meteorological forcing data between October 2003 and September 2023 were processed to drive the Salmon Creek watershed model. Consumptive use data were available for the most recent 6 water years (2018-2023). For earlier water years (2003 – 2017), water use was estimated using the monthly averages from the recent years. Measured flow rates in Salmon Creek are available only between 8/1/1962 and 10/1/1975. A reference station, Austin Creek (Figure 6-4 and Table 6-1), was selected for independent model validation, as detailed in Section 7.3. Measured flow data at this station are available between 8/1/1962 and 9/29/1966, and are missing from 9/30/1966 to 9/30/2003. Therefore, the period from 10/1/1962 to 9/29/1966 — complete water years when flow rates were available at both stations — was selected for model calibration, and no consumptive use data was applied to this period. As shown in Figure 6-3, the annual precipitation during water year 1966 was approximately equal to the 4-year average, 1965 was the wettest year within the 4-year calibration period while 1964 was the driest year. The calibration period from 10/1/1962 to 9/29/1966 was selected for Parameter Estimation—that process is further described in Section 6.2.

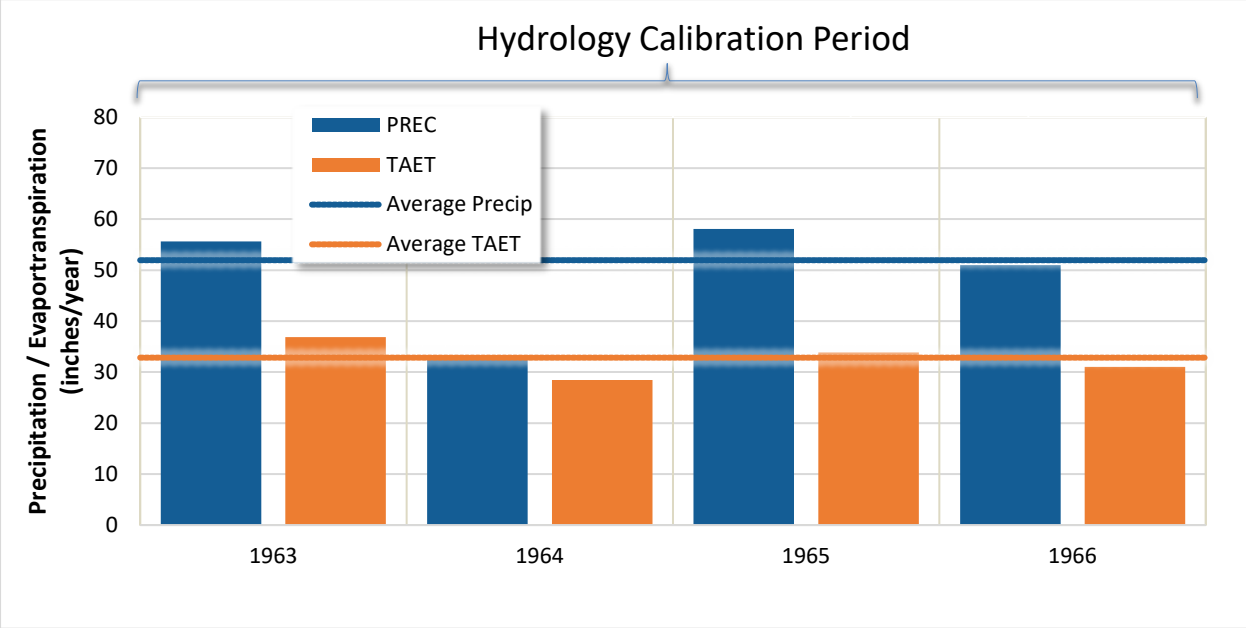

Figure 6-3. Annual average precipitation (PREC) and total evapotranspiration (TAET) between water years 1963 – 1966, along with PEST simulation and hydrology calibration periods.

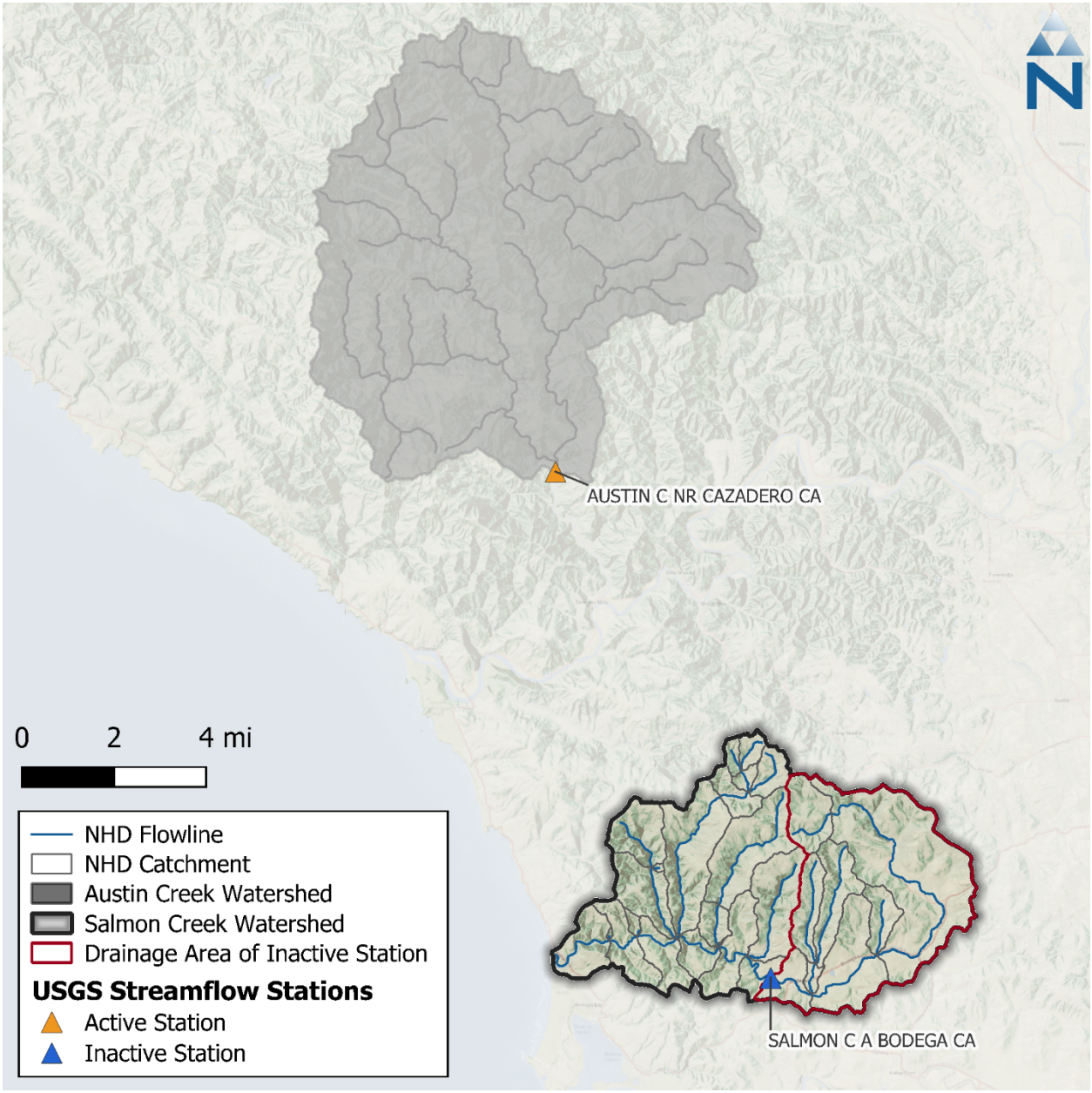

Figure 6-4. USGS streamflow stations in the Salmon Creek watershed.

Table 6-1. Summary of USGS daily streamflow data

Station Name	Station ID	Drainage Area (mi^2)	Start Date	End Date	Status
SALMON C A BODEGA CA	11460920	15.7	8/1/1962	10/1/1975	Inactive
AUSTIN C NR CAZADERO CA	11467200	62.8	6/1/1959	Present	Active

6.1 Calibration Assessment and Metrics

A combination of visual assessments and computed numerical evaluation metrics were used to assess model performance during calibration. Model performance was assessed using graphical comparisons of simulated vs. observed data (e.g., time-series plots, flow duration curves, etc.), quantitative metrics, and qualitative thresholds recommended by Moriasi et al. (2015) and Duda et al. (2012), which are considered highly conservative. Moriasi et al. (2007 and 2015) assign narrative grades for hydrology and water quality modeling to the percent bias (PBIAS), the ratio of the root-mean-square error to the standard deviation of measured data (RSR), and the Nash-Sutcliffe model efficiency (NSE). These metrics are defined as follows:

- The percent bias (PBIAS) quantifies systematic overprediction or underprediction of observations. Positive values of PBIAS reflect a bias towards underestimation, while negative values reflect a bias towards overestimation. Low magnitude values of PBIAS indicate better fit, with a value of 0 being optimal.
- The ratio of the root-mean-square error to the standard deviation of measured data (RSR) provides a measure of error based on the root-mean-square error (RMSE), which indicates error results in the same units as the simulated and observed data but normalized based on the standard deviation of observed data. Values for RSR can be greater than or equal to 0, with a value of 0 indicating perfect fit. Moriasi et al. (2007) provides narrative grades for RSR.
- The Nash-Sutcliffe efficiency (NSE) is a normalized statistic that determines the relative magnitude of the residual variance compared to the measured data variance (Nash and Sutcliffe, 1970). NSE indicates how well the plot of observed versus simulated data fits the 1:1 line. Values for NSE can range between -∞ and 1, with NSE = 1 indicating a perfect fit.

Other metrics were computed and used to assess calibrated model performance, including the Kling-Gupta Efficiency (KGE). This metric can provide additional or complementary information on model performance to the three metrics listed above and is defined as follows:

- The Kling-Gupta Efficiency (KGE) metric is based on the Euclidean Distance between an idealized reference point and a sample's bias, standard deviation, and correlation within a three-dimensional space (Gupta et al. 2009). KGE attempts to address documented shortcomings of NSE, but the two metrics are not directly comparable. A KGE value of 1 indicates perfect fit, with agreement worsening for values less than 1. Knoben et al. (2019) have suggested a KGE value > -0.41 as a benchmark that indicates a model has more predictive skill than using the mean observed flow. Qualitative thresholds for KGE have been used by Kouchi et al. (2017).

Both simulated time series and observed data were binned into subsets of time to highlight seasonal performance and different flow conditions. Hydrograph separation was also performed to assess stormwater runoff vs. baseflow periods to isolate model performance on stormflows and low flows. Table 6-2 is a summary of performance metrics that was used to evaluate the hydrology calibration. As shown in the table, "All Conditions" (i.e., annual interval) for R-squared and NSE is the primary condition typically evaluated during model calibration. For sub-annual intervals, the pattern established in the literature for PBIAS/RME when going from "All Conditions" to sub-annual intervals is to shift the qualitative assessment by one category (e.g., use the "good" range for "very good", "satisfactory" for "good", and so on). This pattern was followed for RSR and NSE qualitative assessments of sub-annual intervals.

Using hydrograph separation to classify baseflow and stormflow provides a more reliable method for assessing low-flow model performance than using the lowest 50% of flows, a metric widely used in hydrology model calibration as a convenient indicator of low-flow model performance. There are several key reasons for this:

1. **Improved Representation of Low-Flow Conditions:** The lowest 50% of flows include not only baseflow but also portions of stormflow as the hydrograph rises and falls. This can mask the true low-flow or baseflow behavior of the system, as the transitions from baseflow to stormflow can have very different physical and hydrological drivers. By using hydrograph separation, baseflow, which is primarily driven by groundwater contributions, can be isolated from storm flows, which are influenced by rainfall (Smakhtin 2001). This provides a clearer, more consistent metric for assessing low-flow conditions during model calibration and performance evaluation.
2. **Reduction in Variability of Metrics:** Because the rising and falling limbs of the hydrograph are affected by factors such as precipitation intensity, antecedent moisture conditions, and catchment characteristics, including portions of these limbs in the low-flow metric can lead to high variability in model performance metrics. This variability can obscure the modeler's ability to accurately assess low-flow performance. Hydrograph separation, on the other hand, offers a cleaner classification, resulting in lower variability and a more stable and reliable assessment of baseflow model performance.
3. **Better Calibration for Baseflow-Driven Processes:** In many hydrological studies, low flows are important for understanding groundwater-surface water interactions, sustaining streamflow during dry periods, and supporting aquatic habitats. Hydrograph separation allows for the explicit calibration of baseflow processes, providing a better assessment of groundwater dynamics and groundwater-fed contributions to the stream network. Without separating baseflow and stormflow, calibration based on the lowest 50% of flows may inadvertently skew model performance statistics by over-emphasizing short-term stormflow events and recession behavior, rather than the sustained low flow processes crucial to many hydrological applications.
4. **Alignment with Process-Based Hydrology:** Hydrograph separation aligns with a process-based understanding of hydrology, where distinct processes govern baseflow and stormflow. This approach respects the inherent differences in generation mechanisms: baseflow is usually a slower, more consistent groundwater-driven process, while stormflow is a quicker response to precipitation events. This distinction is essential for accurately simulating hydrological systems and ensuring model results that are realistic and representative of different flow conditions. Models that capture these distinct flow components are better suited for making predictions about changes in land use, climate, or other factors affecting baseflow and stormflow differently.
5. **Widely Accepted in Hydrological Modeling:** Hydrograph separation techniques are well-established and widely used in hydrological research and practice, offering a consistent framework for distinguishing between baseflow and stormflow (Arnold et al. 1995; Nathan and McMahon 1990). Techniques like those used in the United States Geological Survey (USGS) Hydrograph SEParation (HySEP) methodology provide different options for empirically parsing baseflow time series from storm flows (Sloto and Crouse 1996). The sliding interval method was used to separate both observed and simulated hydrographs at a daily timestep. This provides a consistent approach for the rollup and comparison of hydrograph components. This method is robust because they can be directly applicable to time series data as a function of the upstream drainage area.

.

Table 6-2. Summary of qualitative thresholds for performance metrics used to evaluate hydrology calibration

Performance Metric	Hydrological Condition	Performance Threshold for Hydrology Simulation			
		Very Good	Good	Fair	Poor
Percent Bias (PBIAS)	All Conditions [1]	<5%	5% - 10%	10% - 15%	>15%
	Seasonal Flows [2]	<10%	10% - 15%	15% - 25%	>25%
	Highest 10% of Daily Flow Rates [3]				
	Days Categorized as Storm Flow [4]				
	Days Categorized as Baseflow [4]				
RMSE – Std Dev Ratio (RSR)	All Conditions [1]	≤0.50	0.50 - 0.60	0.60 - 0.70	>0.70
	Seasonal Flows [2]	≤0.40	0.40 - 0.50	0.50 - 0.60	>0.60
Nash-Sutcliffe Efficiency (NSE)	All Conditions [1]	>0.80	0.70 - 0.80	0.50 - 0.70	≤0.50
	Seasonal Flows [2]	>0.70	0.50 - 0.70	0.40 - 0.50	≤0.40
Kling-Gupta Efficiency (KGE)	Monthly Aggregated [5]	≥0.90	0.90 - 0.75	0.75 - 0. 50	<0.50

1. All Flows considers all daily time steps in the model time series.
2. Seasonal Flows consider daily flows during a predefined, seasonal period (e.g., Wet Season and Dry Season). The Wet Season includes the months of October through April. The Dry Season includes the months of May through September.
3. Highest 10% of Flows considers the top 10% of daily flows by magnitude as determined from the observed flow duration curve.
4. Baseflows and Storm flows were determined from analyzing the daily model time series by applying the USGS hydrograph separation approach (Sloto and Crouse 1996).
5. KGE evaluated using thresholds for monthly aggregated time series (Kouchi et al. 2017).

6.2 Parameter Estimation

The model-independent Parameter ESTimation tool (PEST) is a powerful tool used for model parameter estimation, sensitivity analysis, and uncertainty analysis (Doherty 2015). It automates adjusting a specific set of model parameters within a reasonably constrained range of variability, with the objective of minimizing the differences between observed and simulated data. PEST seeks to minimize the sum of Squared Errors (SSE) across all specified observations that can be customized as needed to evaluate complete flow time series or other temporal categorizations such as flow duration intervals, monthly volumes, wet and dry periods, etc. A supervised PEST simulation helps to ensure that recommended outcomes are realistic and representative of the natural system being modeled. PEST is versatile and can be integrated with a wide range of environmental and hydrological models, including LSPC.

Sections 2 through 5 above describe model configuration and quality control methods used to represent physical characteristics of the watershed that are either directly measurable or can be reasonably estimated from available spatial or temporal data. On the other hand, parameters associated with subsurface geology represent one of the areas of uncertainty in the model where optimization of model parameters can improve performance. PEST was used in conjunction with model parameterization guidance documentation (BASINS Technical Note 6 [EPA 2000]) to vary six parameters associated with subsurface geology: the infiltration index parameter (INFILT), the lower zone nominal storage parameter (LZSN), the upper zone nominal storage parameter (UZSN), the non-linear groundwater recession flow parameter (KVARY), the active groundwater recession coefficient (AGWRC), and the interflow recession coefficient (IRC).

The infiltration index parameter (INFILT) is one of the parameters optimized by PEST. Within a given hydrological soil group, TN6 guidance suggests that INFILT typically varies within minimum and maximum values shown in Table 6-3. Some model parameters are codependent. For example, TN6 recommends that the upper zone nominal storage parameter (UZSN) should first be estimated as a percentage of the lower zone nominal storage parameter (LZSN), taking into consideration other physical characteristics such as slope, vegetation cover, and depression storage, and then calibrated. Table 6-4 shows recommended initial values for UZSN as a percentage of LZSN and other physical characteristics. The non-linear groundwater recession coefficient (KVARY) "is used when the observed groundwater recession demonstrates a seasonal variability with a faster recession (i.e., higher slope and lower AGWRC values) during wet periods, and the opposite during dry periods" according to TN6. The active groundwater recession coefficient (AGWRC), the ratio of current groundwater discharge to that of the previous day, was the fourth parameter optimized by PEST. TN6 notes that "the overall watershed recession rate is a complex function of watershed conditions, including climate, topography, soils, and land use" that can be estimated from observed time series, and then adjusted during calibration (EPA 2000). Interflow recession coefficient (IRC), the ratio of the current daily interflow discharge to the interflow discharge on the previous day, affects the rate that interflow is discharged from storage and, therefore, the shape of the hydrograph receding limb after storm events. Model guidance and previous experience suggest that these parameters are both uncertain and very sensitive; therefore, using PEST to explore their impact and optimize performance is worthwhile and beneficial.

Table 6-3. Typical ranges by hydrological soil group for the infiltration index model parameter, INFILT

Hydrological Soil Group	INFILT Typical Ranges (in./hr)		Runoff Potential
	Low	High	
A	0.40	1.00	Low
B	0.10	0.40	Moderate
C	0.05	0.10	Moderate to High
D	0.01	0.05	High

Source: BASINS Technical Note 6 (EPA 2000)

Table 6-4. Recommended initial values for upper zone nominal storage (UZSN) as a percentage of lower zone nominal storage (LZSN) and other physical characteristics

Slope	Vegetation Cover	Depression Storage	UZSN (% of LZSN)
Very Mild	Heavy/Forest	High	14%
Moderate	Moderate	Moderate	8%
Steep	Moderate	Moderate	6%

Source: BASINS Technical Note 6 (EPA 2000)

PEST could have optimized model parameters at the HRU level (up to 85 possible degrees of freedom per parameter for previous HRUs); however, to better manage the search space, those degrees of freedom were constrained to 12 combinations of hydrological soil group (4 types) × slope (3 categories). Figure 6-5 is a schematic of HRU-level LSPC hydrology parameters with the six PEST-optimized parameters and process pathways highlighted. Table 6-5 shows the minimum and maximum parameter value ranges used to constrain PEST optimization by hydrological soil group and slope. Table 6-6 shows the initial and final PEST-optimized estimates for subsurface process parameters, summarized by hydrological soil group and slope—the data bars show the relative magnitude of the initial and estimated parameter value within the PEST min/max range (a full cell indicates the maximum value while an empty cell indicates the minimum value).

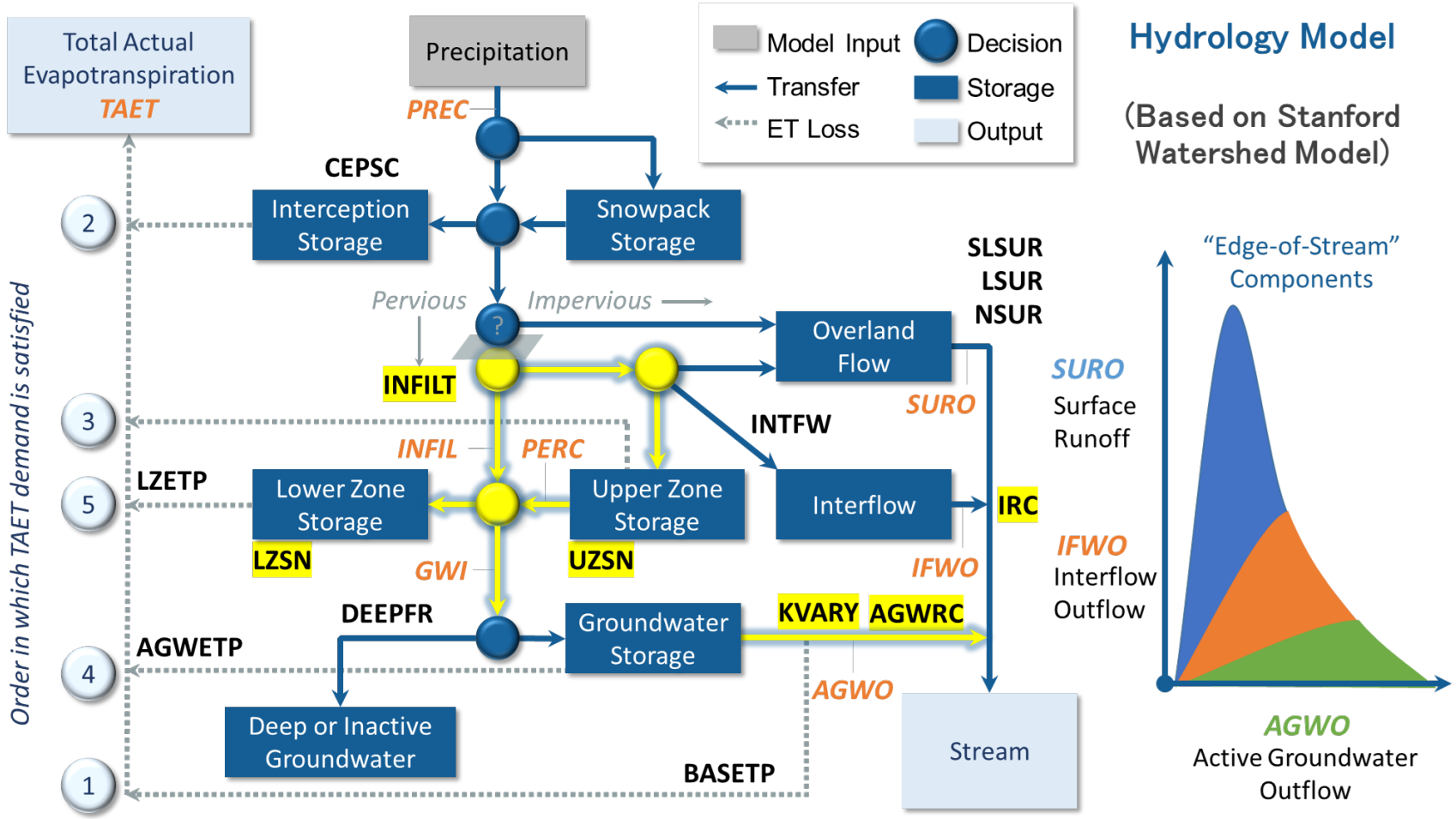

PEST: LSPC parameters and process optimized by Parameter Estimation (PEST) during hydrology calibration.

Figure 6-5. HRU-level LSPC hydrology parameters with PEST-optimized parameters and process pathways highlighted.

Table 6-5. Minimum and maximum parameter value ranges used to constrain PEST optimization, by hydrological soil group and slope

Hydrological Soil Group	Slope	Area (ac)	Area (%)	LZSN		INFILT		KVARY		AGWRC		UZSN (% LZSN)		IRC	
				Min	Max	Min	Max	Min	Max	Min	Max	Min	Max	Min	Max
A	Low	95.4	1.3%	2	15	0.4	1	0.0001	3	0.84	0.999	1	20	0.3	0.85
A	Med	28.0	0.4%	2	15	0.4	1	0.0001	3	0.84	0.999	1	20	0.3	0.85
A	High	15.3	0.2%	2	15	0.4	1	0.0001	3	0.84	0.999	1	20	0.3	0.85
B	Low	126.1	1.7%	2	15	0.1	0.4	0.0001	3	0.85	0.999	1	20	0.3	0.85
B	Med	395.4	5.4%	2	15	0.1	0.4	0.0001	3	0.85	0.999	1	20	0.3	0.85
B	High	1,330.8	18.3%	2	15	0.1	0.4	0.0001	3	0.85	0.999	1	20	0.3	0.85
C	Low	403.4	5.5%	2	15	0.5	1	0.0001	3	0.85	0.999	1	20	0.3	0.85
C	Med	1,170.5	16.1%	2	15	0.5	1	0.0001	3	0.85	0.999	1	20	0.3	0.85
C	High	3,599.9	49.4%	2	15	0.5	1	0.0001	3	0.85	0.999	1	20	0.3	0.85
D	Low	4.9	0.1%	2	15	0.001	0.05	0.0001	3	0.84	0.999	1	20	0.3	0.85
D	Med	17.6	0.2%	2	15	0.001	0.05	0.0001	3	0.84	0.999	1	20	0.3	0.85
D	High	104.1	1.4%	2	15	0.001	0.05	0.0001	3	0.84	0.999	1	20	0.3	0.85

Table 6-6. Initial and final PEST optimized estimates for subsurface process parameters, summarized by hydrological soil group and slope

HSG	Slope	Area (ac)	Area (%)	LZSN		INFILT		KVARY		AGWRC		UZSN (%LZSN)		IRC	
				Initial	Est.	Initial	Est.	Initial	Est.	Initial	Est.	Initial	Est.	Initial	Est.
A	Low	95.4	1.3%	10.18	13.33	0.4	1	0.21	0.15	0.85	0.98	14.26	18.67	0.65	0.85
A	Med	28.0	0.4%	10.18	13.33	0.4	1	0.21	0.15	0.85	0.98	8.15	10.67	0.65	0.85
A	High	15.3	0.2%	10.18	13.33	0.4	1	0.21	0.15	0.85	0.98	6.11	8.00	0.65	0.85
B	Low	126.1	1.7%	12.50	14.97	0.1	0.1	2.50	3.00	0.95	0.93	17.50	20.95	0.58	0.60
B	Med	395.4	5.4%	12.50	14.97	0.1	0.1	2.50	3.00	0.95	0.93	10.00	11.97	0.58	0.60
B	High	1,330.8	18.3%	12.50	14.97	0.1	0.1	2.50	3.00	0.95	0.93	7.50	8.98	0.58	0.60
C	Low	403.4	5.5%	13.00	12.63	0.05	0.05	0.00	0.00	0.97	0.97	18.00	17.49	0.57	0.57
C	Med	1,170.5	16.1%	13.00	12.63	0.05	0.05	0.00	0.00	0.97	0.97	12.00	11.66	0.57	0.57
C	High	3,599.9	49.4%	13.00	12.63	0.05	0.05	0.00	0.00	0.97	0.97	9.00	8.74	0.57	0.57
D	Low	4.9	0.1%	13.00	14.25	0.00684	0.001	2.85	2.83	0.85	1.00	18.00	19.73	0.35	0.30
D	Med	17.6	0.2%	13.00	14.25	0.00684	0.001	2.85	2.83	0.85	1.00	12.00	13.15	0.35	0.30
D	High	104.1	1.4%	13.00	14.25	0.00684	0.001	2.85	2.83	0.85	1.00	9.00	9.87	0.35	0.30

The PEST tool provided limited improvement in model performance at Salmon Creek. Therefore, calibration parameters were further adjusted manually. During the manual calibration process, the following parameters were modified to better capture seasonal variations: Monthly upper zone nominal storage (UZSN), Interflow inflow parameter (INTFW), Interflow recession constant (IRC), and Lower zone evapotranspiration parameter (LZETP). Additionally, because the drainage area of Salmon Creek overlaps with the Pacific Coastal Aquifers, the fraction of groundwater inflow to deep recharge (DEEPFR) was used to represent groundwater loss.

Model parameterization guidance (BASINS Technical Note 6 [EPA 2000]) recommends using non-zero values for the fraction of remaining evapotranspiration from baseflow (BASETP) when significant riparian vegetation is present. As shown in Table 3-2, the watershed is dominated by forest. Therefore, non-zero values of BASETP were applied to forest HRUs to better estimate evapotranspiration from riparian vegetation as active groundwater enters the streambed. In addition, the fraction of remaining evapotranspiration from active groundwater (AGWETP) was applied to scrub HRUs to model direct evaporation from groundwater storage.

Applying non-zero values for DEEPFR, BASETP, and AGWETP improved model performance by increasing simulated water losses. To account for the significant water loss observed in the watershed, the highest values for lower zone nominal storage (LZSN) and infiltration index (INFILT) are set slightly above the ranges recommended by BASINS Technical Note 6. All other parameter values fall within the suggested ranges. The final calibrated values are summarized in Table 6-7.

Table 6-7. Final manual optimized estimates for subsurface process parameters, summarized by hydrological soil group and slope

HSG	Slope	LZSN	INFILT	KVARY	AGWRC	DEEPFR	BASEETP		AGWETP		CEPSC			UZSN		INTFW	IRC		LZETP			
																			Forest		Others	
							Forest	Others	Scrub	Others	Forest	Scrub	Grass & Pasture	Min	Max		Min	Max	Min	Max	Min	Max
A	Low	12.22	0.31	0.00	0.97	0.29	0.20	0.00	0.20	0.00	0.40	0.36	0.34	1.39	2.09	2.00	0.50	0.65	0.83	0.88	0.65	0.69
A	Med	12.22	0.31	0.00	0.97	0.29	0.20	0.00	0.20	0.00	0.40	0.36	0.34	0.80	1.19	2.00	0.50	0.65	0.83	0.88	0.65	0.69
A	High	12.22	0.31	0.00	0.97	0.29	0.20	0.00	0.20	0.00	0.40	0.36	0.34	0.60	0.90	2.00	0.50	0.65	0.83	0.88	0.65	0.69
B	Low	15.00	0.03	0.00	0.97	0.29	0.20	0.00	0.20	0.00	0.40	0.36	0.34	1.54	2.30	2.00	0.50	0.65	0.83	0.88	0.65	0.69
B	Med	15.00	0.03	0.00	0.97	0.29	0.20	0.00	0.20	0.00	0.40	0.36	0.34	1.20	1.80	2.00	0.50	0.65	0.83	0.88	0.65	0.69
B	High	15.00	0.03	0.00	0.97	0.29	0.20	0.00	0.20	0.00	0.40	0.36	0.34	0.90	1.35	2.00	0.50	0.65	0.83	0.88	0.65	0.69
C	Low	16.50	0.02	0.00	0.97	0.29	0.20	0.00	0.20	0.00	0.40	0.36	0.34	1.60	2.40	2.00	0.50	0.65	0.83	0.88	0.65	0.69
C	Med	16.50	0.02	0.00	0.97	0.29	0.20	0.00	0.20	0.00	0.40	0.36	0.34	1.46	2.19	2.00	0.50	0.65	0.83	0.88	0.65	0.69
C	High	16.50	0.02	0.00	0.97	0.29	0.20	0.00	0.20	0.00	0.40	0.36	0.34	1.30	1.94	2.00	0.50	0.65	0.83	0.88	0.65	0.69
D	Low	16.50	0.00	0.00	0.97	0.29	0.20	0.00	0.20	0.00	0.40	0.36	0.34	1.60	2.40	2.00	0.50	0.65	0.83	0.88	0.65	0.69
D	Med	16.50	0.00	0.00	0.97	0.29	0.20	0.00	0.20	0.00	0.40	0.36	0.34	1.46	2.19	2.00	0.50	0.65	0.83	0.88	0.65	0.69
D	High	16.50	0.00	0.00	0.97	0.29	0.20	0.00	0.20	0.00	0.40	0.36	0.34	1.30	1.94	2.00	0.50	0.65	0.83	0.88	0.65	0.69
Min Suggested		2.00	0.00	0.00	0.85	0.00	0.00		0.00		0.01			0.05		1.00	0.30		0.10			
Max Suggested		15.00	0.50	5.00	1.00	0.50	0.20		0.20		0.40			2.00		10.00	0.85		0.90			

6.3 Calibration Results

Using the PEST estimated and manually adjusted parameters, the model was run for water years 1963 through 1966 and calibration performance was evaluated. Note that in all results, modeled flows < 0.01 cfs were set to 0 to match the detection limit of the observed flows. As shown in Table 6-8, performance across the calibration period was "Very Good" for PBIAS with simulated flow volumes underpredicted by 3.7%. Wet season and dry season PBIAS were "Very Good" with 3.6% and 8.5% underprediction, respectively. KGE (calculated with monthly flow values) was "Good" across the entire calibration period (0.89), the dry season (0.85), and the wet season (0.82). Since the hourly precipitation data were obtained from a distant site (i.e., San Francisco International Airport), timing uncertainties may have been introduced into the daily modeling results, leading to poor performance in timing-sensitive metrics such as NSE and RSR. To reduce the influence of these uncertainties, model performance metrics were also evaluated using monthly flow data. As shown in Table 6-9, performance during the calibration period was rated as 'Good' or 'Very Good.' As expected, PBIAS remained unaffected by the change in time step, while both RSR and NSE showed notable improvements compared to results based on daily average time series. These metric values indicate the model is performing well at capturing the observed volume (PBIAS) and trends in wet and dry season flow (RSR, NSE, KGE).

Examination of daily and normalized monthly streamflow (Figure 6-6 and Figure 6-7, respectively) shows that, as indicated by the metrics, the most extreme peaks are slightly overestimated, but general rising/falling patterns in the hydrographs are well captured. Figure 6-8 and Figure 6-9 present the interquartile ranges and averages, respectively, of monthly normalized flow—both show a high degree of correspondence between observed and simulated values. The flow duration curve (FDC) shown in Figure 6-10 indicates that observed flow regime trends are generally well matched by the model. Below the 25th percentile, observed flows are either 0 or below the detection limits; it should be noted that modeled and observed FDCs are calculated independently and flows of the same percentile do not necessarily occur at the same time.

Table 6-8. Summary of daily calibration performance metrics for calibration period (WY 1963 – 1966)

Hydrology Monitoring Locations	Performance Metrics (10/01/1962 – 9/29/1966)														
	PBIAS						RSR			NSE			KGE[1]		
	All	Wet Season	Dry Season	>10th %ile Flows	Storm Flows	Baseflow	All	Wet Season	Dry Season	All	Wet Season	Dry Season	All	Wet Season	Dry Season
SALMON C A BODEGA CA	3.69%	3.58%	8.54%	2.79%	14.82%	-14.15%	0.97	1.00	0.39	0.05	0.00	0.85	0.89	0.85	0.82

[1] Monthly, as specified in Table 6-2.

Very Good | Good | Fair | Poor

\- Overpredicts | + Underpredicts

Table 6-9. Summary of monthly calibration performance metrics

Hydrology Monitoring Locations	Performance Metrics (10/01/1962 – 9/29/1966)											
	PBIAS			RSR			NSE			KGE		
	All	Wet Season	Dry Season	All	Wet Season	Dry Season	All	Wet Season	Dry Season	All	Wet Season	Dry Season
SALMON C A BODEGA CA	3.69%	3.58%	8.54%	0.29	0.34	0.26	0.91	0.88	0.93	0.89	0.85	0.82

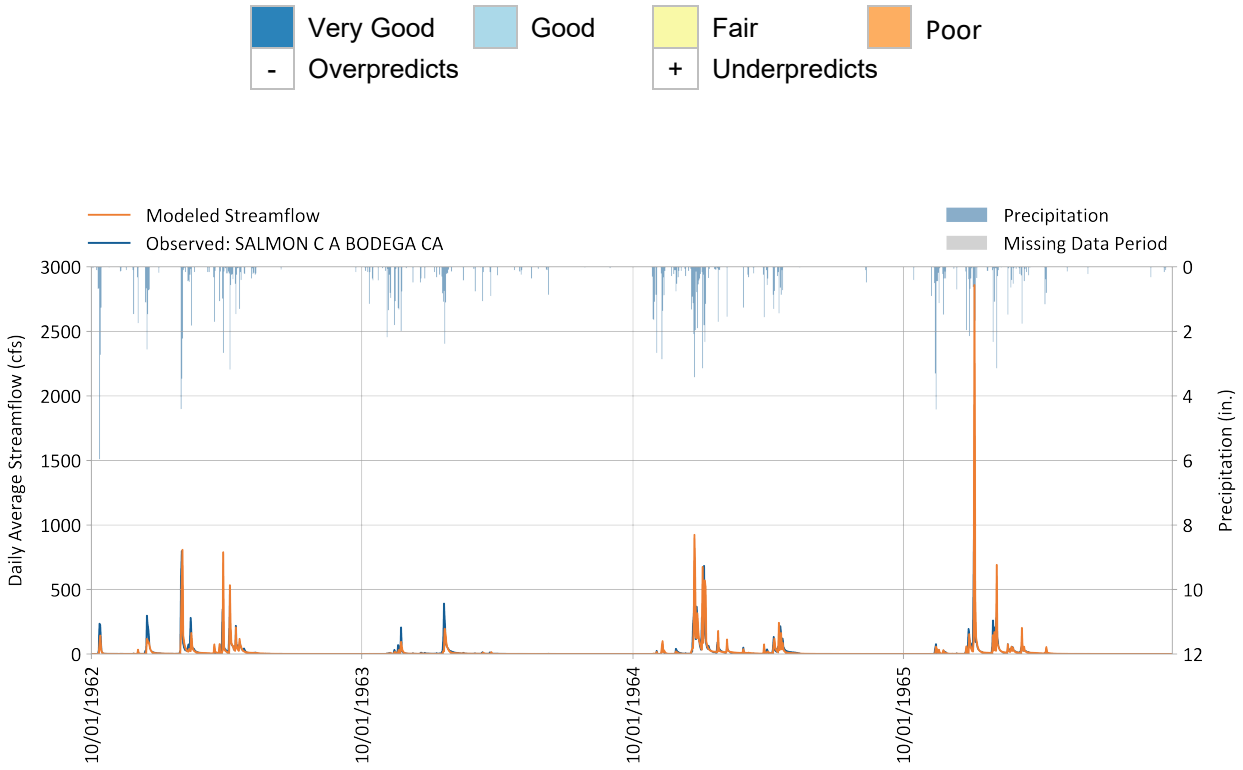

Figure 6-6. Daily simulated vs. observed streamflow for SALMON C A BODEGA CA (11460920).

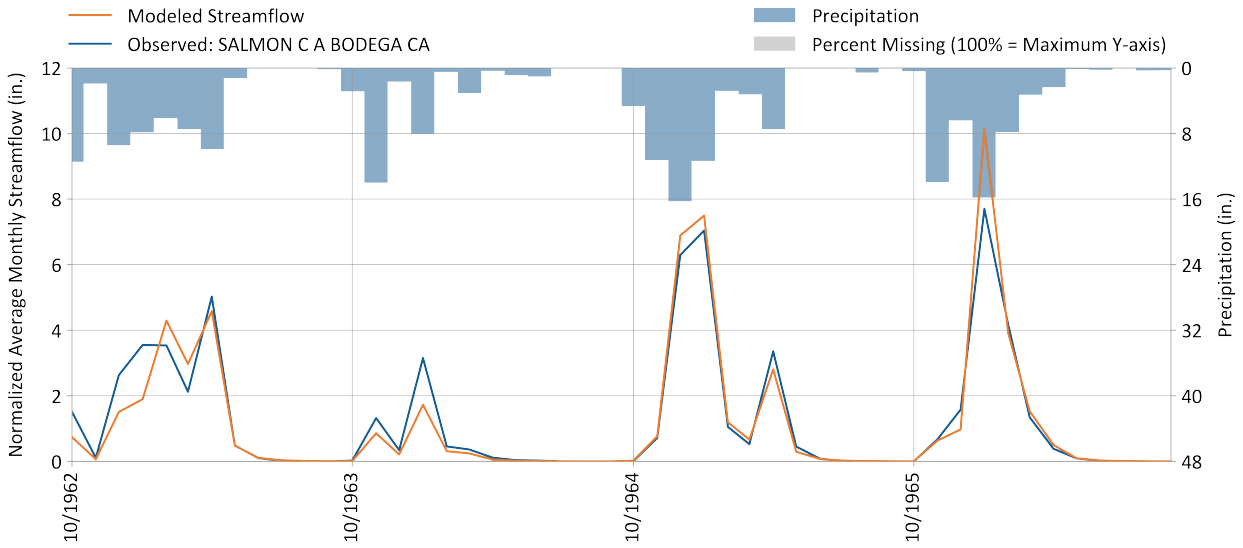

Figure 6-7. Monthly simulated vs. observed streamflow for SALMON C A BODEGA CA (11460920).

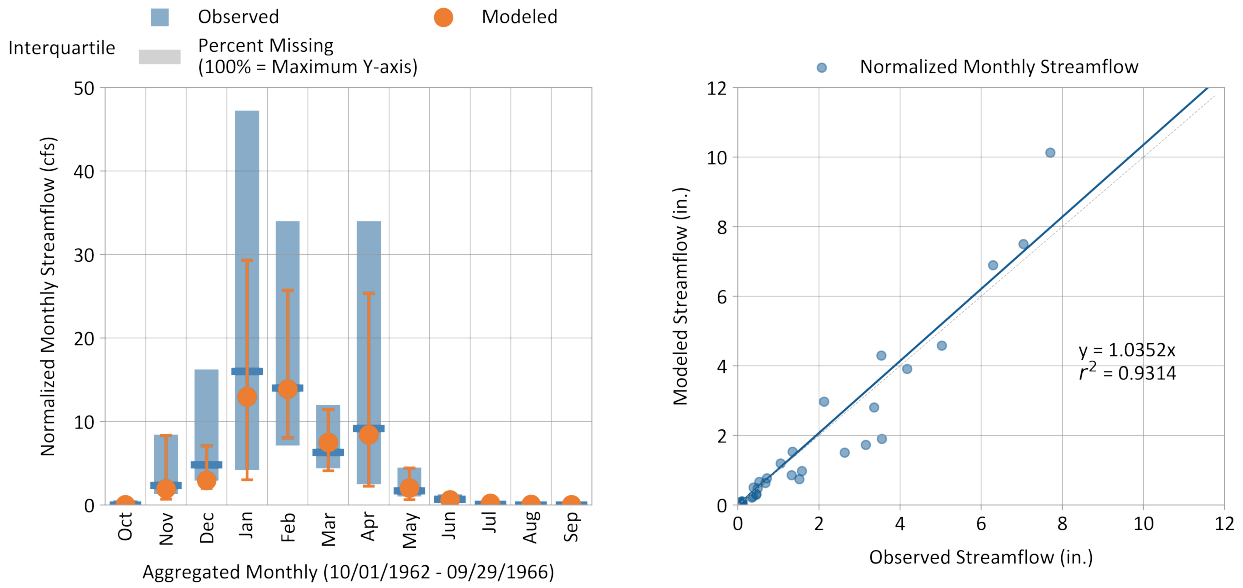

Figure 6-8. Monthly simulated vs. observed streamflow for SALMON C A BODEGA CA (11460920).

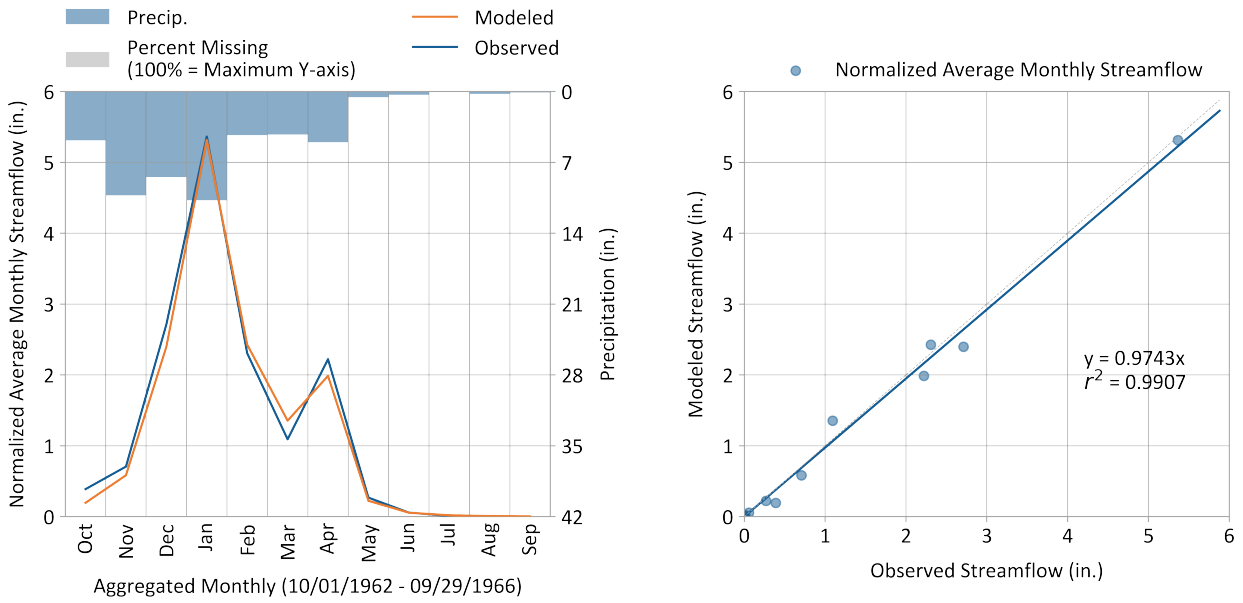

Figure 6-9. Average Monthly simulated vs. observed streamflow for SALMON C A BODEGA CA (11460920).

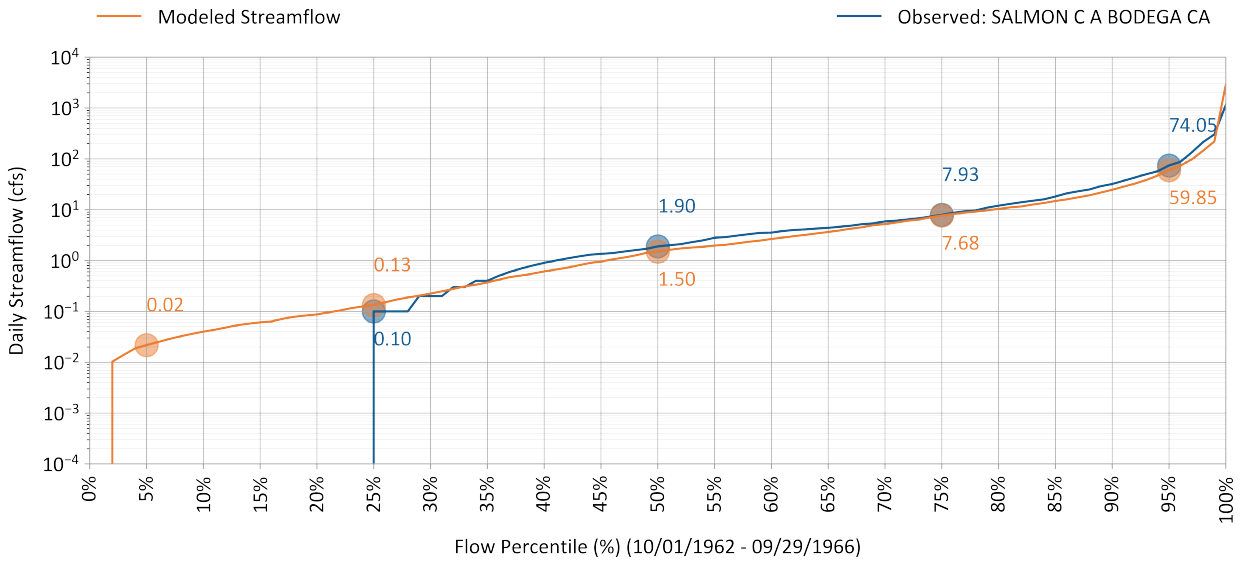

Figure 6-10. Simulated vs. observed flow duration curve for SALMON C A BODEGA CA (11460920).

PBIAS, NSE, and RSR performance values by season and flow regime are shown in Table 6-10, Table 6-11, and Table 6-12, respectively. The "Days Categorized as Baseflow" metric is derived from hydrograph separation. Figure 6-11 and Figure 6-12 show simulated vs. observed sliding-interval hydrograph separation for water year 1966 wet and dry seasons, respectively.

In the Salmon Creek watershed, 93% of rainfall occurs during the days with the highest 50% of flow, and only 25% of days within the lowest 50% of flows are in the wet season. For this unique watershed, flow rates are relatively small. As shown in Figure 6-10, measured flow rates are less than 2.0 cfs more

than half of the time. Greater uncertainty is likely present in flow monitoring at low flows, particularly since values below 0.01 cfs were recorded as zero, introducing additional sources of error. These uncertainties contribute to reduced model performance during low-flow conditions. However, as indicated by the FDC, the current calibrated mode predicts streamflow during low flow conditions well, which benefits management scenarios focused on maintaining minimal flows.

Table 6-10. Simulated vs. observed daily streamflow PBIAS at SALMON C A BODEGA CA (11460920)

Calibration Metrics *(10/01/1962 - 09/29/1966)*	Percent Bias (PBIAS)		
	All Seasons	Wet Season	Dry Season
All Conditions	3.7%	3.6%	8.5%
Highest 10% of Daily Flow Rates	2.8%	2.8%	N/A
Days Categorized as Storm Flow	14.8%	14.8%	10.1%
Days Categorized as Baseflow	-14.1%	-15.3%	8.3%

Table 6-11. Simulated vs. observed daily streamflow NSE at SALMON C A BODEGA CA (11460920)

Calibration Metrics *(10/01/1962 - 09/29/1966)*	Nash-Sutcliffe Efficiency (E)		
	All Seasons	Wet Season	Dry Season
All Conditions	0.05	0.0	0.85
Highest 10% of Daily Flow Rates	-0.51	-0.51	N/A
Days Categorized as Storm Flow	-0.04	-0.11	0.94
Days Categorized as Baseflow	-0.02	-0.11	0.84

Table 6-12. Simulated vs. observed daily streamflow RSR at SALMON C A BODEGA CA (11460920)

Calibration Metrics *(10/01/1962 - 09/29/1966)*	SMSE-Std-Dev. Ratio (RSR)		
	All Seasons	Wet Season	Dry Season
All Conditions	0.97	1.0	0.39
Highest 10% of Daily Flow Rates	1.23	1.23	N/A
Days Categorized as Storm Flow	1.02	1.05	0.24
Days Categorized as Baseflow	1.01	1.05	0.4

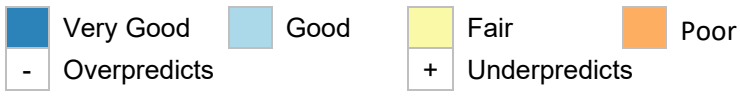

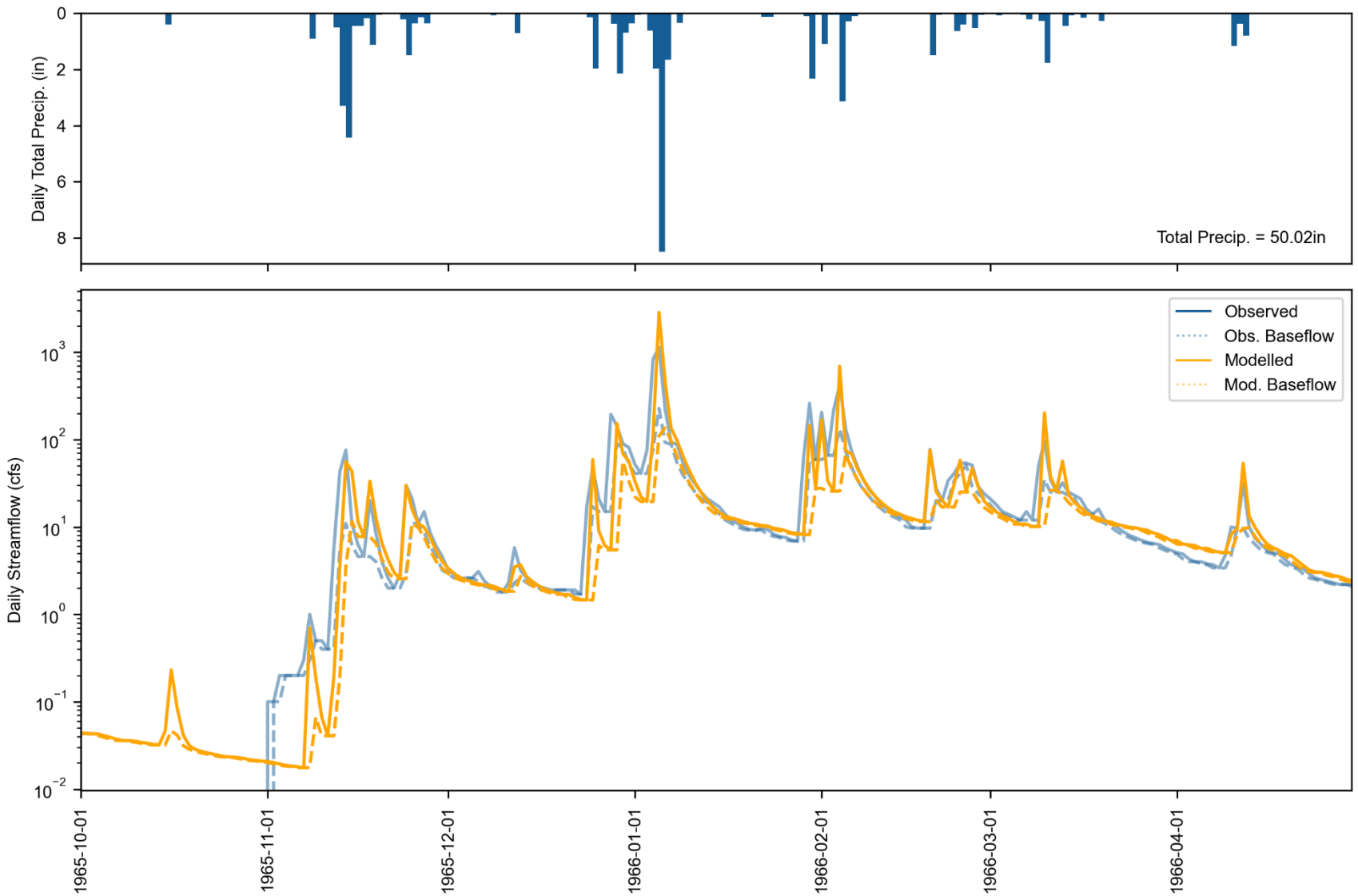

Figure 6-11. Water Year 1966 Wet season daily total precipitation (top) and streamflow (bottom) at SALMON C A BODEGA CA (11460920). Observed and simulated baseflow are calculated with HYSEP.

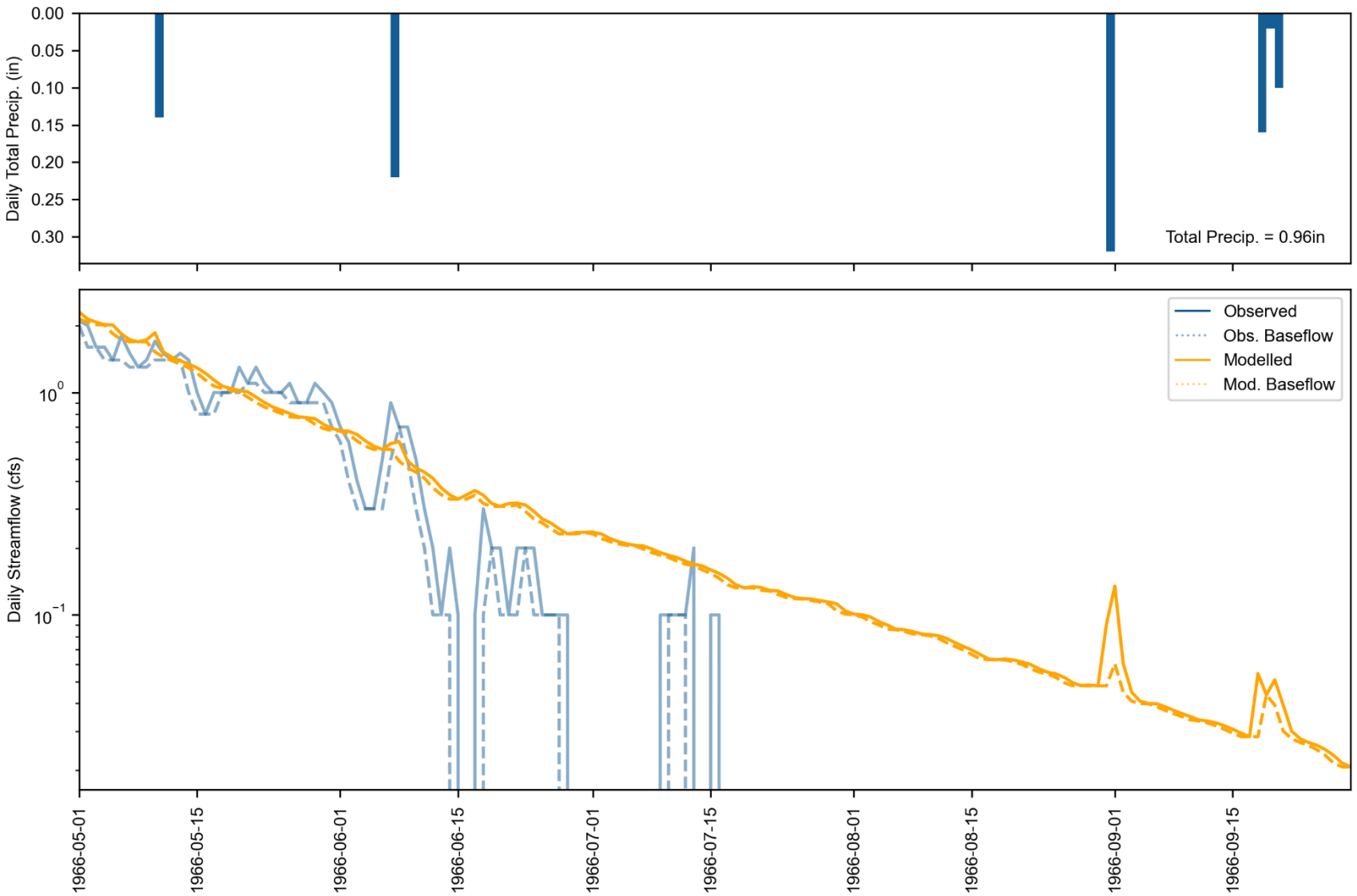

Figure 6-12. Water Year 1966 Dry season daily total precipitation (top) and streamflow (bottom) at SALMON C A BODEGA CA (11460920). Observed and simulated baseflow are calculated with HYSEP.

7 MODEL VALIDATION

The model was calibrated for water years 1963-1966 (4 years) and validated for water years 1967-1969 (the following 3 years). The precipitation data processing workflow involves converting daily observed precipitation values into hourly data using the gridded NLDAS hourly distribution, as outlined in Section 4.1.1. For historical data prior to 1979, there is no available gridded hourly data. Therefore, the hourly distribution from the San Francisco International Airport NOAA station (WBAN:23234) was used to break down daily observed precipitation into hourly values. While observed streamflow data is accessible through 1975, the validation period is limited to 1969 due to the absence of hourly precipitation data at WBAN:23234 from January 1, 1970, to December 31, 1972. As a result, precipitation data was processed only for the historical period from 1961 to 1969.

No withdrawals were applied during the validation period. First, a water budget analysis was conducted for the calibration period. Next, the irrigation water budget was confirmed by normalizing associated inputs and outputs by total irrigated area. This validation check was to confirm that the applied irrigation water, as represented using the coefficients, rates, and methods described in Section 5.1 produced a reasonable and representative average monthly distribution relative to the precipitation and evapotranspiration meteorological forcing data. Irrigation was simulated for the full period from 1963-1969. This section presents results for the water budget analysis (Section 7.1), the validation period performance at the USGS flow station (Section 7.2), and a comparison of flow rates between the calibration USGS flow station and reference USGS flow station (Section 7.3)

7.1 Water Budget

A water budget analysis was conducted to validate a match between the sum of model inputs and outputs. Water inputs include precipitation (both to land segments and water body surfaces) and applied irrigation water. Water outputs include terminal outflow at our assessment point for Salmon Creek, total actual evapotranspiration (from land segments + direct evaporation from water bodies), and total withdrawals (i.e., irrigation and non-irrigation diversion). The water budget was calculated from October 1962 through September 1966, which is the calibration period. The water budget validation showed a close match between all model inputs and outputs—there is a 0.04% difference between inflow and outflow, which represents net volume to system storage over the 4-year simulation period. Figure 7-1 shows the simulated water balance expressed as total volumes and area-normalized annual average depths for water years 1963-1966 at the Salmon Creek flow station.

Figure 7-2 shows monthly average area-normalized simulated water balance components for the same period. In both figures, intermediate values for edge-of-stream outflows prior to stream routing (i.e., surface runoff + interflow outflow + active groundwater outflow) and inflow to active groundwater storage are presented to illustrate the relative scale of those components. The monthly summary also illustrates the expected system lag of approximately 5 months between peak rainfall (Nov-Jan) and peak evapotranspiration (Apr-May).

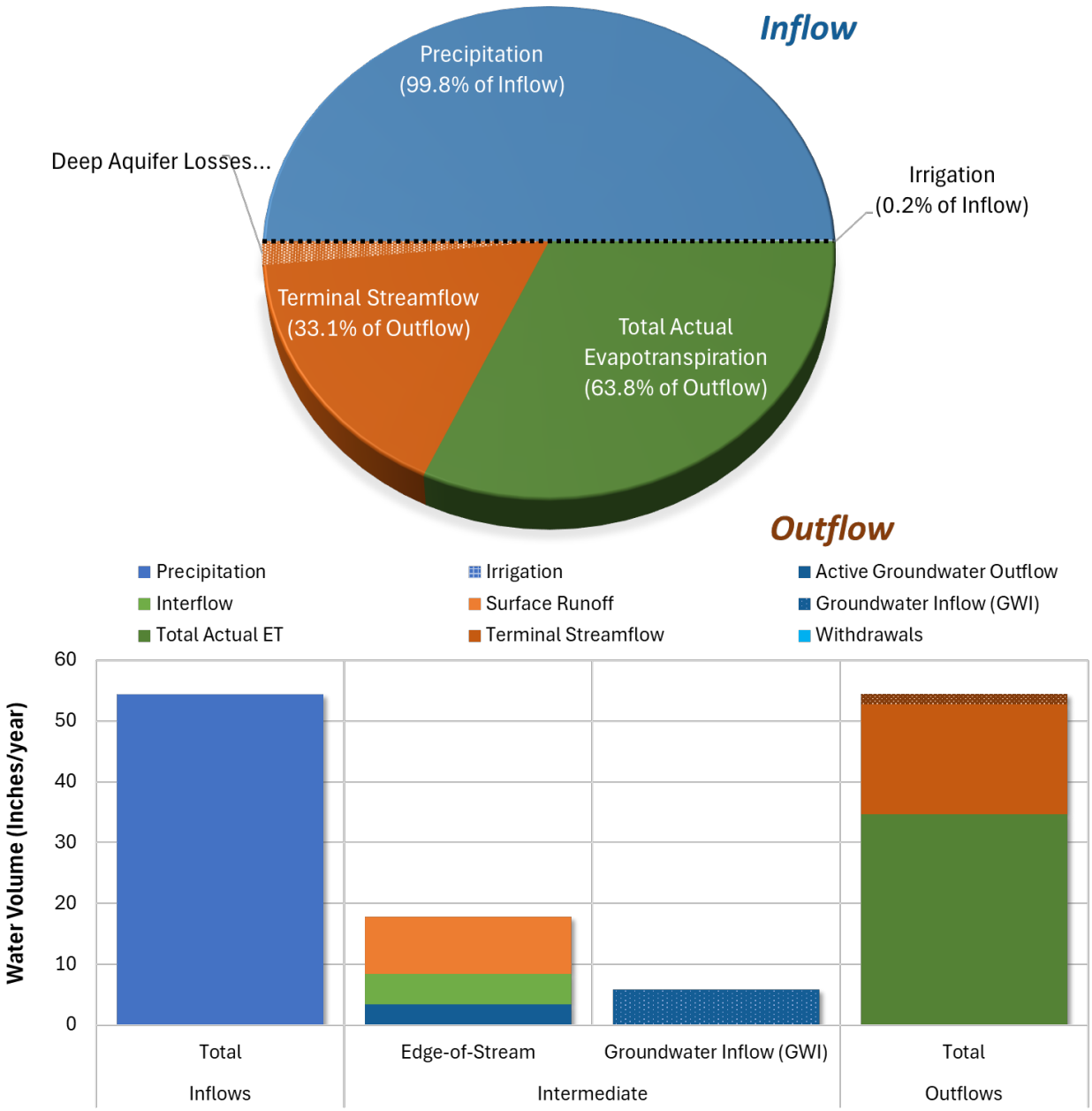

Figure 7-1. Simulated water balance expressed as total volumes and area-normalized annual average depths for the calibration period (water years 1963-1966) at the SALMON C A BODEGA CA (11460920) station.

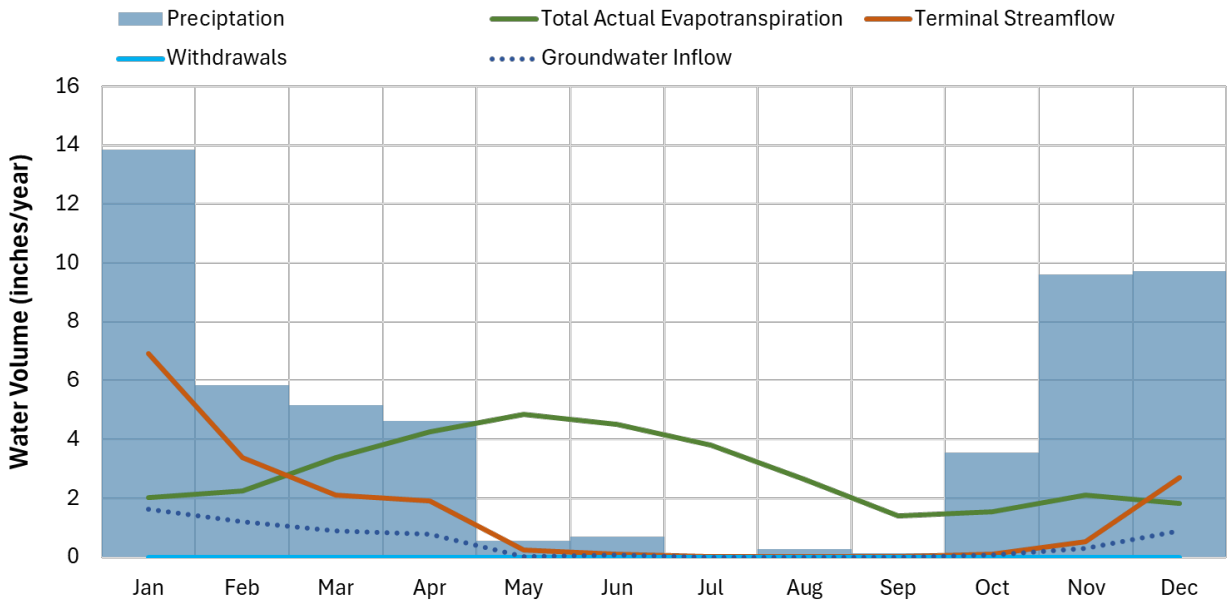

Figure 7-2. Monthly average area-normalized simulated water balance components for water years 1963-1966 at the SALMON C A BODEGA CA (11460920) station. Note that no withdrawals are applied during the calibration period and are discussed in detail in Section 5.

The water budget for applied irrigation volume was also summarized from calibrated model outputs. On average, a total of 19 acre-feet of irrigation water per year was applied on 61 acres of agricultural land in the Salmon Creek model. Irrigation volume was temporally distributed as 41% of potential evapotranspiration so that more irrigation occurred during the drier months, as shown in Figure 7-3. As no withdrawals were applied during the calibration period, the irrigation water applied was assumed to be sourced from groundwater.

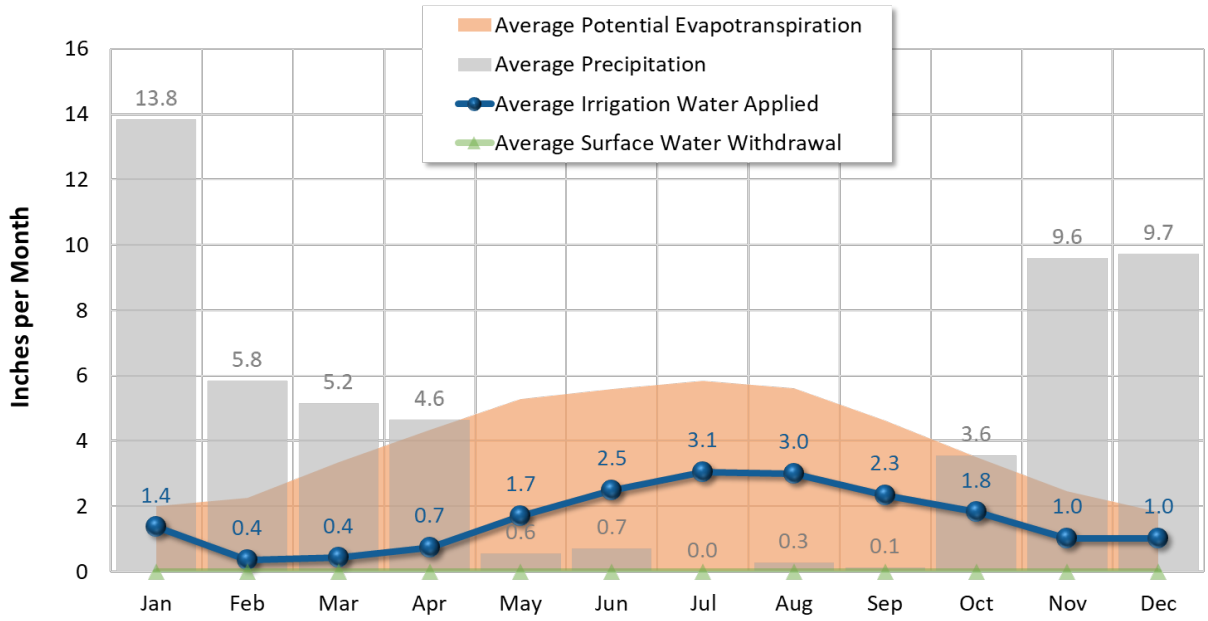

Figure 7-3. Monthly average area-normalized irrigation water balance for irrigated HRUs in the Salmon Creek watershed upstream of 11460920 (average precipitation in the watershed is also plotted for reference).

7.1.1 ET Comparison

Because the Salmon Creek watershed only has one streamflow station for estimating water balance components, evapotranspiration data from OpenET was considered as an alternate source of "observed" evapotranspiration data for validating the simulated spatial distribution and variability of a key predicted model component of the water budget upstream of the streamflow station. The OpenET project is an operational system for generating and distributing ET data at a field scale using an ensemble of six well-established satellite-based approaches for mapping ET (Melton et al. 2022). Within California, OpenET has data beginning in 1999 and uses CIMIS meteorological datasets to compute reference ET and actual ET. OpenET has undergone extensive intercomparison and accuracy assessment conducted using ground measurements of ET. For agricultural areas, results of these assessments demonstrate strong agreement between the satellite-driven ET models and observed flux tower ET data; however, for natural land covers like forests, scrub, and grasslands, which are the dominant land cover types in the Salmon Creek watershed (Table 7-1), the OpenET ensemble is known to be biased towards overprediction (OpenET 2021). OpenET data were used in an exploratory comparison with simulated total actual ET (TAET) and the CIMIS reference ET at the HUC-12 scale and were not used for calibration because of the known biases. In highly agricultural watersheds, OpenET could prove to be a valuable data point for model calibration and validation, however, in the Salmon Creek watershed, OpenET closely resembles CIMIS reference ET.

For the Salmon Creek watershed, monthly total OpenET, CIMIS reference ET, and LSPC TAET by HUC-12 and watershed-wide were compared for the period with available OpenET data (October 2003 – September 2023). As seen in Figure 7-4, OpenET is similar in magnitude and timing to the CIMIS reference ET and both data sets are high, as expected for reference ET. When estimated as annual average observed precipitation minus annual average observed streamflow, actual ET (and a storage component) is approximately 67% of the outflow portion of the water budget. This is close to the simulated value of 65% from the calibration period (see Section 7.1) and 60% for the OpenET period.

In the Salmon Creek watershed, ET datasets were compared as the annual average totals for: (1) OpenET, (2) TAET, (3) PEVT (CIMIS reference ET), and (4) PREC. These comparisons are shown as bar charts in Figure 7-5 and indicate that TAET is 79% of OpenET, OpenET is 96% of CIMIS reference ET, and total annual precipitation is 128% of OpenET (Figure 7-5)—note the inverted phase shift between the two (Figure 7-4).

Table 7-1. Summary of HRU area grouped by land cover for HUC-12s within the Salmon watershed

HUC-12		HRU Land Cover Area (%)									
Name	Area (ac)	Developed Impervious	Developed Pervious	Barren	Forest	Scrub	Grassland	Pasture	Agriculture	Irrigation	Water
Salmon Creek	22,396	0.09%	5.34%	0.00%	47.48%	25.69%	10.18%	8.35%	2.48%	0.27%	0.11%

Color Gradient: Lowest | Low | Med | High | Highest

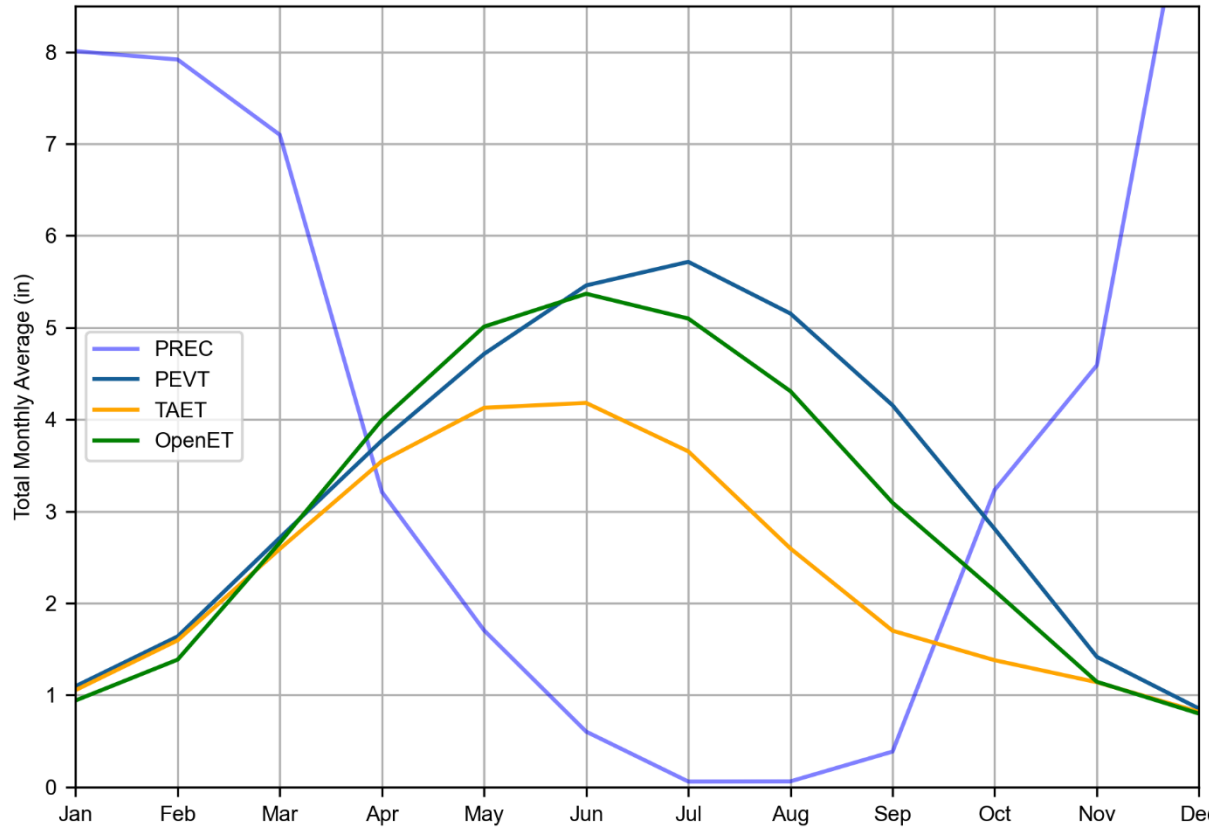

Figure 7-4. Comparison of average monthly totals from October 2003 – September 2023 for rainfall (PREC), potential ET (PEVT), OpenET, and simulated total actual ET (TAET) for the Salmon Creek watershed.

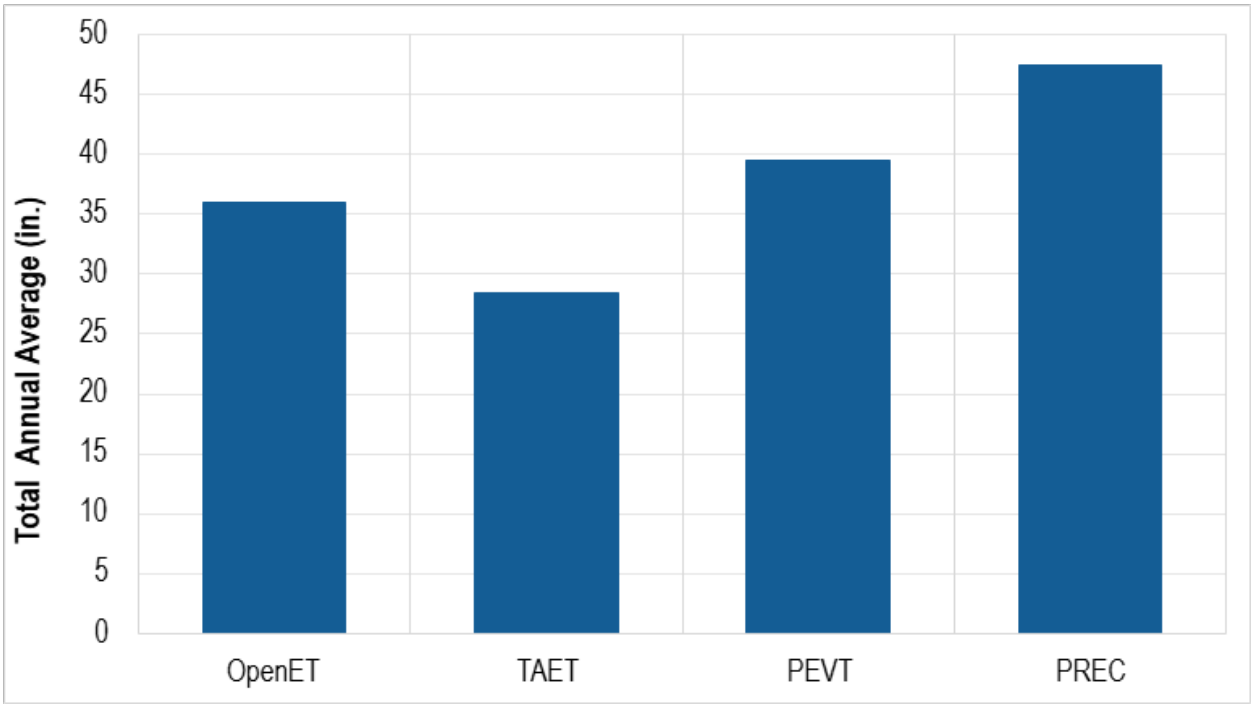

Figure 7-5. Annual average OpenET, simulated total actual ET (TAET), CIMIS reference ET (PEVT), and annual average precipitation (PREC) within the Salmon Creek watershed.

7.2 Hydrology

Across the validation period (water years 1967 to 1969) hydrologic performance was similar to the calibration period. Note that in all results, modeled flows less than 0.01 cfs were set to 0 to match the detection limit of the observed flows. Over the validation period, PBIAS is "Very Good" and slightly overpredicted while seasonal PBIAS values were "Good" to "Very Good" (Table 7-2 and Table 7-4). However, NSE and RSR indicate poor performance, particularly during the wet season (Table 7-2, Table 7-5 and Table 7-6); All these validation metrics were computed using daily average time series and included higher resolution flow-regime metrics like the highest 10% of flows, storm flows, and baseflow. As discussed in Section 6.3, using hourly precipitation data from a distant station introduces timing uncertainties into the daily modeling results. To reduce the influence of these uncertainties, model performance with monthly flow data was evaluated. Table 7-3 is a summary of model calibration vs. validation performance metrics computed using monthly time series, as recommended by Moriasi et al. (2015). As expected, PBIAS is not impacted by the time step change; however, both RSR and NSE, which are timing sensitive, show notable performance improvement compared to using daily average time series.

As with the calibration period, flow time series plots, monthly aggregate figures, and the FDC were also created for the validation period, and are shown in Figure 7-6 to Figure 7-10. Figure 7-11 and Figure 7-12 show simulated vs. observed sliding-interval hydrograph separation for water year 1967 wet and dry seasons, respectively. Overall, the simulated flow rates show good agreement with the observed flow rates.

Table 7-2. Summary of daily validation performance metrics for validation period (WY 1967 – 1969).

Hydrology Monitoring Locations	Performance Metrics (10/1/1966 – 9/30/1969)														
	PBIAS						RSR			NSE			KGE[1]		
	All	Wet Season	Dry Season	>10th %ile Flows	Storm Flows	Baseflow	All	Wet Season	Dry Season	All	Wet Season	Dry Season	All	Wet Season	Dry Season
SALMON C A BODEGA CA	-0.02%	0.20%	-10.69%	2.16%	11.82%	-16.02%	0.70	0.73	0.62	0.50	0.46	0.61	0.97	0.95	0.87

1. Monthly, as specified in Table 6-2.

Very Good | Good | Fair | Poor

\- Overpredicts | + Underpredicts

Table 7-3. Summary of calibration and validation performance metrics using monthly average.

Calibration Metrics for Monthly Flow	Calibration: 10/01/1962 - 09/29/1966			Validation: 10/01/1966 - 09/30/1969		
	All	Wet Season	Dry Season	All	Wet Season	Dry Season
Count:	48	28	20	36	21	15
PBIAS	3.70%	3.60%	8.50%	0.00%	0.20%	-10.70%
RSR	0.29	0.34	0.26	0.21	0.25	0.34
NSE	0.91	0.88	0.93	0.95	0.94	0.88
KGE	0.89	0.85	0.82	0.97	0.95	0.87

1. RSR is the ratio of the root-mean-square error to the standard deviation of observations

Very Good Good Fair Poor

\- Overpredicts + Underpredicts

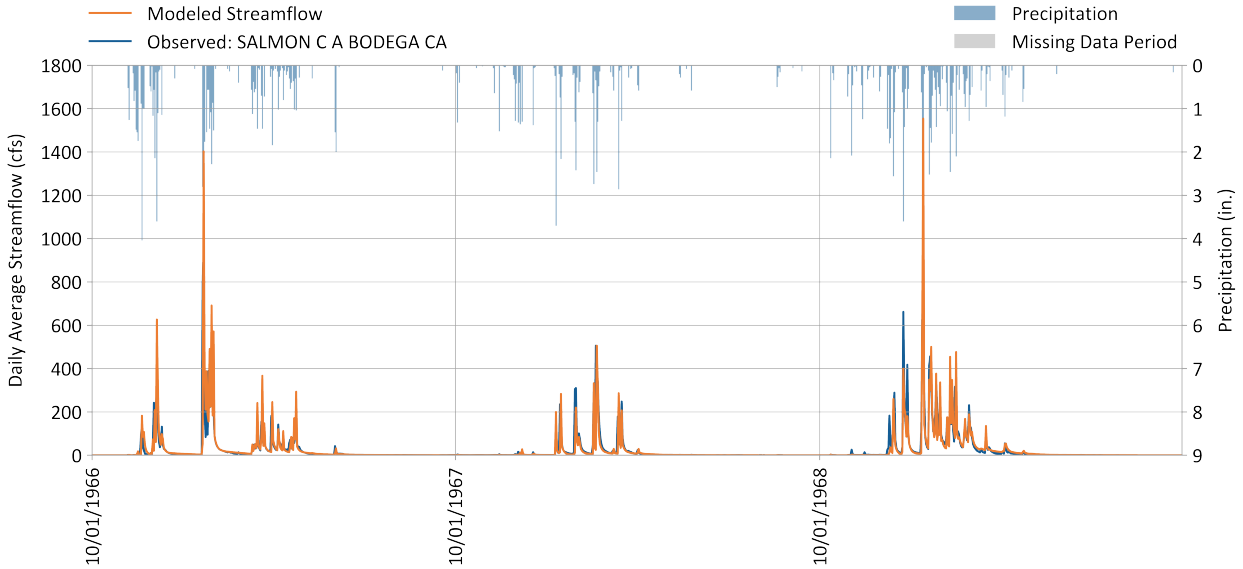

Figure 7-6. Daily simulated vs. observed streamflow for SALMON C A BODEGA CA (11460920).

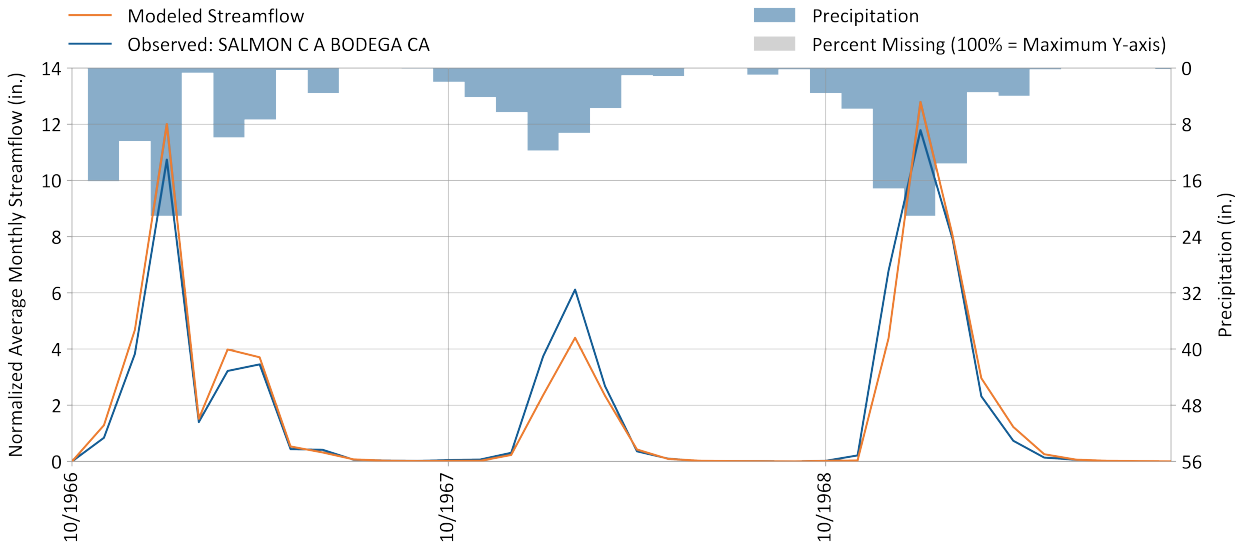

Figure 7-7. Monthly simulated vs. observed streamflow for SALMON C A BODEGA CA (11460920).

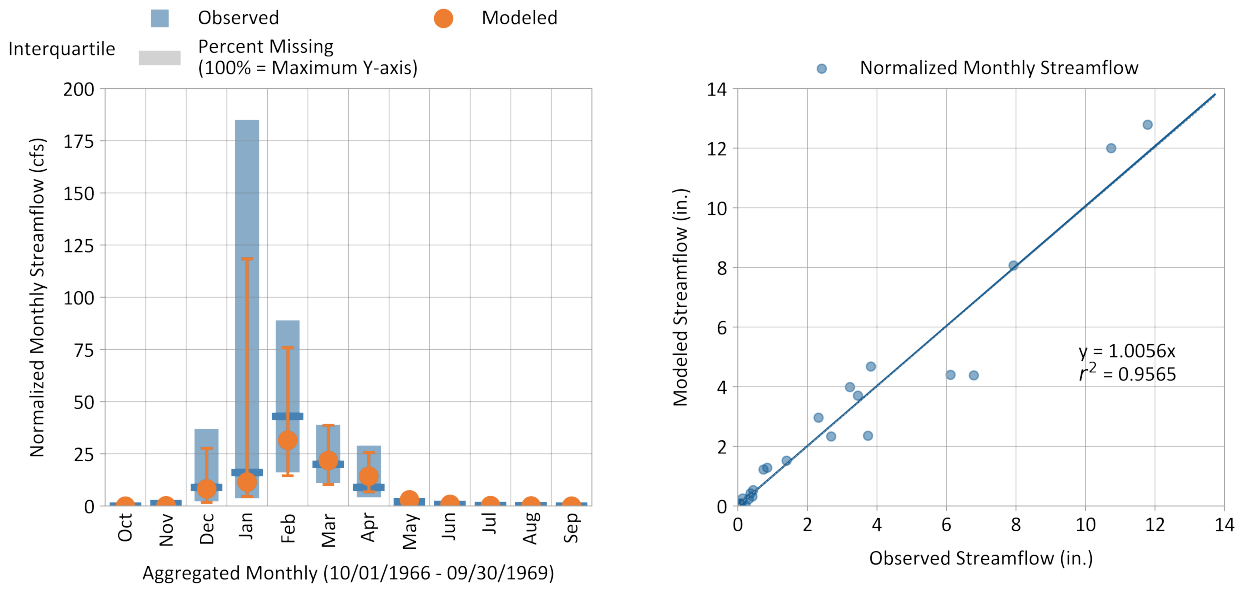

Figure 7-8. Monthly simulated vs. observed streamflow for SALMON C A BODEGA CA (11460920)

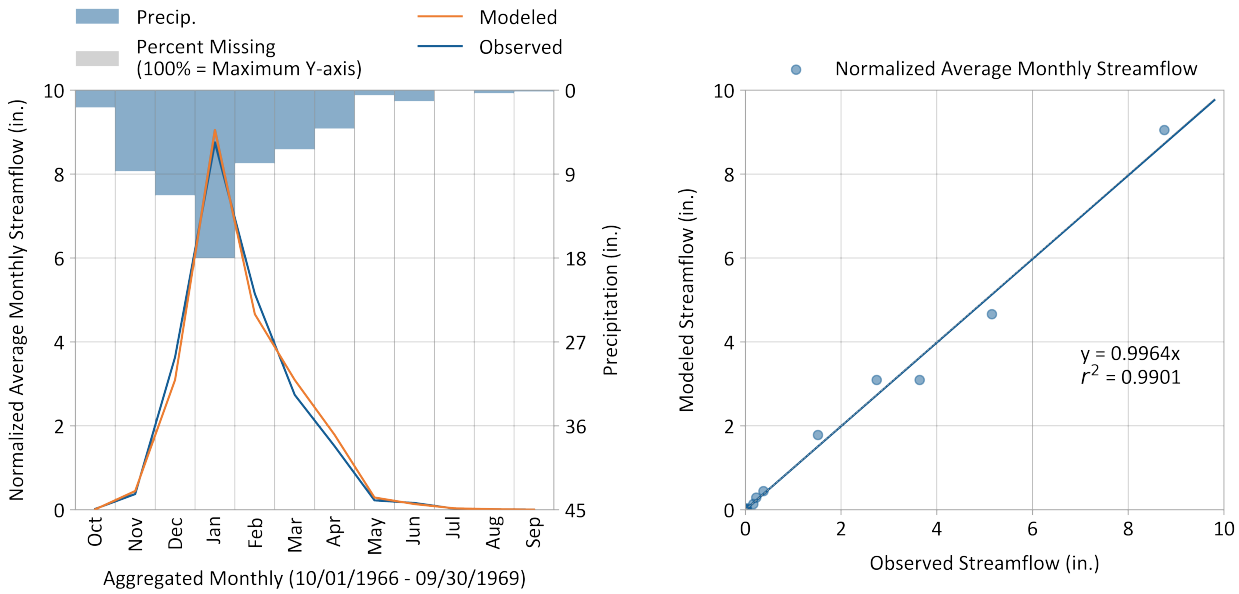

Figure 7-9. Average monthly simulated vs. observed streamflow for SALMON C A BODEGA CA (11460920).

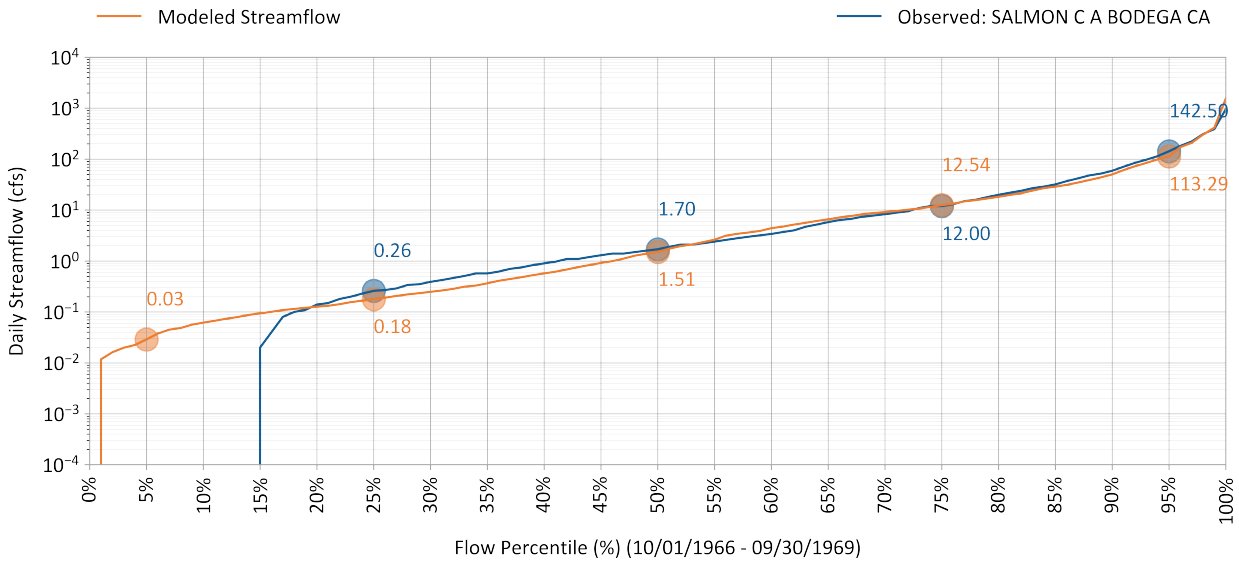

Figure 7-10. Simulated vs. observed flow duration curve for SALMON C A BODEGA CA (11460920).

Table 7-4. Simulated vs. observed daily streamflow PBIAS at SALMON C A BODEGA CA (11460920)

Validation Metrics *(10/01/1966 - 09/30/1969)*	Percent Bias (PBIAS)		
	All Seasons	Wet Season	Dry Season
All Conditions	-0.0%	0.2%	-10.7%
Highest 10% of Daily Flow Rates	2.2%	2.2%	N/A
Days Categorized as Storm Flow	11.8%	11.7%	24.0%
Days Categorized as Baseflow	-16.0%	-15.9%	-20.7%

Table 7-5. Simulated vs. observed daily streamflow NSE at SALMON C A BODEGA CA (11460920)

Validation Metrics *(10/01/1966 - 09/30/1969)*	Nash-Sutcliffe Efficiency (E)		
	All Seasons	Wet Season	Dry Season
All Conditions	0.5	0.46	0.61
Highest 10% of Daily Flow Rates	-0.15	-0.15	N/A
Days Categorized as Storm Flow	0.45	0.37	0.43
Days Categorized as Baseflow	0.53	0.49	0.86

Table 7-6. Simulated vs. observed daily streamflow RSR at SALMON C A BODEGA CA (11460920)

Validation Metrics *(10/01/1966 - 09/30/1969)*	SMSE-Std-Dev_Ratio (RSR)		
	All Seasons	Wet Season	Dry Season
All Conditions	0.7	0.73	0.62
Highest 10% of Daily Flow Rates	1.07	1.07	N/A
Days Categorized as Storm Flow	0.74	0.8	0.76
Days Categorized as Baseflow	0.69	0.72	0.37

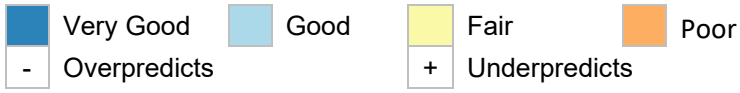

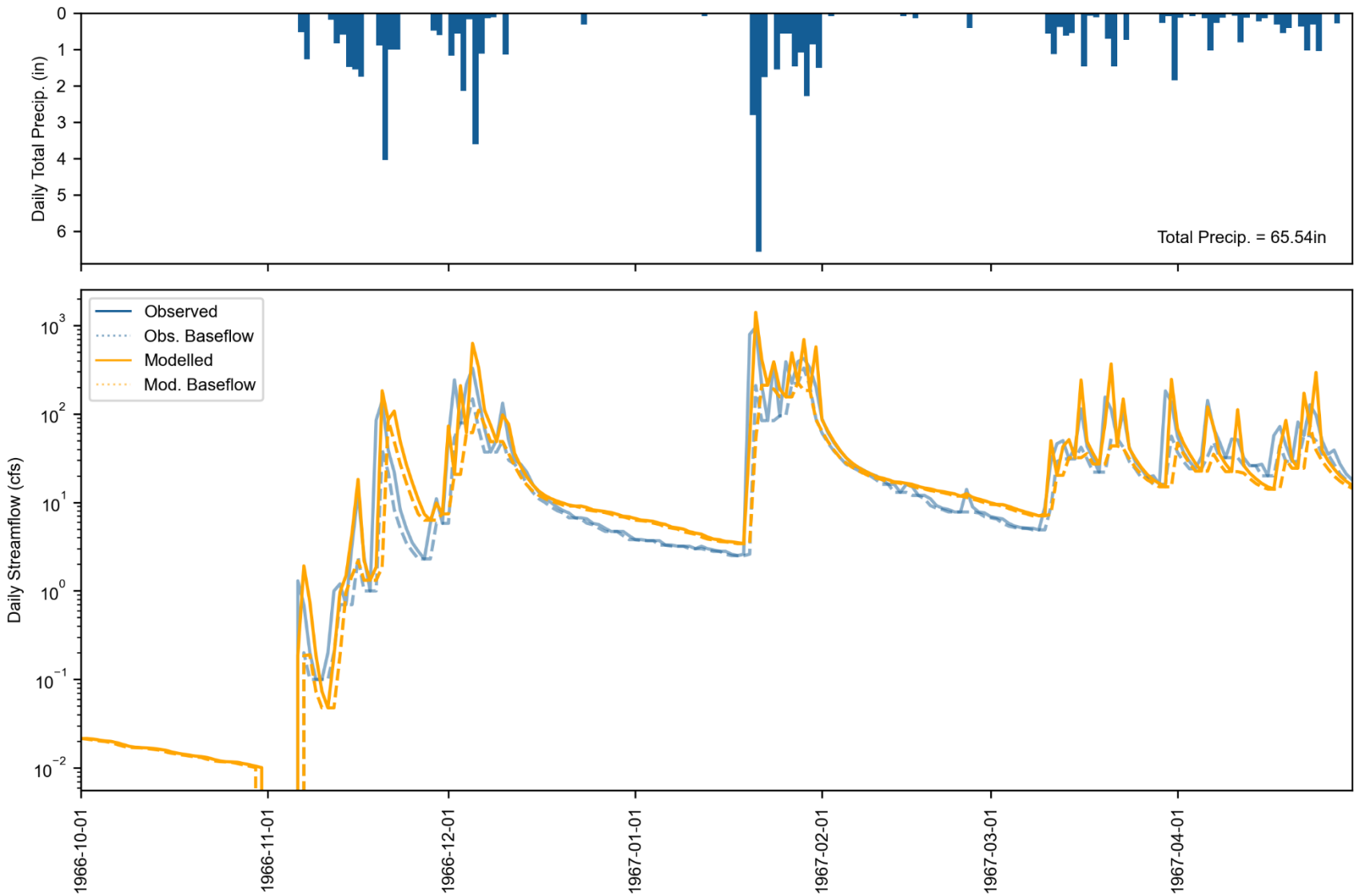

Figure 7-11. Water Year 1967 Wet season daily total precipitation (top) and streamflow (bottom) at SALMON C A BODEGA CA (11460920). Observed and simulated baseflow are calculated with HYSEP.

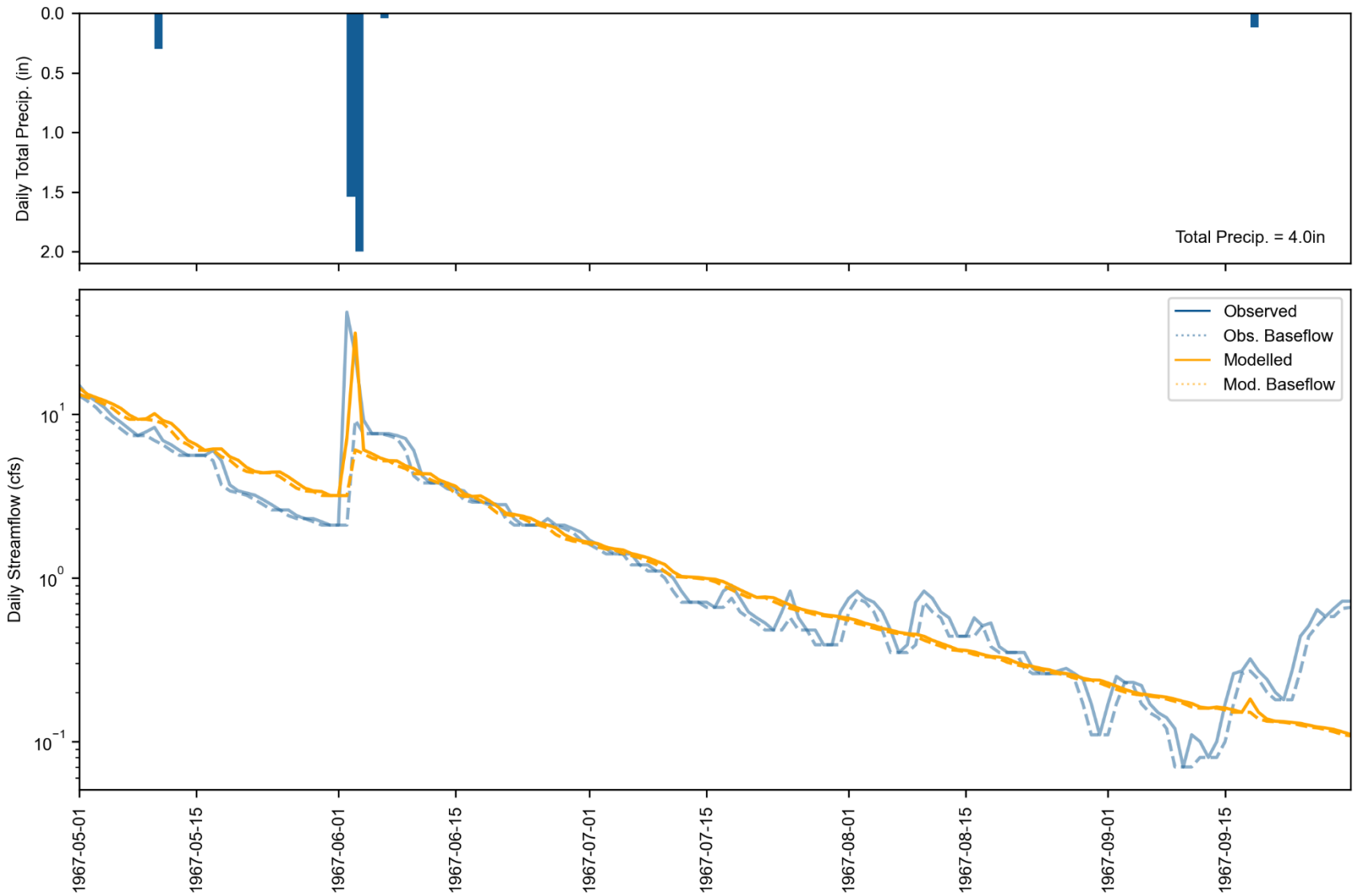

Figure 7-12. Water Year 1967 Dry season daily total precipitation (top) and streamflow (bottom) at SALMON C A BODEGA CA (11460920). Observed and simulated baseflow are calculated with HYSEP.

7.3 Comparison to Reference USGS Flow Station

Since the calibration flow station in Salmon Creek (USGS 11460920) is no longer active and lacks recent flow rate data, the recent years (calendar years 2005 through 2023) were selected for independent model validation by comparing the modeled flow in Salmon Creek to observed flow at a reference flow station, Austin Creek near Cazadero, CA (USGS 11467200). Those two USGS flow stations are shown in Figure 6-4 and Table 6-1. The USGS flow station 11467200 lies north of the Salmon Creek watershed. The drainage area of this station is dominated by forest, and covers about 62.8 mi², which is approximately four times the size of USGS 11460920. This station has been active since 6/1/1959, although data gaps exist between 9/30/1966 and 9/30/2003. A comparison of watershed characteristics for the Salmon Creek watershed and the Austin Creek watershed is summarized in Table 7-7.

The Austin Creek reference flow station was selected for the following reasons:

- It features land cover characteristics similar to those of Salmon Creek.
- Its proximity to USGS 11460920 suggests that it likely shares similar meteorological and geological conditions.
- It is currently active, with continuous flow rate data available through the present.

Table 7-7. Characteristics of calibration (USGS 11460920) and reference (USGS 11467200) stations

Comparison (8/1/1962 - 9/29/1966)	USGS 11460920	USGS 11467200
Drainage Area (mile^2)	15.7	62.8
Dominate Landuse	Forest	Forest
Data Coverage	8/1/1962 - 10/1/1975	6/1/1959 - 2/10/2025 (no data between 9/30/1966 - 9/30/2003)
Maximum Flow (cfs)	1140	7870
Minimum Flow (cfs)	0	0.1
Mean Annual Precipitation (in.)	47.5	64.08
Mean Elevation (ft)	460	1011
Forest Percentage	36.20%	54.90%
Lake/Ponds Percentage	0.05%	0.01%
Developed Land (Urban) Percentage	5.60%	2.30%
Impervious Percentage	0.30%	0.10%
CIMIS Zone	4	4

Linear regressions of monthly precipitation and flow volumes between the assessment points at Salmon Creek and Austin Creek were conducted during two periods:

- 8/1/1962 - 9/29/1969, the full period with flow data available at both the calibration and the reference USGS stations.
- 1/1/2005 – 12/31/2023, the long-term recent period.

In this analysis, precipitation and flow volumes from both watersheds were normalized by their respective drainage areas to eliminate bias due to differences in watershed size. Intercepts were set to zero, and slopes were primarily used to compare precipitation and flow volumes between the two locations. Linear regressions for precipitation and flow volumes are shown in Figure 7-13 and Figure 7-14, respectively. As shown in Figure 7-13, precipitation depths in the Salmon Creek watershed are consistently lower than those in the Austin Creek watershed. On average, precipitation in the Salmon Creek watershed is approximately 80% of that in the Austin Creek watershed for both analyzed periods. For the flow volume comparisons, two linear regressions were performed for the period from 8/1/1962 to 9/29/1969: one comparing measured monthly flow depths in Salmon Creek to measured monthly flow depths in Austin Creek, and the other comparing modeled monthly flow depths in Salmon Creek to measured monthly flow depths in Austin Creek. For the more recent period from 1/1/2005 to 12/31/2023, due to the absence of measured flows at Salmon Creek, only one regression was conducted to compare modeled monthly flow depths in Salmon Creek to measured values in Austin Creek. All three regressions yielded comparable slope values, indicating consistently lower flow depths in Salmon Creek, which are approximately half of those observed in Austin Creek.

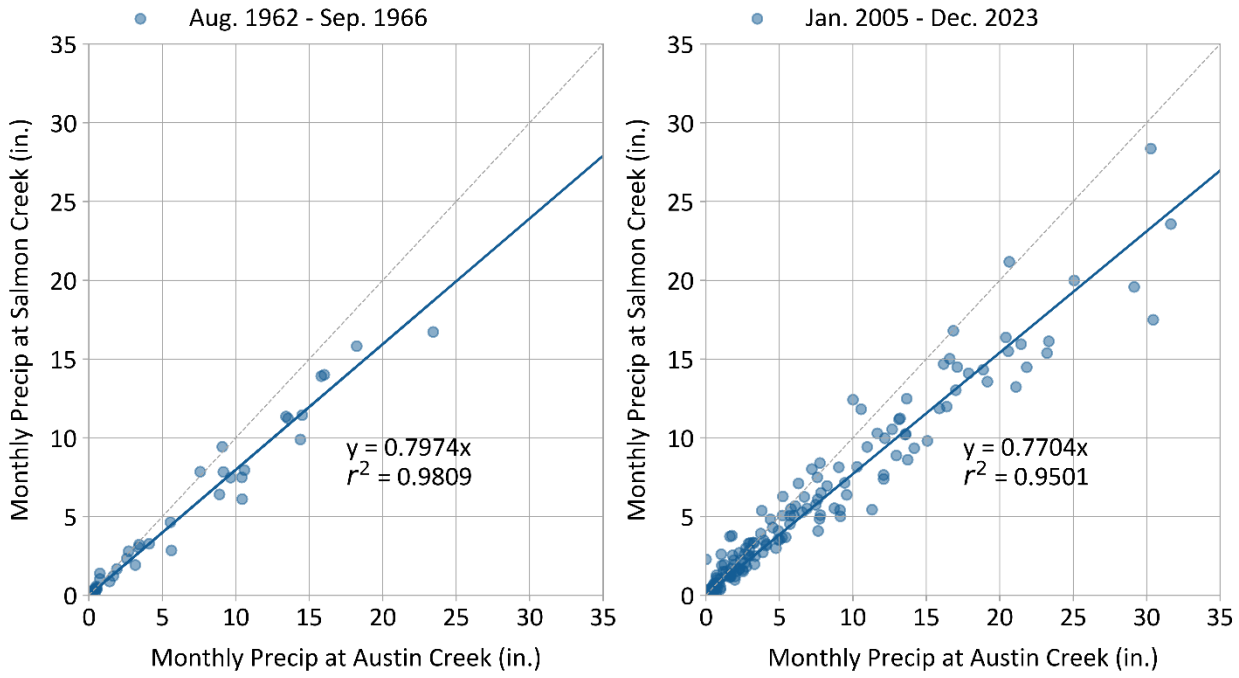

Figure 7-13. Linear regression of monthly precipitation between SALMON C A BODEGA CA (11460920) and AUSTIN C NR CAZADERO CA (11467200) during the calibration period (left) and recent long-term period (right).

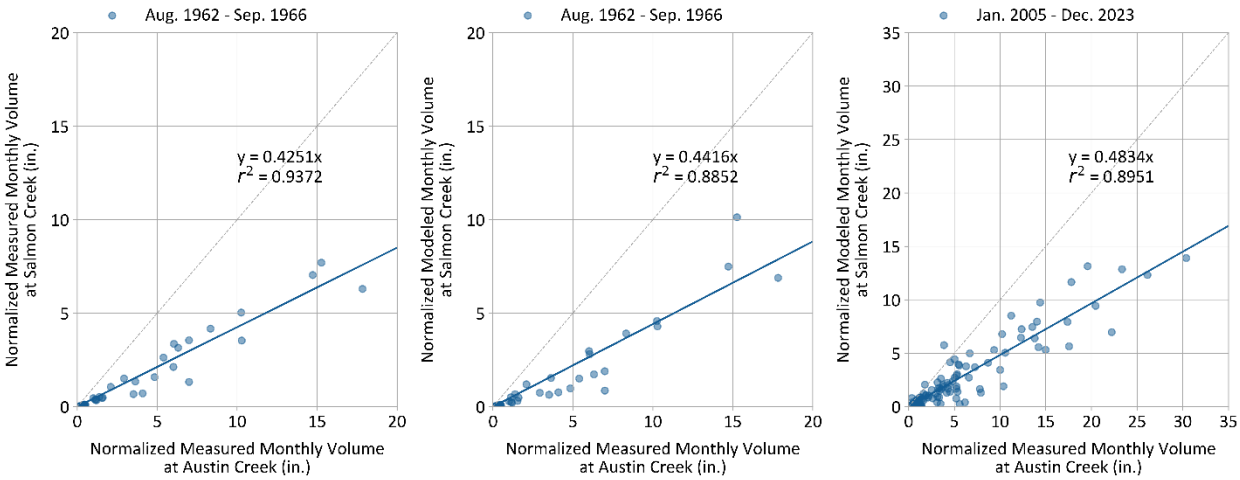

Figure 7-14. Linear regression of monthly flow volumes between SALMON C A BODEGA CA (11460920) and AUSTIN C NR CAZADERO CA (11467200).

Additional linear regressions were conducted on monthly storm flow volumes estimated using two methods. In the first method, storm volumes were separated from total flow using the HYSEP function, which partitions streamflow into baseflow and surface runoff components (Sloto and Crouse 1996). In the second method, storm volumes were estimated as the total flow on days with recorded precipitation. The regression results are shown in Figure 7-15 and Figure 7-16. Both regressions are consistent with those based on total flow volumes and indicate that storm depths at the Salmon Creek

station are consistently lower, and the storm flow depths are approximately half of those observed at the Austin Creek station.

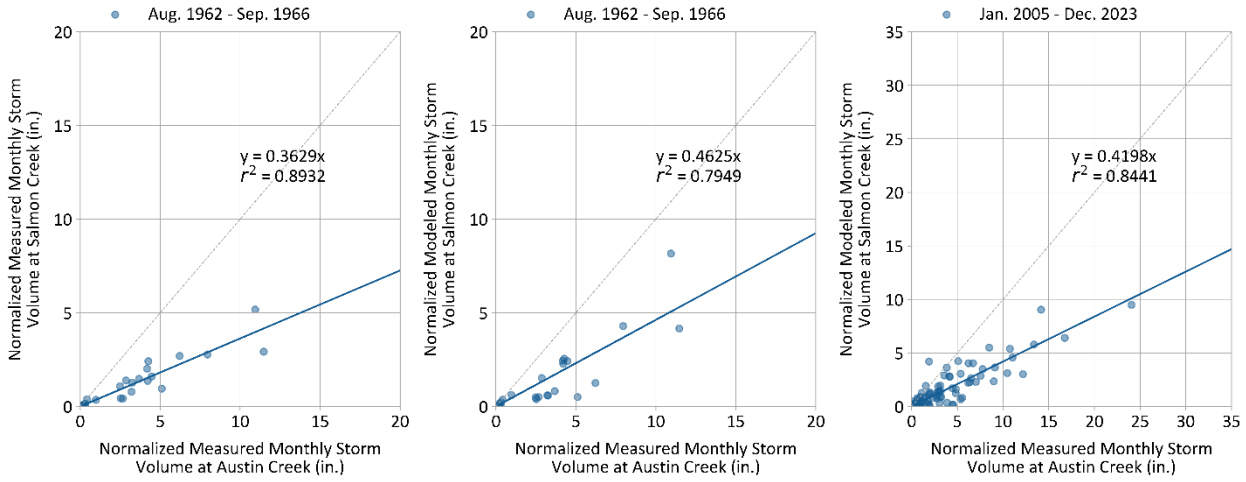

Figure 7-15. Linear regression of monthly storm volumes between SALMON C A BODEGA CA (11460920) and AUSTIN C NR CAZADERO CA (11467200). The storm volumes were estimated with HYSEP function.

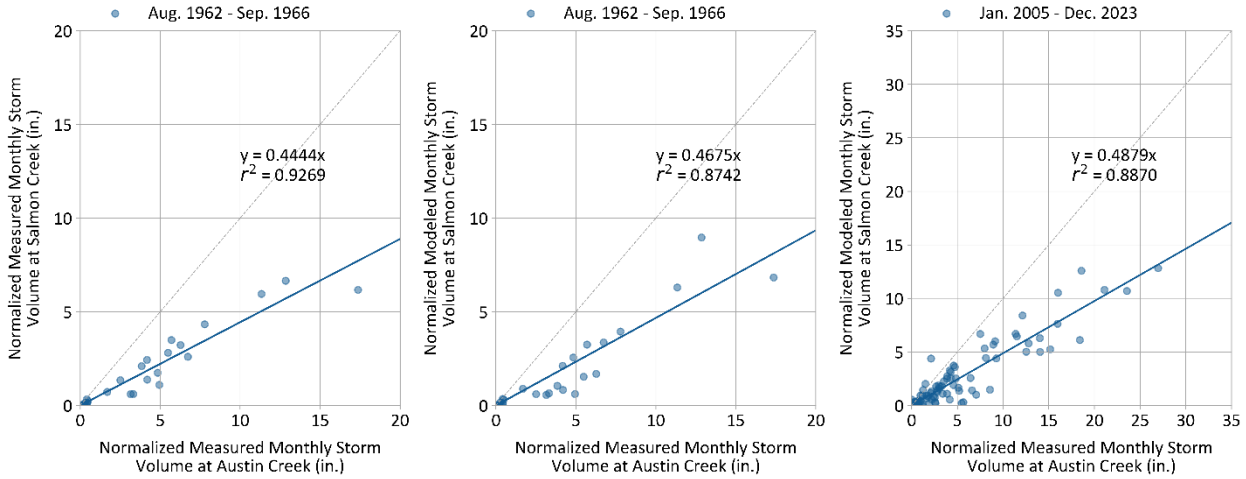

Figure 7-16. Linear regression of monthly storm volumes between SALMON C A BODEGA CA (11460920) and AUSTIN C NR CAZADERO CA (11467200). Storm volume is defined as the flow volume on rain days.

The changes in precipitation and flow rate in each watershed were calculated, and then the differences between the two watersheds were compared as an additional validation of the model's ability to capture temporal changes in flow rates. Two periods were selected for this analysis: the calibration period and a more recent period from 10/1/2019 to 9/29/2023. This period was selected to ensure an equal number of days in both periods. Figure 7-17 and Figure 7-18 are the FDC plots for observed flows at the Austin Creek station and modeled flows at the Salmon Creek station, respectively. Figure 7-19 presents the percentage change in flow rates in a bar chart. Flow rates were grouped into five bins from highest to lowest values: high flows, moist conditions, mid-range flows, dry conditions, and low

flows. At both stations, flow rates have declined in the recent period, with low flows reaching zero. At both locations, the low-flow regime shows the greatest reduction, followed by the dry and mid-range conditions. Table 7-8 lists the numeric flow rate reductions by flow regimes in recent years at both stations. On average, flow rates decreased by 37% at the Austin Creek station and 51% at the Salmon Creek station. These percentage reductions are comparable between the two stations. The reductions in flow rates can be attributed to decreases in precipitation over these two periods. As shown in Table 7-9, the average precipitation decreased by 25% in the Austin Creek watershed and 31% in the Salmon Creek watershed. The greater reduction in precipitation in the Salmon Creek watershed aligns with the larger flow rate reductions observed at the Salmon Creek station.

The comparison to the reference station shows that the magnitude differences between the modeled flows at the calibration station and those at the reference station are relatively consistent across both the earlier period, which includes the calibration and validation periods, and the more recent period.

Despite these magnitude differences, the modeled flows at the calibration station exhibit similar temporal patterns to those observed at the reference station.

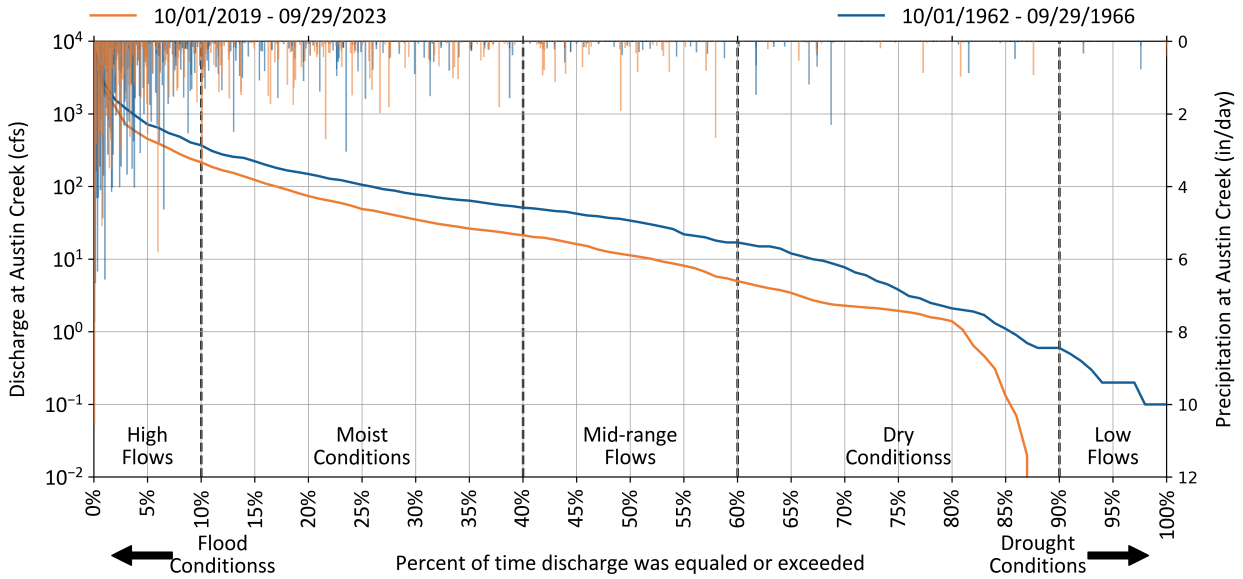

Figure 7-17. Observed flow duration curve for AUSTIN C NR CAZADERO CA (11467200) during the calibration and recent periods.

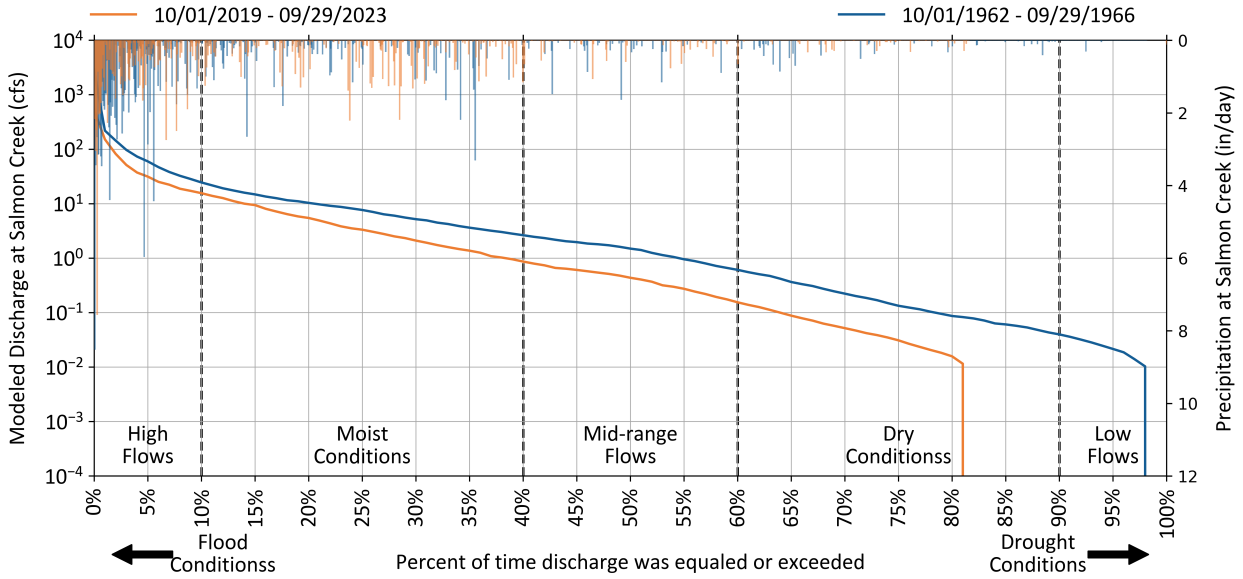

Figure 7-18. Observed flow duration curve for SALMON C A BODEGA CA (11460920) during the calibration and recent periods.

Table 7-8. Change in flow rates between the calibration and recent periods at SALMON C A BODEGA CA (11460920) and AUSTIN C NR CAZADERO CA (11467200)

FDC Flow Regime	Average daily flow (cfs) at Austin Creek				Average daily flow (cfs) at Salmon Creek			
	10/1/1962-9/29/1966	10/1/2019-9/29/2023	Diff.	% Diff.	10/1/1962-9/29/1966	10/1/2019-9/29/2023	Diff.	% Diff.
High Flows (<10%)	1244.5	845.2	-399.3	-32%	137.9	67.8	-70.1	-51%
Moist Conditions (10% - 40%)	134.4	69.9	-64.5	-48%	9.0	4.8	-4.2	-47%
Mid-range Flows (40% - 60%)	34.4	12.1	-22.2	-65%	1.5	0.5	-1.1	-70%
Dry Conditions (60% - 90%)	6.8	2.1	-4.8	-70%	0.2	0.1	-0.1	-70%
Low Flows (>90%)	0.3	0.0	-0.3	-100%	0.0	0.0	-0.0	-100%
All Conditions (Combined)	171.9	108.1	-63.8	-37%	16.8	8.3	-8.5	-51%

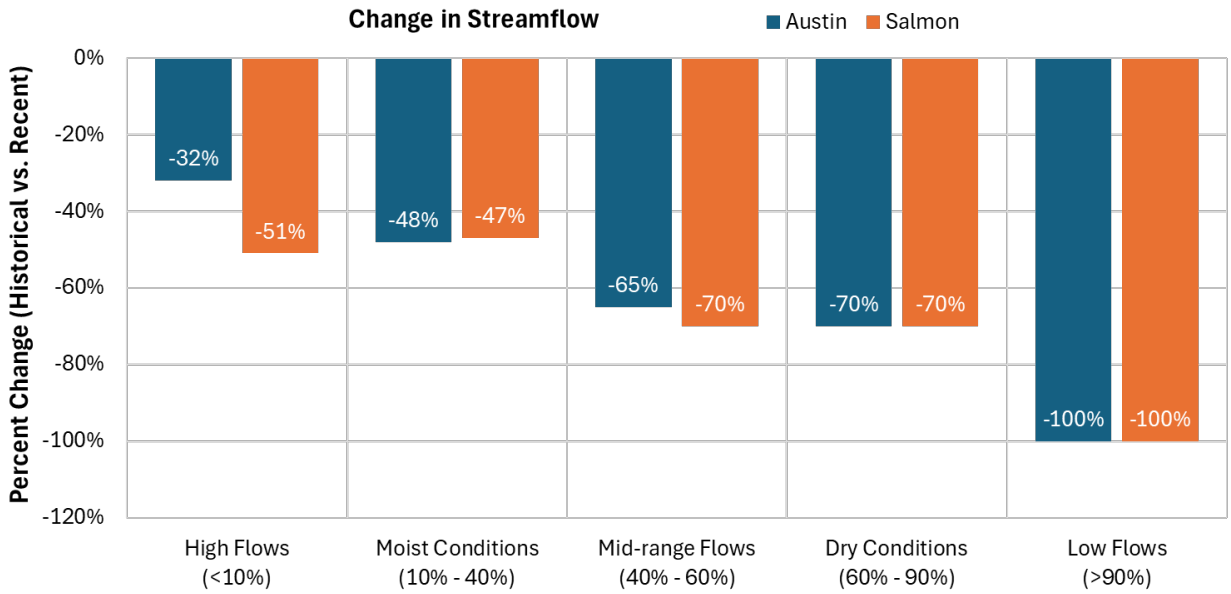

Figure 7-19. Change in flow rates between the calibration and recent periods at SALMON C A BODEGA CA (11460920) and AUSTIN C NR CAZADERO CA (11467200).

Table 7-9. Change in precipitation between the calibration and recent periods at SALMON C A BODEGA CA (11460920) and AUSTIN C NR CAZADERO CA (11467200)

FDC Flow Regime	Average annual precipitation (in.) at Austin Creek				Average annual precipitation (in.) at Salmon Creek			
	10/1/1962-9/29/1966	10/1/2019-9/29/2023	Diff.	% Diff.	10/1/1962-9/29/1966	10/1/2019-9/29/2023	Diff.	% Diff.
High Flows (<10%)	45.7	27.3	-18.4	-40%	34.9	18.9	-16.0	-46%
Moist Conditions (10% - 40%)	11.3	13.7	2.4	21%	10.0	11.6	1.6	15%
Mid-range Flows (40% - 60%)	1.4	3.8	2.4	173%	2.1	2.2	0.1	6%
Dry Conditions (60% - 90%)	2.3	1.0	-1.3	-55%	2.2	1.2	-1.0	-45%
Low Flows (>90%)	0.4	0.3	-0.2	-43%	0.1	0.1	0.0	10%
All Conditions (Combined)	61.1	46.0	-15.1	-25%	49.3	34.0	-15.3	-31%

8 SUMMARY

This report documented the configuration, calibration, and validation of an LSPC hydrology model for the Salmon Creek watershed. The Water Board may use this model to help facilitate water use planning to ensure adequate, minimal water supplies for critical purposes. The Salmon Creek watershed model provides a comprehensive planning and decision-making tool by serving as an evaluation platform for (1) simulating existing instream flows that integrate current water management activities and consumptive uses and (2) evaluating the range of impacts of alternative management scenarios, including water allocation, changes in demand, and the impact of extreme events (e.g., droughts, atmospheric rivers, etc.).

The Salmon Creek watershed model was configured based on authoritative and comprehensive data sets suitable for characterizing hydrology within the region. The model is based on HRUs, which capture physical attributes controlling the rainfall-runoff response and are driven by long-term meteorological forcing time series representing the spatial and temporal range of precipitation and evapotranspiration conditions in the watershed. The model was calibrated and validated at the USGS streamflow station located at Salmon Creek at a point draining almost 45% of the total watershed area, which is the only data set with available data within the whole Salmon Creek watershed.

Overall, the model performance during the calibration period (water years 1963–1969) across the evaluated PBIAS performance metrics ranged from "Very Good" to "Good." Metrics during the validation period (1967–1969) at the same station were also generally in the "Very Good" to "Good" range. However, the model showed poor performance in the RSR and NSE metrics. In this study, hourly precipitation distribution data during the calibration and validation periods were obtained from a distant site, San Francisco International Airport. This may have introduced timing uncertainties into the daily modeling results, leading to poor performance in timing-sensitive metrics such as NSE and RSR. When model performance metrics were evaluated using monthly flow data, the influence of timing errors was reduced, and RSR and NSE showed notable improvements compared to results based on the daily average time series.

The model was also validated by comparing monthly flow volumes as well as the temporal variations of flow rates at the calibration flow station with those at a reference USGS flow station on Austin Creek, located north of the study area. Austin Creek has similar drainage area characteristics and provides high-quality data. Linear regressions of monthly flow volumes indicated consistently lower flow depths in Salmon Creek, which are approximately half of those observed in Austin Creek. Additionally, flow rates at both locations are lower in the recent period, with low flows reaching zero. A higher percentage reduction was observed at the Salmon Creek flow station, aligning with the greater reduction in precipitation observed in the Salmon Creek watershed. Those analyses show that the modeled flows at the calibration station exhibit similar temporal patterns to those observed at the reference station.

In conclusion, the Salmon Creek watershed model is a robust platform for representing existing conditions and setting up future management scenarios. An important benefit of the model development approach used to build the watershed model and described in this report is that it is designed in a modular way where key components can be refined and improved over time as new and better information becomes available.

9 REFERENCES

Arcement, G.J., JR., Schneider, V.R., 1989. Guide for selecting Manning's roughness coefficients for natural channels and flood plains. USGS Water-Supply Paper 2339.

Bent, G.C., Waite, A.M., 2013. Equations for Estimating Bankfull Channel Geometry and Discharge for Streams in Massachusetts. U.S. Geological Survey Scientific Investigations Report 2013–5155 62. https://doi.org/https://doi.org/10.3133/sir20135155

Chapra, S.C.; Pelletier, G.J.; Tao, H.; 2008. QUAL2K: A Modeling Framework for Simulating River and Stream Water Quality, Version 2.11: Documentation and Users Manual.

Cosgrove, B.A., Lohmann, D., Mitchell, K.E., Houser, P.R., Wood, E.F., Schaake, J.C., Robock, A., Marshall, C., Sheffield, J., Duan, Q., Luo, L., Higgins, R.W., Pinker, R.T., Tarpley, J.D., Meng, J., 2003. Real-time and retrospective forcing in the North American Land Data Assimilation System (NLDAS) project. Journal of Geophysical Research: Atmospheres 108, 8842. https://doi.org/10.1029/2002jd003118

Daly, C., G. H. Taylor, W. P. Gibson, T. W. Parzybok, G. L. Johnson, P. A. Pasteris, 2000. High-Quality Spatial Climate Data Sets for the United States and Beyond. Transactions of the ASAE 43, 1957–1962. https://doi.org/10.13031/2013.3101

Daly, C., Neilson, R.P., Phillips, D.C., 1994. A Statistical-Topographic Model for Mapping Climatological Precipitation over Mountainous Terrain. J Appl Meteorol Climatol 33, 140–158.

Daly, C., Taylor, G., Gibson, W., 1997. The Prism Approach to Mapping Precipitation and Temperature, in: 10th AMS Conf. on Applied Climatology. Reno, NV, pp. 10–12.

Gibson, W.P., Daly, C., Kittel, T., Nychka, D., Johns, C., Rosenbloom, N., McNab, A., Taylor, G.H., 2002. Development of a 103-Year High-Resolution Climate Data Set for the Conterminous United States, in: Proceedings of the 13th AMS Conference on Applied Climatology. Portland, OR, pp. 181–183.

Hamon, W.R., 1963. Estimating potential evapotranspiration. Transactions of the American Society of Civil Engineers, 128(1), pp.324-338.

Henn, B., Newman, A.J., Livneh, B., Daly, C., Lundquist, J.D., 2018. An assessment of differences in gridded precipitation datasets in complex terrain. J Hydrol (Amst) 556, 1205–1219. https://doi.org/10.1016/j.jhydrol.2017.03.008

Kim, S., Paik, K., Johnson, F.M., Sharma, A., 2018. Building a Flood-Warning Framework for Ungauged Locations Using Low Resolution, Open-Access Remotely Sensed Surface Soil Moisture, Precipitation, Soil, and Topographic Information. IEEE J Sel Top Appl Earth Obs Remote Sens 11, 375–387. https://doi.org/10.1109/JSTARS.2018.2790409

LACFCD (Los Angeles County Flood Control District), 2020. WMMS Phase I Report: Baseline Hydrology and Water Quality Model. Prepared for the Los Angeles County Flood Control District by Paradigm Environmental. Alhambra, CA.

Looper, J.P., Vieux, B.E., 2012. An assessment of distributed flash flood forecasting accuracy using radar and rain gauge input for a physics-based distributed hydrologic model. J Hydrol (Amst) 412–413, 114–132. https://doi.org/10.1016/j.jhydrol.2011.05.046

McCandless, T.L., 2003a. Maryland stream survey: Bankfull discharge and channel characteristics in the Allegheny Plateau and the Valley and Ridge hydrologic region. Annapolis, MD.

McCandless, T.L., 2003b. Maryland Stream Survey: Bankfull Discharge and Channel Characteristics in the Coastal Plain Hydrologic Region. Annapolis, MD.

McCandless, T.L., Everett, R.A., 2002. Maryland stream survey: Bankfull discharge and channel characteristics in the Piedmont hydrologic region. Annapolis, MD.

McGourty, G., et al. 2020. Agricultural water use accounting provides path for surface water use solutions. California Agriculture, 74(1), 46–57. https://doi.org/10.3733/CA.2020A0003

Mitchell, K.E., Lohmann, D., Houser, P.R., Wood, E.F., Schaake, J.C., Robock, A., Cosgrove, B.A., Sheffield, J., Duan, Q., Luo, L., Higgins, R.W., Pinker, R.T., Tarpley, J.D., Lettenmaier, D.P., Marshall, C.H., Entin, J.K., Pan, M., Shi, W., Koren, V., Meng, J., Ramsay, B.H., Bailey, A.A., 2004. The multi-institution North American Land Data Assimilation System (NLDAS): Utilizing multiple GCIP products and partners in a continental distributed hydrological modeling system. Journal of Geophysical Research: Atmospheres 109. https://doi.org/10.1029/2003jd003823

Quirmbach, M., Schultz, G.A., 2002. Comparison of rain gauge and radar data as input to an urban rainfall-runoff model. Water Science and Technology 45, 27–33. https://doi.org/10.2166/wst.2002.0023

State Water Resource Control Board, 2024. Watershed Supply and Demand Allocations: Salmon Creek Work Plan https://www.waterboards.ca.gov/waterrights/water_issues/programs/supply-and-demand/

Sloto, R. A., & Crouse, M. Y. (1996). HYSEP: A computer program for streamflow hydrograph separation and analysis (No. 96-4040). US Geological Survey. https://pubs.usgs.gov/publication/wri964040

Sutherland, R.C., 2000. Methods for Estimating the Effective Impervious Area of Urban Watersheds, Technical Note 58, in: Scueler, T.R., Holland, H.K. (Eds.), The Practice of Watershed Protection. Center for Watershed Protection, Ellicot City, MD, pp. 193–195.

Xia, Y., Mitchell, K., Ek, M., Cosgrove, B., Sheffield, J., Luo, L., Alonge, C., Wei, H., Meng, J., Livneh, B., Duan, Q., Lohmann, D., 2012a. Continental-scale water and energy flux analysis and validation for North American Land Data Assimilation System project phase 2 (NLDAS-2): 2. Validation of model-simulated streamflow. Journal of Geophysical Research Atmospheres 117. https://doi.org/10.1029/2011JD016051

Xia, Y., Mitchell, K., Ek, M., Sheffield, J., Cosgrove, B., Wood, E., Luo, L., Alonge, C., Wei, H., Meng, J., Livneh, B., Lettenmaier, D., Koren, V., Duan, Q., Mo, K., Fan, Y., Mocko, D., 2012b. Continental-scale water and energy flux analysis and validation for the North American Land Data Assimilation System project phase 2 (NLDAS-2): 1. Intercomparison and application of model products. Journal of Geophysical Research Atmospheres 117, 3109. https://doi.org/10.1029/2011JD016048